TÜRKİYE
FIRAT UNIVERSITY
GRADUATE SCHOOL OF NATURAL AND APPLIED SCIENCES

N-soliton solutions, M-lump waves and physical phenomena between N-soliton solutions and M-lump waves for some types of partial differential equations

Hajar Farhan Ismael

Ph.D. Thesis

Department of Mathematics

June 2022

TÜRKİYE
FIRAT UNIVERSITY
GRADUATE SCHOOL OF NATURAL AND APPLIED SCIENCES

Department of Mathematics

Ph.D. Thesis

N-soliton solutions, M-lump waves and physical phenomena between N-soliton solutions and M-lump waves for some types of partial differential equations

Author

Hajar Farhan Ismael

Supervisor

Prof. Dr. Hasan BULUT

June 2022
Elaziğ

TÜRKİYE
FIRAT UNIVERSITY
GRADUATE SCHOOL OF NATURAL AND APPLIED SCIENCES

Department of Mathematics

Ph.D. Thesis

Title:	N-soliton solutions, M-lump waves and physical phenomena between N-soliton solutions and M-lump waves for some types of partial differential equations
Author:	Hajar Farhan Ismael
Submission Date:	10.5.2022
Defense Date:	10.6.2022

THESIS APPROVAL

This thesis, which was prepared according to the thesis writing rules of the Graduate School of Natural and Applied Sciences, Fırat University, was evaluated by the committee members who have signed the following signatures and was unanimously approved after the defense exam made open to the academic audience.

		Signature
Supervisor:	Prof. Dr. Hasan BULUT Firat University, Faculty of Science	Approved
Chair:	Prof. Dr. Reşat YILMAZER Firat University, Faculty of Science	Approved
Member:	Assoc. Prof. Dr. Asıf YOKUŞ Firat University, Faculty of Science	Approved
Member:	Assoc. Prof. Dr. Hacı Mehmet BAŞKONUŞ Harran University, Faculty of Education	Approved
Member:	Assoc. Prof. Dr. Nuri Murat YAĞMURLU İnönü University, Faculty of Science	Approved

This thesis was approved by the Administrative Board of the Graduate School on .../.../....

Prof. Dr. Kürşat Esat ALYAMAÇ
Director of the Graduate School

DECLARATION

This thesis is dedicated to my parents (Farhan & Mariyah) and my family (Karmina, Masa and Mila).

June 2022

Hajar Farhan Ismael

PREFACE

All glory be to Almighty Allah, the Giver of Mathematics wisdom, Who inspired me to compose my thesis report with His might and will. I would like to express my thanks to my thesis supervisor, Prof. Dr. Hasan Bulut, for his continuous advice, support, patience, and many helpful suggestions during carrying out this Ph.D. thesis. My heartfelt thanks go to my beloved parents Farhan Ismael and Mariya Nasrullah for their immense support in whatever it takes to be me. Special thanks to my lovely wife Karmina Kamal for her continuous support and many helpful suggestions and my daughters (Masa and Mila). Special thanks go to my beloved brother (Vaheel) and sisters (Hivi, Jiyan and Arzo). I would also like to extend my thanks to Mr. Mohammad Hasan Maronisi for his continuous support and help. My deep gratitude also goes to my colleagues, too.

Hajar Farhan Ismael

Elaziğ, 2022

Contents

Page

Abstract

N-soliton solutions, M-lump waves and physical phenomena between N-soliton solutions and M-lump waves for some types of partial differential equations

Hajar Farhan Ismael

Ph.D. Thesis

FIRAT UNIVERSITY
Graduate School of Natural and Applied Sciences

Department of Mathematics
June 2022, Page: vii-98

This research looks at the exact solutions to various nonlinear models in many nonlinear science disciplines. The simplified Hirota's method and long wave method are used to explore N-soliton solutions, complex multi-soliton waves, M-lump waves and interaction phenomena of N-soliton with M-lump waves. The nonlinear models that studied in this thesis are as follows: the (2+1)-dimensional Bogoyavlenskii–Schieff equation, the extended (2+1)-dimensional shallow water wave model, the (2+1)-dimensional Bogoyavlenskii's generalized breaking soliton equation, the (2+1)-dimensional Date-Jimbo-Kashiwara-Miwa equation, the (2+1)-dimensional Bogoyavlensky-Konopelchenko equation, the (2+1)-dimensional Korteweg-De Vries equation with the extension of time-dependent coefficients, and the (3+1)-dimensional generalized Kadomtsev-Petviashvili equation. The velocity of one-M-lump solution is stated. Straight lines of motion that M-lump waves travel among them are also addressed.

Besides, we newly extend the modified expansion function method to construct new wave solutions of partial differential equations. By using this newly modified method we can obtain novel and more analytic solutions comparing to modified expansion function method. Also, comparison between new and obtained solutions are presented successfully.

Keywords: N-soliton solutions; M-lump waves; Interaction phenomena; Hirota's method; Newly modified method

ÖZET

Kısmi diferansiyel denklemlerin bazı türleri için N-soliton çözümleri, M-yığın dalgaları ve N-soliton çözümleri ile M-yığın dalgası arasındaki fiziksel olaylar

Hajar Farhan Ismael

Doktora Tezi

FIRAT ÜNİVERSİTESİ
Fen Bilimleri Enstitüsü

Matematik Anabilim Dalı

Haziran 2022, Sayfa: vii-98

Bu araştırma, birçok doğrusal olmayan bilim disiplinindeki çeşitli doğrusal olmayan modellerin kesin çözümlerini incelemektedir. Basitleştirilmiş Hirota ve bir uzun dalga yöntemi, N-soliton çözümlerini, karmaşık multi-soliton dalgalarını, M-lump dalgalarını ve N-soliton'un M-lump dalgaları ile etkileşim fenomenini keşfetmek için kullanılır. Bu tezde ele alınan doğrusal olmayan modeller şunlardır: (2+1)-boyutlu Bogoyavlenskii–Schieff denklemi, genişletilmiş (2+1)-boyutlu sığ su dalgası modeli, (2+1)-boyutlu Bogoyavlenskii'nin genelleştirilmiş kırılma solitonu denklemi, (2+1) boyutlu Date-Jimbo-Kashiwara-Miwa denklemi, (2+1) boyutlu Bogoyavlensky-Konopelchenko denklemi, (2+1) boyutlu Korteweg-De Vries denklemi ile zamanın uzaması -bağımlı katsayılar, (3+1) boyutlu genelleştirilmiş Kadomtsev-Petviashvili denklemi. Verilen bulgular daha önce yayınlanmış sonuçlarla karşılaştırılır. Bir-M-topak çözümünün hızı belirtilmiştir. M-yumru dalgalarının aralarında hareket ettiği düz hareket çizgileri de ele alınır.

Ayrıca, kısmi diferansiyel denklemlerin yeni dalga çözümlerini oluşturmak için değiştirilmiş genişleme fonksiyonu yöntemini yeni genişlettik. Bu yeni değiştirilmiş yöntemi kullanarak, değiştirilmiş genişleme fonksiyonu yöntemine kıyasla yeni ve daha analitik çözümler elde edebiliriz. Ayrıca yeni ve elde edilen çözümlerin karşılaştırılması da başarılı bir şekilde sunulmaktadır.

Anahtar Kelimeler: N-soliton çözümleri; M-yumru dalgaları; Etkileşim olayları; Hirota'nın yöntemi; Yeni değiştirilmiş yöntem

List of Figures

Symbols and abbreviations

Symbols

α	: Alpha
β	: Beta
γ	: Gamma
μ	: Mu
ϕ	: Phi
ψ	: psi
Ψ	: Psi
ρ	: rho
Φ	: Phi
ξ	: xi
∂_x^{-1}	: Integration with respect to x
$\prod$	: A product over a set of terms
$\sum$	: Sum over a set of terms
∂	: Partial derivative
D_x	: Hirota deivative with respect to x

Abbreviations

PDE	: Partial differential equation
NPDEs	: Nonlinear partial differential equations
DJKM	: Date–Jimbo–Kashiwara–Miwa
BS	: Bogoyavlenskii-Schieff
BK	: Bogoyavlensky-Konopelchenko
KdV	: Korteweg–De Vries
gKP	: generalized Kadomtsev-Petviashvili
BE	: Boussinesq equations
MEFM	: Modified exponential function method

1. Introduction

One of the fundamental problems in the theory of differential equations is the Cauchy problem. The problem requires finding a solution to a differential equation that satisfies what is known as the initial values. Only the simplest differential equations, usually constant-coefficient and linear can be explicitly resolved. As classified, Laplace's method is used to solve linear ordinary differential equations and the Fourier transform method to find the solution of linear partial differential equations, and in the modern soliton theory, the isomonodromic transform method and the inverse scattering transform method are systematical methods that have been developed to find solutions of nonlinear ordinary and partial differential equations, respectively.

Nonlinear partial differential equations are frequently used to characterize a variety of complex nonlinear phenomena that happen in nonlinear sciences such as plasma physics, optical fibers, chemical processes, biological sciences, mathematical physics, and so on. Nonlinear partial differential equations have a wide variety of roles in applied mathematics, making it critical to obtain exact solutions for various types of equations. The general form of NPDE is as follows:

Partial differential equation as one of the important fields of mathematics describe various phenomena in physics and engineering for example the Bogoyavlenskii–Schieff equation in (2+1)-dimensions arise in plasma physics [**1**]. The shallow-water wave model is a set of hyperbolic partial differential equations that describe the flow below a pressure surface in a fluid [**2**]. The (2+1)-dimensional Bogoyavlenskii's breaking soliton equation and the (2+1)-dimensional Bogoyavlensky-Konopelchenko equation characterize the (2+1)-dimensional interaction between a long wave about the x axis interacting with a Riemann wave on the y axis [**3**, **4**]. The (2+1)-dimensional Date–Jimbo–Kashiwara–Miwa equation can be utilized in applied mathematics to model water waves with low surface tension and long wavelengths [**5**]. The Korteweg–de Vries equation is a mathematical model of waves on shallow water surfaces [**6**]. A generalized Kadomtsev-Petviashvili equation in (3+1)-dimensions arises in fluid mechanics and plasma physics [**7**]. Therefore, finding exact solutions to nonlinear evolution equations has piqued the scientific community's attention since they describe the evolution of complicated nonlinear processes in physics and engineering.

According to various applications of PDEs in different areas of sciences, various techniques have been presented and developed to explore dynamical behaviors of PDEs that occur in our globe such as the first integral method [**8**, **9**], the Backland transformation [**10**, **11**], a double Laplace transformation [**12**], the scattering method [**13**], a long-wave method [**14**], the ansatz method [**15**], the Darboux transformation [**16**], the Lie group method [**17**], the simplified Hirota method [**18**, **19**, **20**], the symbolic computations method [**21**, **22**, **23**], the generalized exponential rational function [**24**, **25**], a Taylor series expansion approach [**26**], the Riemann-Hilbert method [**27**, **28**], a generalized (G'/G)-expansion method [**29**], the $(1/G')$-expansion method [**30**, **31**, **32**], the $(G'/G, 1/G')$-expansion method [**33**], the $(m + G'/G)$-expansion method [**34**, **35**, **36**], the $(m + 1/G')$-expansion method [**37**], the (G'/G^2)-expansion method [**38**], a generalized Kudryashov method [**39**], the modified extended direct algebraic method [**40**], the improved mapping approach [**41**], the Pfaffian method [**42**, **43**], the inverse spectral transform method [**44**], the Jacobi elliptic function method [**45**, **46**], and so on.

1.1. Aim of the Thesis

The aim of thesis is to construct the exact solutions to several nonlinear partial differential equations. The simplified Hirota's method and long-wave method will be used to find multiple soliton waves, Complex multiple soliton solutions, M-lump waves, fusion solutions, and interaction physical phenomena solutions. Also, we will newly extend modified expansion function method to construct new and more analytical solution of PDEs.

1.2. Outline of Thesis

The following is an outline of the thesis's structure: Part one includes an overview of nonlinear partial differential equations and their applications. Part 2 of this thesis defines various key concepts, including classical differential equations and solitary wave solutions. Part 3 describes the simplified Hirota's method, a long-wave method, and newly extend modified expansion function method employed in this thesis. Part 4 discusses the applications of the approaches described in Part 3 to certain nonlinear physical models. Part 5 contains the results as well as a discussion of the stated results from Part 4. In section 6, we present the study's result.

2. FUNDAMENTAL DEFINITIONS

Definition 2.1. Partial differential equation is a differential equation that has more than one independent variable with one or more dependent variables [**47**].

Definition 2.2. The largest derivative that appears in the equation is called the order of the differential equation [**47**].

Definition 2.3. A partial differential equation is considered to be linear [**47**] if and only if the following conditions are met:

- The dependent variable's exponent and each partial derivative included in the equation are both one.
- There are no cross–terms that is, terms such as uu' or $u'u''$ in which the function or its derivatives occur more than once.

Otherwise, differential equation is said to be nonlinear differential equation.

Definition 2.4. Non-homogeneous partial differential equations are those in which all of the terms of a PDE contain the dependant variable or its partial derivatives [**47**].

Definition 2.5. A solitary wave is a self-reinforcing wave packet that keeps its form while moving at a regular speed. Soliton solutions are constructed by using the following formula:

$$f = f_N = \sum_{\mu=0,1} \exp\left(\sum_{i=1}^{N} \mu_i \psi_i + \sum_{1\leq i<j\leq N}^{(N)} \mu_i \mu_n A_{ij}\right), \tag{2.1}$$

The notation $\sum\limits_{\mu=0,1}$ is a summation that takes over all possible combinations $\mu_i = 0,1$ for $i = 1,2,...,N$ [**48**].

Definition 2.6. Lump waves are rational function solutions and localized in all directions in the space [**49**].

Definition 2.7. Rogue waves are a kind of rational function solution, which have amplitude more than twice the background waves and appear from nowhere and disappear without a trace [**49**].

Definition 2.8. Breathers are solutions that are periodic in time or space and localized in one certain direction [**49**].

Definition 2.9. The Hirota bilinear operator, and defined by Hirota direct method [**48**] as

$$D_x^i D_y^j D_t^k a.b = (\partial_x - \partial_{x'})^i (\partial_y - \partial_{y'})^j (\partial_t - \partial_{t'})^k a\,(x,y,t) \times b\,(x',y',t')\Big|_{x=x',y=y',t=t'}. \tag{2.2}$$

For instance

$$
\begin{aligned}
&D_x(a.b) = a_x b - a b_x = -D_x(b.a),\\
&D_x D_t(a.b) = a_{xt} b - a_x b_t - a_t b_x + a b_{xt} = D_x D_t(b.a),\\
&D_x^2\left(a.b\right) = a_{xx} b - 2 a_x b_x + a b_{xx} = D_x^2\left(b.a\right),\\
&D_x D_t\left(a.a\right) = 2\left(a a_{xt} - a_x a_t\right),
\end{aligned}
$$

where D is a binary operator and is called the Hirota derivative.

3. Simplified Hirota's and long wave methods

In this chapter, we use the simplified Hirota's method and long wave method on some nonlinear partial differential equations to construct N-soliton solutions and M-lump waves, respectively. Also, to find physical interaction phenomena between multi-soliton solution and M-lump wave, we use both methods together.

3.1. The (2 + 1)-Dimensional Bogoyavlenskii-Schieff equation

In present work, we investigate the exact solutions of the BS equation that describes a nonlinear phenomenon in plasma physics by the Hirota bilinear form. The BS equation has an essential role in clarifying the (2 + 1)-dimensional interaction of the Riemann wave propagating through the y-axis with a long wave propagating through the x-axis. Deem integrable BS equation of higher-order in (2 + 1)-dimension as follows

$$4u_{xt} + 4u_x u_{xy} + 2u_{xx}u_y + u_{xxxy} + \partial_x^{-1} u_{yyy} + 4\alpha u_{xy} = 0, \tag{3.1}$$

where $u = u(x, y, t)$ and α is real. This equation was derived by uniting the dual spatial generalizations of the KdV equation, integrating the closed ring with both the KP equation and the Bogoyavlenskii equation. Song-Ju et al. [**50**] studied N-soliton solutions to the BS equation via reporting its Lax pair when $\alpha = 0$. Wazwaz [**51**] derived two extensions of the BS equation and demonstrated that the extension terms do not ruin the integration of the standard Bogoyavlenskii–Schieff equation. Yong et al. [**52**] constructed novel solutions of the BS equation via utilizing the Riccati equation expansion method. Ray and Vinita [**53**] used the Lie group method to study a similarity reduction of Eq. (3.1).

Applying the logarithmic transform

$$u\,(x, y, t) = 2\frac{\partial}{\partial x}\left(\log\left(f\,(x, y, t)\right)\right), \tag{3.2}$$

on Eq. (3.1), the reader can obtain

$$\begin{aligned}
&f_y\left(2{f_{xx}}^2 - 4f_x\left(2af_x + f_{xxx}\right)\right) + 2{f_y}^3\\
&- 2f\left(f_{xx}\left(2f_t - f_{xxy}\right) + 2f_x\left(2f_{xt} + 2af_{xy} + f_{xxxy}\right)\right)\\
&+ 4f_x\left(-f_{xy}f_{xx} + f_x\left(2f_t + f_{xxy}\right)\right)\\
&- f^2\left(f_{yyy} + 4f_{xxt} + 4af_{xxy} + f_{xxxxy}\right)\\
&+ f_yf\left(3f_{yy} + 4af_{xx} + f_{xxxx}\right) = 0.
\end{aligned} \tag{3.3}$$

Now, to retrieve the multi-soliton solutions to the Eq. (3.1), we use the function $f = f(x, y, t)$ as stated in Eq. (2.1) and related necessary constants and functions are introduced as the following form

$$A_{ij} = \frac{(k_i - k_j + l_i - l_j)(k_i - k_j - l_i + l_j)}{(k_i + k_j + l_i - l_j)(k_i + k_j - l_i + l_j)}, \tag{3.4}$$

$$\psi_i = e^{k_i(x+l_i y+w_i t)+\alpha_i}, \tag{3.5}$$

$$w_i = \frac{1}{4}\left(-4\alpha l_i - {k_i}^2 l_i - {l_i}^3\right). \tag{3.6}$$

Here k_i, l_i, w_i are real scalars.

3.1.1. Multi-soliton and Fusional solutions

In this portion, we explore the features of the BS equation of higher order, such as one-, two-, and three-soliton solutions and a general form of fusional solutions. First, we try to find multi soliton solutions to the Eq. (3.1). When $N = 1$, we get

$$f = 1 + \mathrm{e}^{k_1(x+l_1 y+w_1 t)+\alpha_1}, \tag{3.7}$$

where w_1 is defined in Eq. (7). Plugging Eq. (8) into Eq. (2), the result is

$$u = k_1 - k_1 \tanh\left(\frac{1}{8}k_1\left(\left(4\alpha l_1 + {k_1}^2 l_1 + {l_1}^3\right)t - 4x - 4l_1 y\right)\right). \tag{3.8}$$

This equation is a kink soliton solution.
When $N = 2$, we get

$$f = 1 + \mathrm{e}^{\psi_1} + \mathrm{e}^{\psi_2} + A_{12}\mathrm{e}^{\psi_1+\psi_2}, \tag{3.9}$$

here w_1, w_2 are defined in Eq. (3.6) and A_{12} is defined in Eq. (3.4). Inserting Eq. (3.9) into Eq. (3.2), we gain the two-soliton solution of Eq. (3.1) as follows

$$u = \frac{2\left(k_1\mathrm{e}^{\psi_1} + k_2\mathrm{e}^{\psi_2} + A_{12}(k_1 + k_2)\mathrm{e}^{\psi_1+\psi_2}\right)}{1 + \mathrm{e}^{\psi_1} + \mathrm{e}^{\psi_2} + A_{12}\mathrm{e}^{\psi_1+\psi_2}}. \tag{3.10}$$

When $N = 3$, we have

$$f = 1 + \mathrm{e}^{\psi_1} + \mathrm{e}^{\psi_2} + \mathrm{e}^{\psi_3} + A_{12}\mathrm{e}^{\psi_1+\psi_2} + A_{13}\mathrm{e}^{\psi_1+\psi_3} + A_{23}\mathrm{e}^{\psi_2+\psi_3} + A_{123}\mathrm{e}^{\psi_1+\psi_2+\psi_3}, \tag{3.11}$$

where $A_{123} = A_{12}A_{13}A_{23}$. Here $\psi_i\,(i = 1, 2, 3)$ are defined in Eq. (3.5) and $A_{ij}\,(1 \le i < j \le 3)$ are defined in Eq. (3.4). Putting Eq. (3.11) into Eq. (3.2), we obtain a 3-soliton solution of the BS equation of higher order. The 1-soliton, 2-solitom, and 3-soliton solutions of BS equation of higher order are plotted graphically (see Figure 3.1, Figure 3.2 and Figure 3.3).

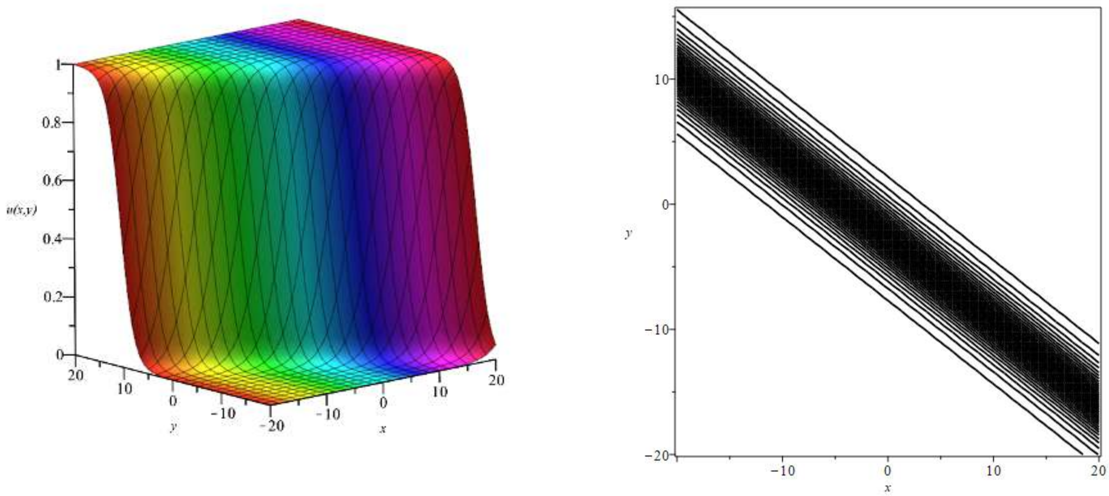

(a) One-soliton solution

(b) Contour plot of one-soliton solution

Figure 3.1. One-soliton solution and its corresponding contour plot drawn when $t = 2, k_1 = \frac{1}{2}, l_1 = \frac{3}{2}, \alpha = -2$.

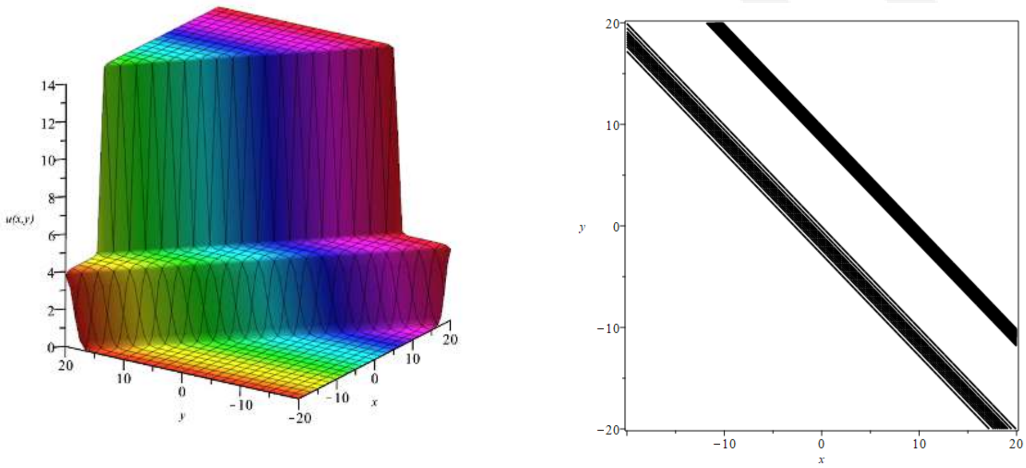

(a) Two-soliton solution

(b) Contour plot of two-soliton solution

Figure 3.2. Two-soliton solution and its corresponding contour plot drawn when $t = 2, k_1 = 2, k_2 = 5, l_1 = 1, l_2 = 1, \alpha_1 = 0, \alpha_2 = 1, \alpha = -2$.

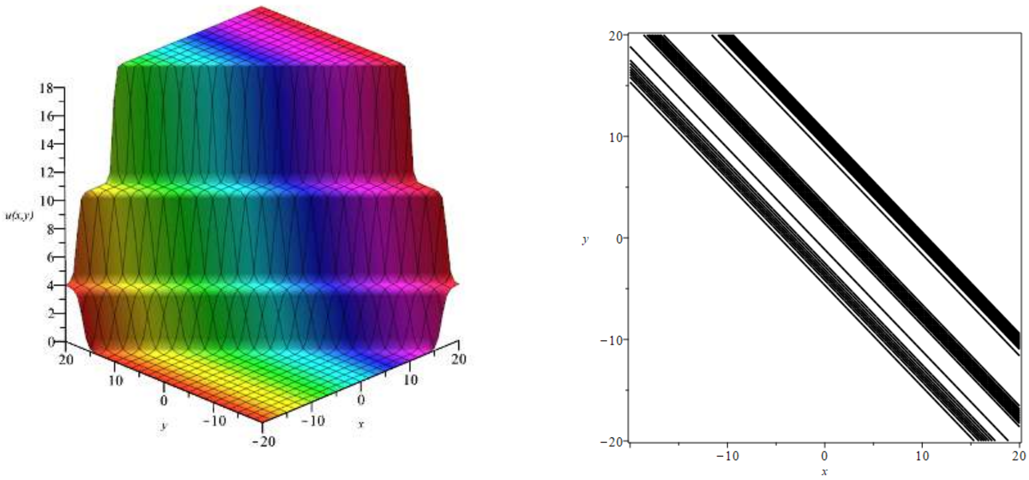

(a) Three-soliton solution

(b) Contour plot of three-soliton solution

Figure 3.3. Three-soliton solution and its corresponding contour plot drawn when $t = 4, k_1 = 2, k_2 = 3, k_3 = 4, l_1 = 1, l_2 = 1, l_3 = 1, \alpha_1 = 1, \alpha_2 = 2, \alpha_3 = 3, \alpha = -2$.

Taking $\alpha = 0$, one can get the N-soliton solutions which was reported by Song-Ju et al. [**50**]. To guarantee the existence of N-soliton solution to the differential equation, we suggest readers to study Ref. [**54**]. Now to explore the features of fusional solutions we choose suitable values for the constants $A_{ij} = 0\,(1 \leq i < j \leq N)$. When $N = 2, N = 3$ and $N = 4$, we have

$$f_2 = 1 + \mathrm{e}^{k_1(x+l_1y+w_1t)+\alpha_1} + \mathrm{e}^{k_2(x+l_2y+w_2t)+\alpha_2}, \tag{3.12}$$

$k_1 = -1, k_2 = 2, l_1 = -1, l_2 = 2.$

$$f_3 = 1 + \mathrm{e}^{\psi_1} + \mathrm{e}^{\psi_2} + \mathrm{e}^{\psi_3}, \tag{3.13}$$

$k_1 = \frac{1}{2}, k_2 = 1, k_3 = \frac{3}{2}, l_1 = \frac{1}{2}, l_2 = 1, l_3 = \frac{3}{2}.$

$$f_4 = 1 + \mathrm{e}^{\psi_1} + \mathrm{e}^{\psi_2} + \mathrm{e}^{\psi_3} + \mathrm{e}^{\psi_4}, \tag{3.14}$$

$k_i = l_i\,(i = 1, 2, 3, 4).$

$$f_N = 1 + \sum_{i=1}^{N} e^{\psi_i}, \qquad (k_i = l_i)\,, \tag{3.15}$$

where $\psi_i\,(i = 1, 2, 3, ...N)$ is defined in Eq. (3.5), and Eq. (3.15) is a general form of fusional solutions. The features of Eqs. (3.13-3.15) are plotted as shown in Figure 3.4.

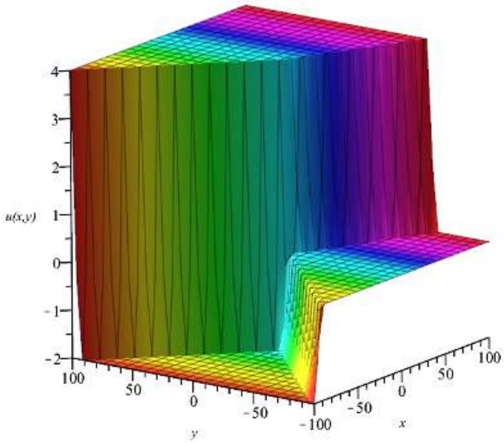

(a) 1-fusional solution

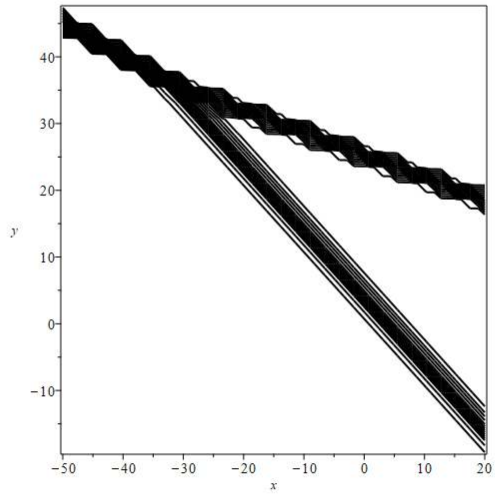

(b) Contour plot of 1-fusional solution

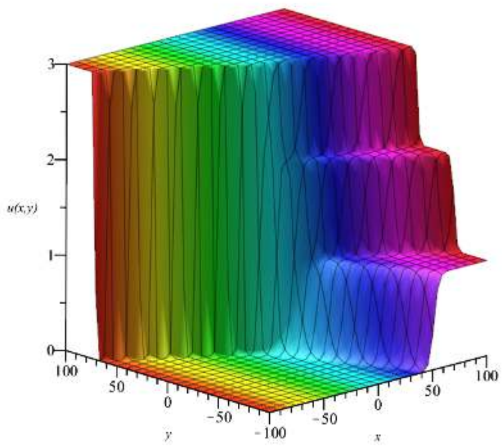

(c) 2-fusional solution

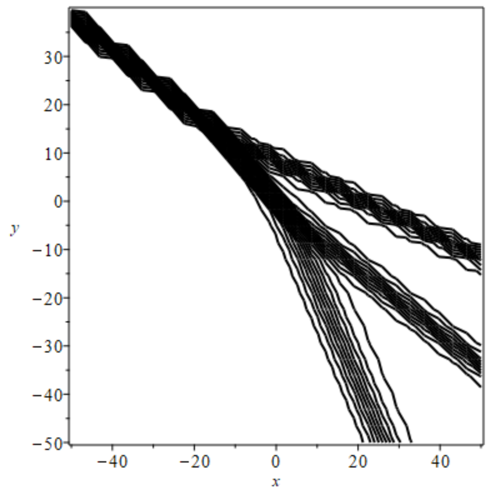

(d) Contour plot of 2-fusional solution

Figure 3.4. 3D figure plotted when $t = 2, \alpha_1 = -1, \alpha_2 = -1, a = -1, \alpha_3 = -10, \alpha = -1$.

3.1.2. Quadratic solutions

In this section, we analyze the real and complex lump solutions of Eq. (3.1). First, we define the quadratic form

$$f = (a_1 x + a_2 y + a_3 t + a_4)^2 + (b_1 x + b_2 y + b_3 t + b_4)^2 + c, \tag{3.16}$$

and replace it in Eq. (3.2), one could get an algebraic system. Solving the obtained solutions, the following case is deduced

$$a_2 = 2\mathrm{i}\sqrt{\alpha}a_1, a_3 = 0, b_2 = -2\left({a_1}^2 - \mathrm{i}\sqrt{\alpha}b_1\right), b_3 = -4\alpha {a_1}^2. \tag{3.17}$$

Inserting Eq. (3.17) into Eq. (3.2), we have

$$u = \frac{2\left(b_1 + 2a_1\left(a_4 + a_1 x + 2\mathrm{i}\sqrt{\alpha}a_1 y\right)\right)}{b_4 + c - 4\alpha {a_1}^2 t + b_1 x - 2\left({a_1}^2 - \mathrm{i}\sqrt{\alpha}b_1\right) y + \left(a_4 + a_1 x + 2\mathrm{i}\sqrt{\alpha}a_1 y\right)^2}. \tag{3.18}$$

This equation represents a complex soliton solution of the BS equation of higher-order (see Figure 3.5).

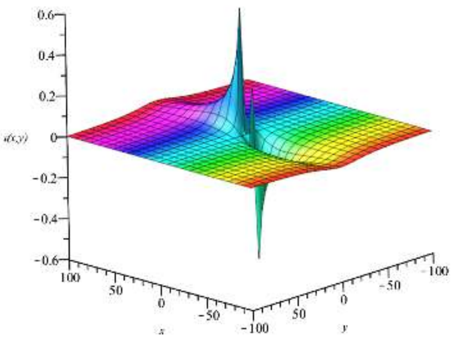

(a) Real part of Eq. (3.18)

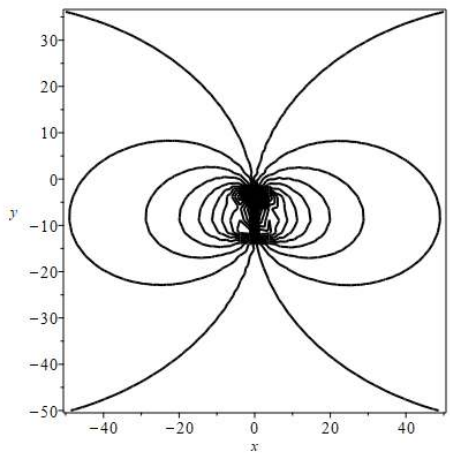

(b) Contour plot of real part

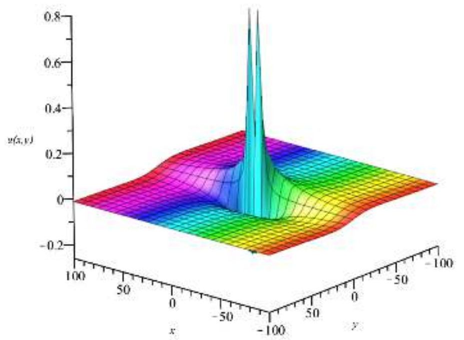

(c) Imaginary part of Eq. (3.18)

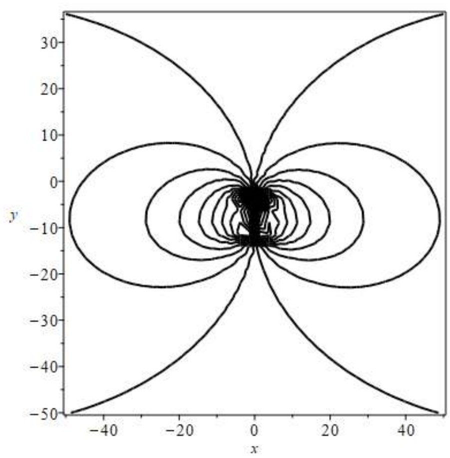

(d) Contour plot of imaginary part

Figure 3.5. 3D figure plotted when $t = 2, a_1 = 2, a_4 = 2, b_1 = 2, b_4 = 0.2, c = 1, \alpha = 1$.

3.1.3. M-Lump solutions

To study M-lump waves, we will apply long-wave method on Eq. (3.1). Manakov and Zakharov [**55**] were the first to introduce the lump wave. After that, Satsuma and Ablowitz [**56**] used long wave limit method for constructing multi-lump waves. In this section, the long-wave method is used to construct M-lumps solutions from 2N-soliton solutions. To analyze a 1-lump solution from Eq. (3.9), we let $\frac{k_1}{k_2} = O(1),\ k_i \to 0, e^{\alpha_i} = -1\ \ (i = 1, 2)$, then we have

$$f_2 = \phi_1\phi_2 + B_{12}. \tag{3.19}$$

Here

$$\begin{aligned} \phi_i &= x + l_i y + \rho_i t, \\ \rho_i &= -\frac{1}{4}\left(4\alpha l_i + {l_i}^3\right), \\ B_{ij} &= \frac{4}{(l_i - l_j)^2} \quad i < j. \end{aligned} \tag{3.20}$$

Now plugging Eq. (3.20) along with $l_1 = a_1 + b_1\mathrm{i}, l_2 = a_1 - b_1\mathrm{i} = l_1^*$ into Eq.(3.2), one can get

$$\begin{aligned} u &= 2\frac{\partial}{\partial x}\left((x' + a_1 y')^2 + {b_1}^2 y'^2 - \frac{1}{{b_1}^2}\right) \\ &= \frac{4\,(x' + a_1 y')}{(x' + a_1 y')^2 + {b_1}^2 y'^2 - \frac{1}{{b_1}^2}}, \end{aligned} \tag{3.21}$$

where

$$\begin{aligned} x' &= x + \frac{1}{2}{a_1}^3 t + \frac{1}{2} t a_1 {b_1}^2, \\ y' &= y - a_1 t - \frac{3}{4}{a_1}^2 t + \frac{1}{4}{b_1}^2 t. \end{aligned} \tag{3.22}$$

The above equation is a M-lump solution of the suggested equation as shown in Figure 3.6, which decays as $O\left(\frac{1}{x^2}, \frac{1}{y^2}\right)$ for $|x|, |y| \to \infty$ and move with the velocity

$$v_x = -\frac{1}{2}{a_1}^3 - \frac{1}{2}a_1{b_1}^2,$$

and

$$v_y = a_1 + \frac{3}{4}{a_1}^2 - \frac{1}{4}{b_1}^2.$$

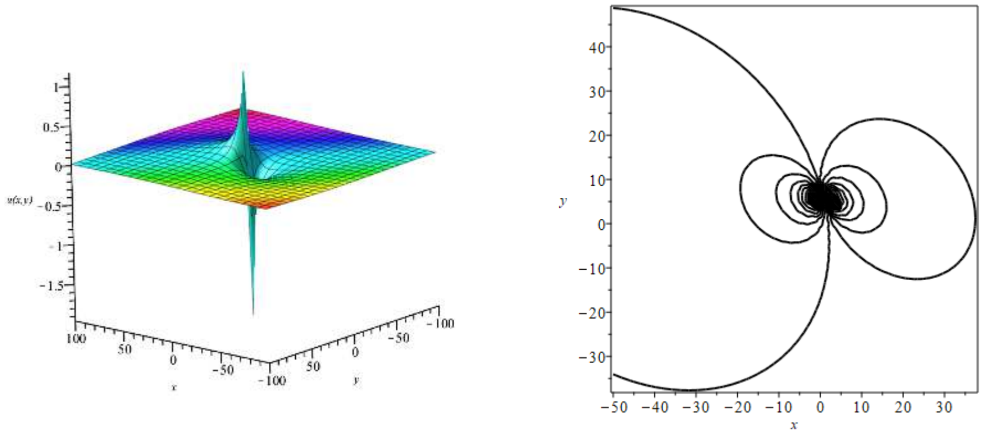

(a) One-M-lump wave **(b)** Contour plot of one-M-lump wave

Figure 3.6. 1-M-Lump solution plotted when $t = 2, a_1 = 1/4, b_1 = 1, \alpha = 3$.

For study a 2-lump solution from Eq. (2.1), we choose $N = 4$, $k_i \to 0$, and $e^{\alpha_i} = -1$ $(i = 1, 2, 3, 4)$, then f_4 takes the following form

$$\begin{aligned} f_4 = {} & \phi_1\phi_2\phi_3\phi_4 + B_{12}\phi_3\phi_4 + B_{13}\phi_2\phi_4 + B_{14}\phi_2\phi_3 + B_{23}\phi_1\phi_4 \\ & + B_{24}\phi_1\phi_3 + B_{34}\phi_1\phi_2 + B_{12}B_{34} + B_{13}B_{24} + B_{14}B_{23}, \end{aligned} \tag{3.23}$$

where ϕ_i, ρ_i, B_{ij} for $i, j = 1, 2, 3, 4$ is defined in Eq. (3.20). After putting Eq. (3.23) into Eq. (3.2), the results give us the two-M-lump solution as seen in Figure 3.7.

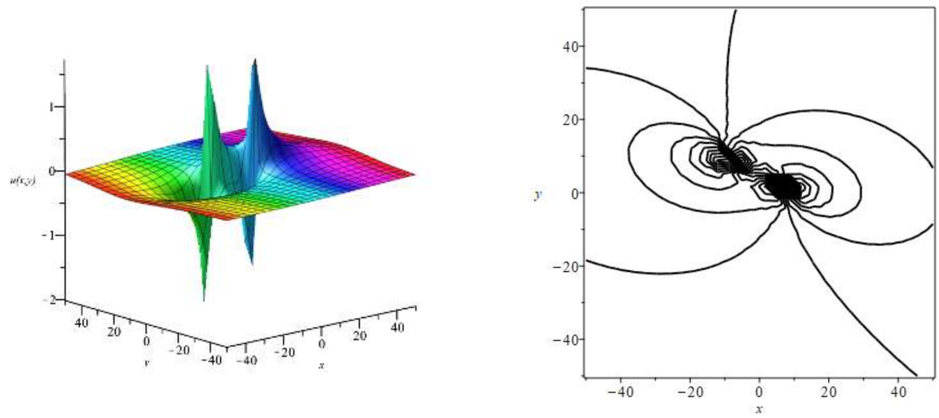

(a) 2-M-lump wave **(b)** Contour plot of 2-M-lump wave

Figure 3.7. 2-M-Lump solution plotted when $t = 2, a_1 = 1/2, b_1 = 4/3, a_2 = 1/3, b_2 = 3/2, \alpha = 3$.

3.1.4. Interaction solutions between M-lump and solitary waves

In this section, we will scrutinize interaction between M-lump and solitary waves. First, we find the interaction between M-lump and soliton solution. Let, we have $N = 3$ in Eq. (2.1), and choosing $\frac{k_1}{k_2} = O(1)$, $k_i \to 0, e^{\alpha_i} = -1$ $(i = 1, 2)$, then f_3 become

$$f_3 = \phi_1\phi_2 + B_{12} + (\phi_1\phi_2 + B_{12} + C_{23}\phi_1 + C_{13}\phi_2 + C_{13}C_{23})e^{\psi_3}. \tag{3.24}$$

The constants $C_{m3}\,(m = 1, 2)$ are defined as

$$C_{m3} = -\frac{4k_3}{{k_3}^2 - {l_m}^2 + 2l_m l_3 - {l_3}^2}, \qquad m = 1, 2. \tag{3.25}$$

Putting Eq. (3.24) into Eq. (3.2), the result is an interaction phenomena that appear between M-lump solution and a 1-soliton solution (see Figure 3.8).

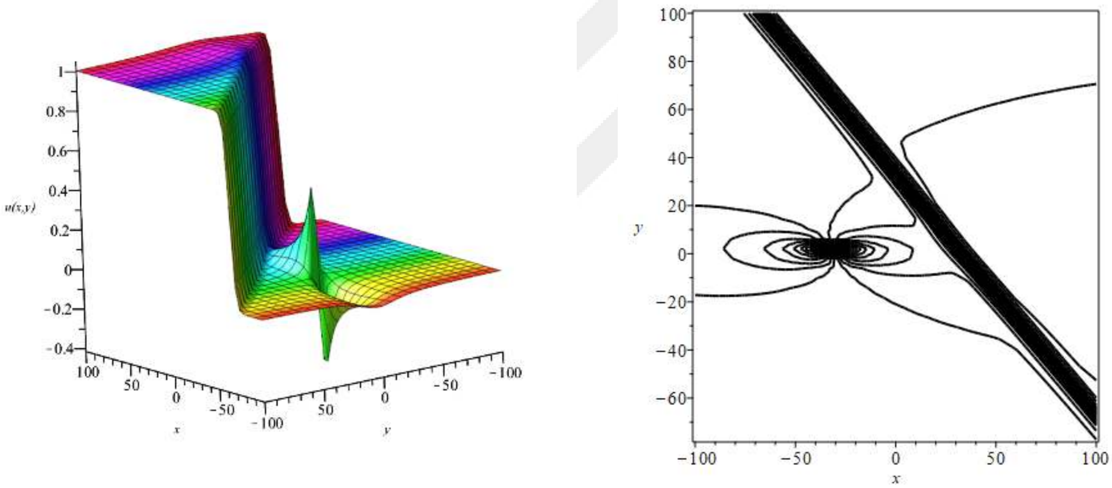

(a) Mixed one-M-lump-one-soliton wave

(b) Contour plot of mixed one-M-lump-one-soliton wave

Figure 3.8. 3D figure plotted when $a = 1/2, b = 7/2, k_3 = 1/2, l_3 = 1, \alpha = 3, t = 10$.

Let, we have $N = 4$ in Eq. (2.1), and letting $\frac{k_1}{k_2} = O(1)$, $k_i \to 0$, and $e^{\alpha_i} = -1$ $(i = 1, 2, 3, 4)$, then f_4 become

$$f_4 = f_3 + \Psi_2 e^{\psi_4} + A_{34}e^{\psi_3+\psi_4}\left(\Psi_1 + \Psi_2 - \phi_1\phi_2 - B_{12} + C_{13}C_{24} + C_{14}C_{23}\right), \tag{3.26}$$

where

$$\Psi_1 = \phi_1\phi_2 + B_{12} + C_{23}\phi_1 + C_{13}\phi_2 + C_{13}C_{23},$$

$$\Psi_2 = \phi_1\phi_2 + B_{12} + C_{24}\phi_1 + C_{14}\phi_2 + C_{14}C_{24}.$$

The constants $C_{m4}\,(m = 1,2,3)$ are defined as follows

$$C_{m4} = -\frac{4k_4}{{k_4}^2 - {l_m}^2 + 2l_m l_4 - {l_4}^2}. \tag{3.27}$$

Substituting Eq. (3.26) into Eq. (3.2) a result gives us a solution that describes physical interaction solution between M-lump and 2-soliton solution as presented graphically in Figure 3.9.

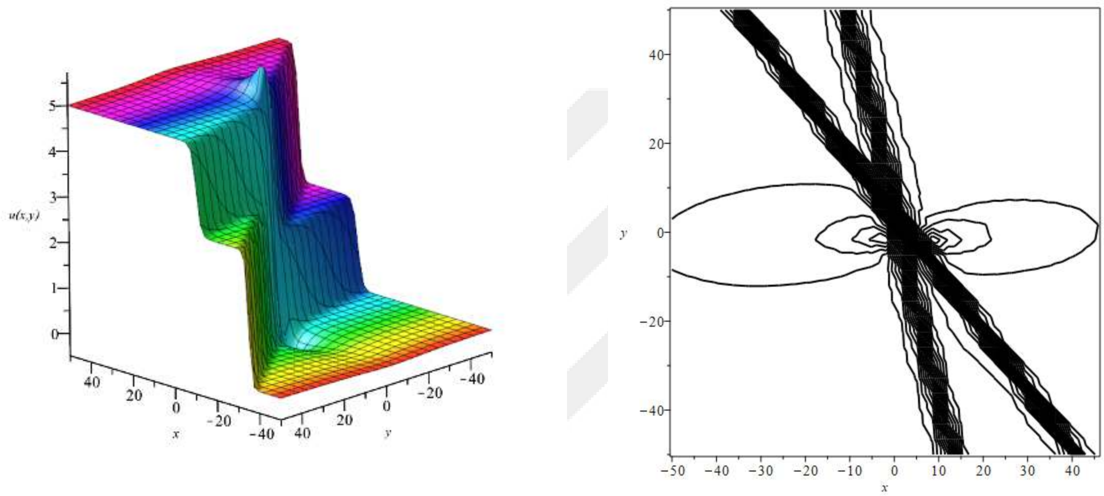

(a) Mixed one-M-lump-two-soliton wave

(b) Contour plot of mixed one-M-lump-two-soliton wave

Figure 3.9. 3D figure plotted when $a_1 = -1/2, b_1 = 5/2, l_3 = 1/4, k_3 = 1, l_4 = 3/4, k_4 = 3/2, \alpha = 1, t = 2$.

Finally, we analyze the interaction solution between M-lump wave and fusion solution. By taking the constant A_{34}, which is defined in Eq. (3.4) to be zero in Eq. (3.26), then f_4 becomes equivalent to

$$f_4 = \phi_1\phi_2 + B_{12} + \Psi_1 e^{\psi_3} + \Psi_2 e^{\psi_4}. \tag{3.28}$$

Putting the above equation into Eq. (3.2) a result represents the interaction between M-lump and fusion solutions (see Figure 3.10).

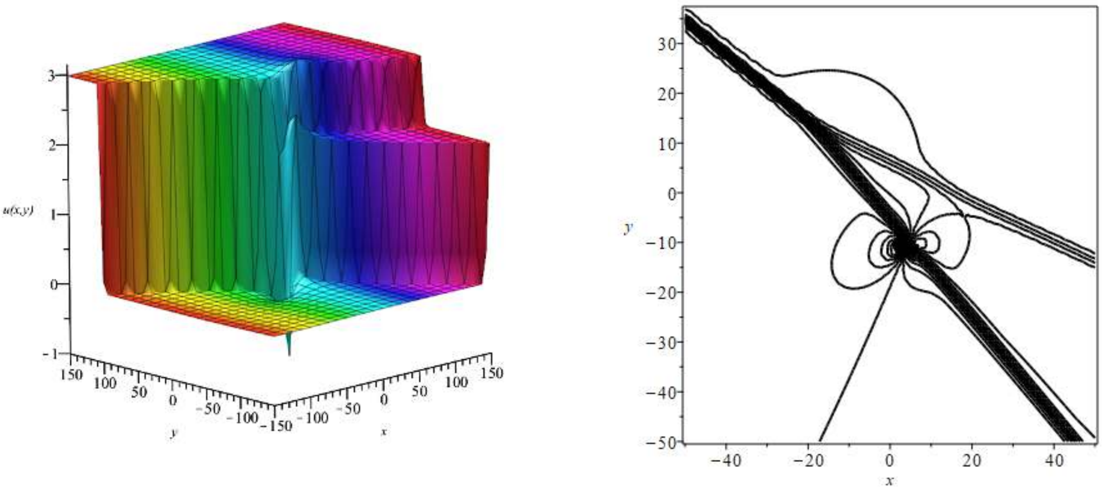

(a) Mixed one-M-lump-one-fusion wave

(b) Contour plot of mixed one-M-lump-one-fusion wave

Figure 3.10. 3D figure plotted when $a_1 = -1/2, b_1 = 1, l_3 = 1, k_3 = 1, l_4 = 3/2, k_4 = 3/2, \alpha = -1, t = 10$.

3.2. The extended shallow water wave model

Consider the extended shallow water wave model in (2 +1)-dimensions as follows

$$u_{yt} + 3u_{xxxy} - 3u_{xx}u_y - 3u_x u_{xy} + \alpha u_{xy} = 0, \tag{3.29}$$

where α is constant and $u = u(x, y, t)$. The dynamics of shallow water waves can be shown in multiple locations, such as river islands, lakes, and streams. Harun-Or-Roshid & Ma [**57**], studied the dynamics shallow water model in (2 +1)-dimension by using $u = -2(\log(f))_x$, as a variable transformation, and obtained Hirota bilinear form as

$$\left(D_y D_t + D_x^3 D_y + \alpha D_x D_y\right) f.f = 0.$$

In this thesis via the logarithmic variable transformation that depends on the Hirota bilinear method, we focus to investigate and construct multi-soliton, complex multi-soliton, fusion, breather, one-lump, the interaction between kink soliton and one-lump, and periodic lump solutions to the model. Consider the following variable transformation [**2**]

$$u = -6(\log(f))_x, \tag{3.30}$$

and apply it on Eq. (3.29), whenever $f = f(x, y, t)$ is defined in Eq. (2.1), we can rewrite

Eq. (3.29) as

$$\begin{aligned}&\frac{6f_{yt}f_x}{f^2}-\frac{12f_tf_yf_x}{f^3}-\frac{12\alpha f_yf_x{}^2}{f^3}+\frac{6f_yf_{xt}}{f^2}+\frac{6f_tf_{xy}}{f^2}+\frac{12\alpha f_xf_{xy}}{f^2}-\frac{6f_{xyt}}{f}+\\&\frac{6\alpha f_yf_{xx}}{f^2}+\frac{108f_xf_{xy}f_{xx}}{f^3}-\frac{6\alpha f_{xxy}}{f}-\frac{108f_x{}^2f_{xxy}}{f^3}-\frac{36f_yf_xf_{xxx}}{f^3}-\\&\frac{36f_{xy}f_{xxx}}{f^2}+\frac{72f_xf_{xxxy}}{f^2}+\frac{18f_yf_{xxxx}}{f^2}-\frac{18f_{xxxxy}}{f}=0,\end{aligned}\tag{3.31}$$

here $f=f(x,y,t)$. Simplifying Eq. (3.31) to its bilinear form, we get

$$\left(\frac{\left(3D_yD_t+9D_x^3D_y+3\alpha D_xD_y\right)f.f}{f^2}\right)_x=0.\tag{3.32}$$

By integrate Eq. (3.32) with respect to x, simplify the result and letting the constant of integration to be zero, we get

$$\left(D_yD_t+3D_x^3D_y+\alpha D_xD_y\right)f.f=0,\tag{3.33}$$

where D is the Hirota bilinear operator defined in Eq. (2.2).

3.2.1. N-soliton Solutions

To obtain the 1-soliton solution of the studied model, we assume

$$f=1+\mathrm{e}^{k_1x+l_1y-w_1t+\alpha_1},\tag{3.34}$$

where

$$w_i=\alpha k_i+3k_i{}^3,\qquad i=1,2,...,N.\tag{3.35}$$

Here, k_i, l_i and w_i are arbitrarily selected constants. Plugging Eq.(3.35) and Eq. (3.34) into Eq. (3.30), we acquire

$$u=-\frac{6k_1\mathrm{e}^{k_1x+l_1y-\left(k_1\alpha+3k_1{}^3\right)t+\alpha_1}}{1+\mathrm{e}^{k_1x+l_1y-\left(k_1\alpha+3k_1{}^3\right)t+\alpha_1}}.\tag{3.36}$$

This is a single-soliton solution to the model as shown in Figure 3.11 in three-dimensions. To investigate the double-soliton solution of Eq. (3.29), we assume f as follows

$$\begin{aligned}f=&1+\mathrm{e}^{k_1x+l_1y-w_1t+\alpha_1}+\mathrm{e}^{k_2x+l_2y-w_2t+\alpha_2}+\\&A_{12}\mathrm{e}^{k_1x+l_1y-w_1t+k_2x+l_2y-w_2t+\alpha_2+\alpha_1},\end{aligned}\tag{3.37}$$

where

$$A_{ij}=\frac{\left(k_i-k_j\right)\left(l_i-l_j\right)}{\left(k_i+k_j\right)\left(l_i+l_j\right)},\qquad\left(1\le i<j\le N\right).\tag{3.38}$$

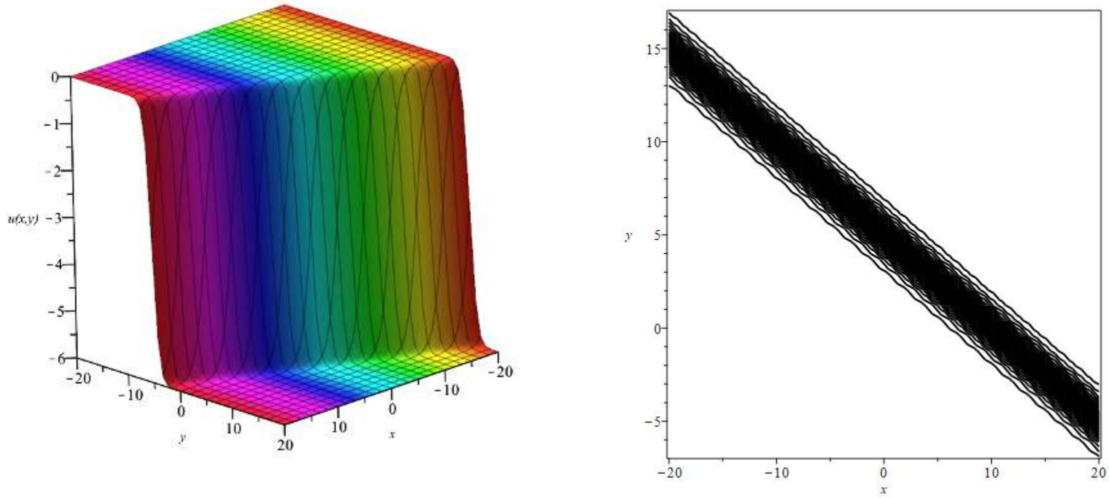

(a) One-soliton wave

(b) Contour plot of one-soliton wave

Figure 3.11. One-soliton solution plotted when $t = 2, k_1 = 1, l_1 = 2, \alpha_1 = 0, \alpha = 2$.

Putting Eq. (3.37) with Eq. (3.38) into Eq. (3.30), we gain

$$u = -\frac{6\left(k_1 e^{\gamma_1} + k_2 e^{\gamma_2} + \frac{(k_1-k_2)(l_1-l_2)}{l_1+l_2} e^{\gamma_3}\right)}{1 + e^{\gamma_1} + e^{\gamma_2} + \frac{(k_1-k_2)(l_1-l_2)}{(k_1+k_2)(l_1+l_2)} e^{\gamma_3}}, \tag{3.39}$$

where

$$\gamma_1 = k_1 x + l_1 y - \left(\alpha k_1 + 3{k_1}^3\right) t + \alpha_1, \tag{3.40}$$

$$\gamma_2 = k_2 x + l_2 y - \left(\alpha k_2 + 3{k_2}^3\right) t + \alpha_2, \tag{3.41}$$

and

$$\gamma_3 = (k_1 + k_2)\, x + (l_1 + l_2)\, y - \left(\left(k_1 \alpha + 3{k_1}^3\right) + \left(k_2 \alpha + 3{k_2}^3\right)\right) t + \alpha_1 + \alpha_2. \tag{3.42}$$

This is the two-soliton solution to the studied model as shown in Figure 3.12 in three-dimension.

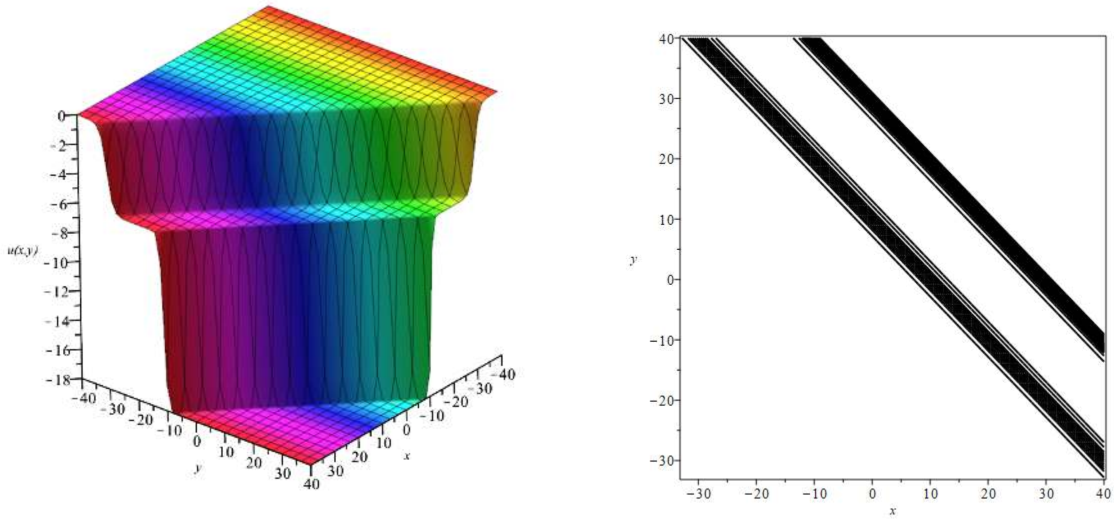

(a) Two-soliton wave **(b)** Contour plot of two-soliton wave

Figure 3.12. Double-soliton solution plotted when $t = 2, k_1 = 1, k_2 = 2, l_1 = 1, l_2 = 2, \alpha_1 = 0, \alpha_2 = 0, \alpha = 2$.

To investigate the 3-soliton solution of Eq. (3.29), we assume f as follows

$$f = 1 + e^{\psi_1} + e^{\psi_2} + e^{\psi_3} + A_{12}e^{\psi_1+\psi_2} + A_{13}e^{\psi_1+\psi_3} + A_{23}e^{\psi_2+\psi_3} + A_{123}e^{\psi_1+\psi_2+\psi_3}, \tag{3.43}$$

where

$$\psi_i = k_i x + l_i y - w_i t + \alpha_i, \qquad (i = 1, 2, 3) \tag{3.44}$$

and

$$A_{123} = A_{12}A_{13}A_{23}. \tag{3.45}$$

The values of A_{12}, A_{13}, A_{23} are defined in Eq. (3.38). Putting Eq. (3.43) with Eqs. (3.44) and (3.45) into Eq. (3.30). As a result, we obtain the three-soliton solution to the model (see Figure 3.13).

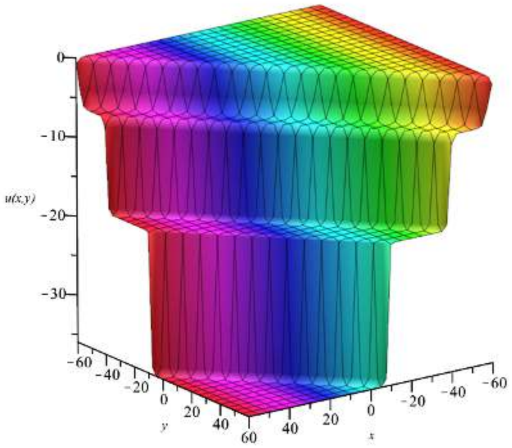

(a) Three-soliton wave

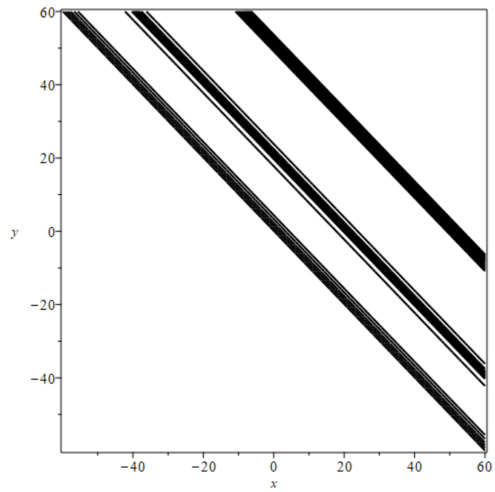

(b) Contour plot of three-soliton wave

Figure 3.13. Triple-soliton solution plotted when $t = 2, k_1 = 1, k_2 = 2, k_3 = 3, l_1 = 1, l_2 = 2, l_3 = 3, \alpha_1 = 0, \alpha_2 = 0, \alpha_3 = 0, \alpha = -2$.

3.2.2. Complex N-soliton solutions

To study the complex one-, two-, and three-soliton solutions to the model under consideration, we assume

$$f = \mathrm{i} + \mathrm{e}^{k_1 x + l_1 y - w_1 t + \alpha_1}, \quad \mathrm{i} = \sqrt{-1}, \tag{3.46}$$

where w_1 is defined in Eq. (3.44). Inserting Eq. (3.46) into Eq. (3.30), we get

$$u = -\frac{6k_1 \mathrm{e}^{k_1 x + l_1 y - \left(\alpha k_1 + 3{k_1}^3\right)t + \alpha_1}}{\mathrm{i} + \mathrm{e}^{k_1 x + l_1 y - \left(\alpha k_1 + 3{k_1}^3\right)t + \alpha_1}}. \tag{3.47}$$

This is the complex 1-soliton solution as presented in Figure 3.14.

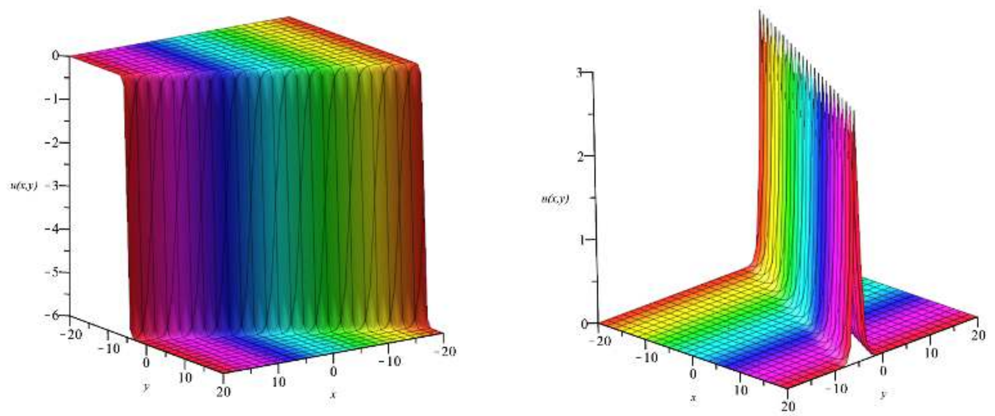

(a) Real wave solution of Eq. (3.47)

(b) Imaginary wave solution of Eq. (3.47)

Figure 3.14. 3D surfaces drawn by setting $t = 2, k_1 = 1, l_1 = 2, \alpha_1 = 0, \alpha = 2$.

To reveal a complex 2-soliton solution, the function f is given by

$$f = \mathrm{i} + \mathrm{e}^{k_1 x + l_1 y - w_1 t + \alpha_1} + \mathrm{e}^{k_2 x + l_2 y - w_1 t + \alpha_2} + A_{12} \mathrm{e}^{k_1 x + l_1 y - w_1 t + k_2 x + l_2 y - w_1 t + \alpha_2 + \alpha_1}, \tag{3.48}$$

where

$$A_{12} = -\frac{\mathrm{i}\,(k_1 - k_2)\,(l_1 - l_2)}{(k_1 + k_2)\,(l_1 + l_2)}.$$

The constants w_1, w_2 are defined in Eq. (3.44). Substituting Eq. (3.48) into Eq. (3.30), we get

$$u = -\frac{6\left(k_1 \mathrm{e}^{\gamma_1} + k_2 \mathrm{e}^{\gamma_2} - \frac{\mathrm{i}(k_1 - k_2)(l_1 - l_2)}{l_1 + l_2} \mathrm{e}^{\gamma_3}\right)}{\mathrm{i} + \mathrm{e}^{\gamma_1} + \mathrm{e}^{\gamma_2} - \frac{\mathrm{i}(k_1 - k_2)(l_1 - l_2)}{(k_1 + k_2)(l_1 + l_2)} \mathrm{e}^{\gamma_3}}. \tag{3.49}$$

The functions γ_1, γ_2, and γ_3 are given in Eqs. (3.40), (3.41) and (3.42), respectively. Eq. (3.49) is the complex two-soliton solution to the studied model as shown in Figure 3.15.

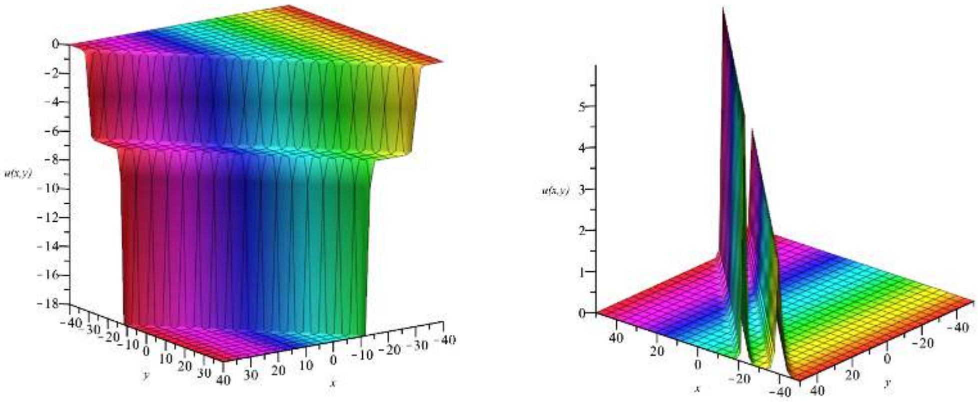

(a) Real wave solution of Eq. (3.49)

(b) Imaginary wave solution of Eq. (3.49)

Figure 3.15. 3D surfaces drawn by setting $t = 2, k_1 = 1, k_2 = 2, l_1 = 1, l_2 = 2, \alpha_1 = 0, \alpha_2 = 4, \alpha = 2$.

To construct the complex 3-soliton solution, we assume that the function f is equal to

$$f = \mathrm{i} + \mathrm{e}^{\psi_1} + \mathrm{e}^{\psi_2} + \mathrm{e}^{\psi_3} + A_{12}\mathrm{e}^{\psi_1+\psi_2} + A_{13}\mathrm{e}^{\psi_1+\psi_3} + A_{23}\mathrm{e}^{\psi_2+\psi_3} + B\mathrm{e}^{\psi_1+\psi_2+\psi_3}, \tag{3.50}$$

where

$$A_{ij} = -\frac{\mathrm{i}\,(k_i - k_j)\,(l_i - l_j)}{(k_i + k_j)\,(l_i + l_j)}, \qquad i < j, \tag{3.51}$$

and

$$B = -\,\mathrm{i}\frac{(k_1 - k_2)\,(k_1 - k_3)\,(k_2 - k_3)}{(k_1 + k_2)\,(k_1 + k_3)\,(k_2 + k_3)} \times \frac{(l_1 - l_2)\,(l_1 - l_3)\,(l_2 - l_3)}{(l_1 + l_2)\,(l_1 + l_3)\,(l_2 + l_3)}. \tag{3.52}$$

By putting Eq.(3.50) with Eqs. (3.51) and (3.52) into Eq. (3.50) as a result, we derive the complex three-soliton solution (see Figure 3.16).

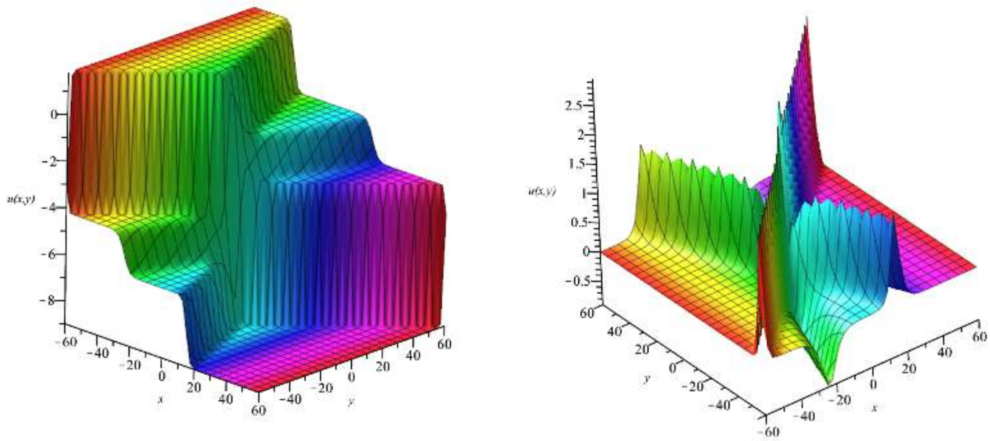

(a) Real wave solution of complex 3-soliton solution **(b)** Imaginary wave solution of complex 3-soliton solution

Figure 3.16. 3D surfaces of a complex three-soliton solution drawn by setting $t = 2, k_1 = 0.5, k_2 = -0.3, k_3 = 1, l_1 = 0.2, l_2 = 0.1, l_3 = -1, \alpha_1 = 4, \alpha_2 = -1, \alpha_3 = 2, \alpha = -2$.

3.2.3. The fusion soliton solutions

In this portion, we analyze the fusion solutions to the Eq. (3.29). In order to find the 1-fusion solution, we introduce the 2-soliton solution by setting the value of $A_{12} = 0$ in Eq. (3.38). For this purpose, we choose $k_1 = -1, k_2 = 2, l_1 = 1$, and $l_2 = 1$, we gain

$$u(x, y, t) = \frac{6e^{(3+\alpha)t-x+y+\alpha_1} - 12e^{2x+y-(24+2\alpha)t+\alpha_2}}{1 + e^{(3\alpha)t-x+y+\alpha_1} + e^{2x+y-(24+2\alpha)t+\alpha_2}}. \tag{3.53}$$

This is a 1-fusion soliton solution as shown in Figure 3.17.

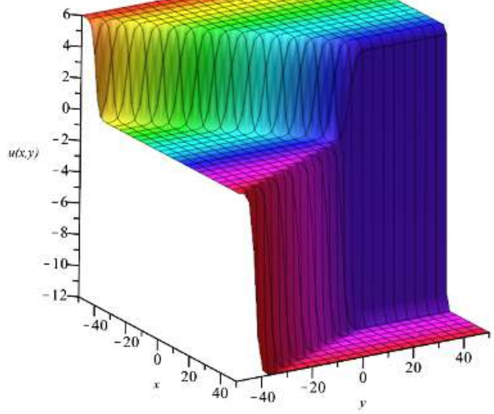

(a) Real wave solution of complex 3-soliton solution

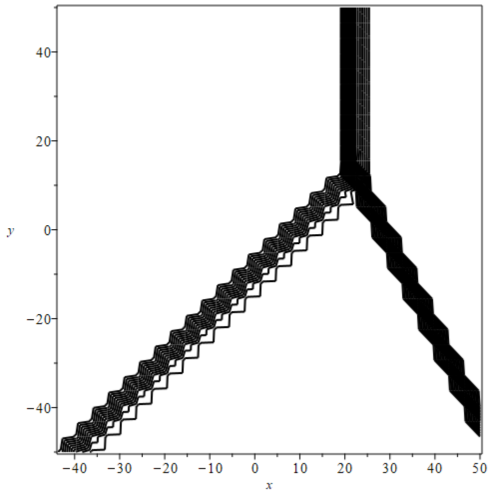

(b) Imaginary wave solution of complex 3-soliton solution

Figure 3.17. 3D plot of Eq. (3.53) plotted when $t = 2, \alpha_1 = -1, \alpha_2 = -1, \alpha = 2$.

When we set $k_1 = -1, k_2 = 2, k_3 = 3, l_1 = 1, l_2 = 1, l_3 = 1$ and plugging them into Eq. (3.43), we have

$$f = 1 + e^{(3+\alpha)t - x + y + \alpha_1} + e^{2x + y - 2(12+\alpha)t + \alpha_2} + e^{3x + y - 3(27+\alpha)t + \alpha_3}. \tag{3.54}$$

Putting Eq. (3.54) into Eq. (3.30), the outcome is

$$u(x,t) = \frac{6e^{\Omega_1} - 12e^{\Omega_2} - 18e^{\Omega_3}}{1 + e^{\Omega_1} + e^{\Omega_2} + e^{\Omega_3}}, \tag{3.55}$$

where

$$\begin{aligned} \Omega_1 &= (3+k)\,t - x + y + \alpha_1, \\ \Omega_2 &= 2x + y - (24 + 2k)\,t + \alpha_2, \\ \Omega_3 &= 3x + y - (81 + 3k)\,t + \alpha_3. \end{aligned} \tag{3.56}$$

This is 2-fusion solution of Eq. (3.29) as seen in Figure 3.18.

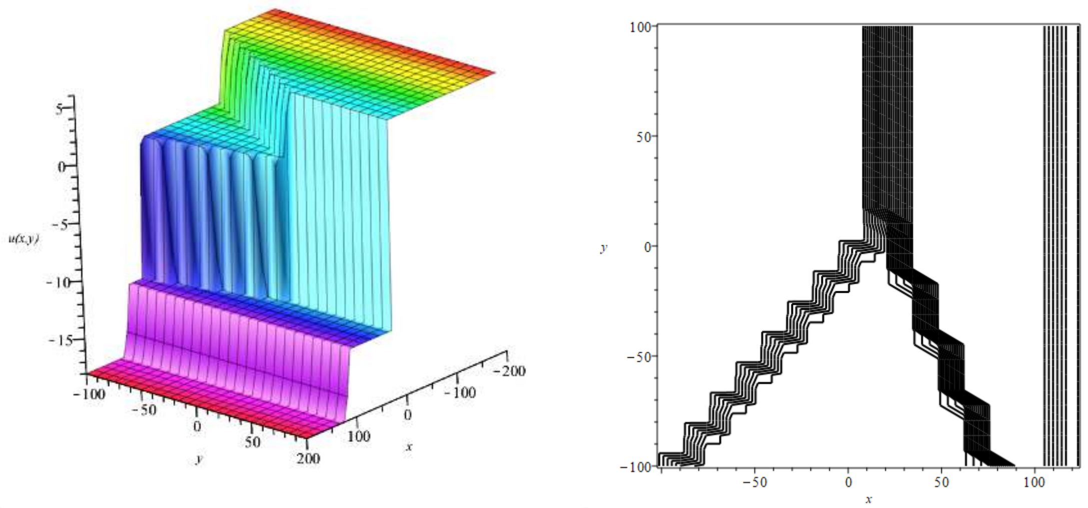

(a) Real wave solution of complex 3-soliton solution **(b)** Imaginary wave solution of complex 3-soliton solution

Figure 3.18. 3D plot of Eq. (3.55) plotted when $t = 2, \alpha_1 = 1, \alpha_2 = -1, \alpha_3 = -1, \alpha = 1$.

3.2.4. The breather solutions

In order to analyze and present the breather solution to the studied model, we define the following parameters:

$$k_1 = 1 - \mathrm{i}, k_2 = 1 + \mathrm{i}, l_1 = 1 + \mathrm{i}, l_2 = 1 - \mathrm{i}, \alpha_1 = 0, \alpha_2 = 0. \tag{3.57}$$

Plugging Eq. (3.57) into Eq. (3.48) and putting the outcome result into Eq. (3.30), we get

$$u(x, y) = \frac{(6 + 6\mathrm{i})\,\mathrm{e}^{x+y}\left((1 - \mathrm{i})\,\mathrm{e}^{(1+\mathrm{i})(x+y)} + \mathrm{i}\mathrm{e}^{(1+\mathrm{i})(6\mathrm{i}+\alpha)t} - \mathrm{e}^{(1-\mathrm{i})(\alpha-6\mathrm{i})t+2\mathrm{i}(x+y)}\right)}{\mathrm{e}^{2(\alpha-6)t+\mathrm{i}(x+y)} + \mathrm{e}^{(1+\mathrm{i})(6\mathrm{i}+\alpha)t+x+y} + \mathrm{e}^{(1-\mathrm{i})(\alpha-6\mathrm{i})t+(1+2\mathrm{i})(x+y)} - \mathrm{e}^{(2+\mathrm{i})(x+y)}}. \tag{3.58}$$

This equation present the breather solution to the studied model as shown in Figure 3.19.

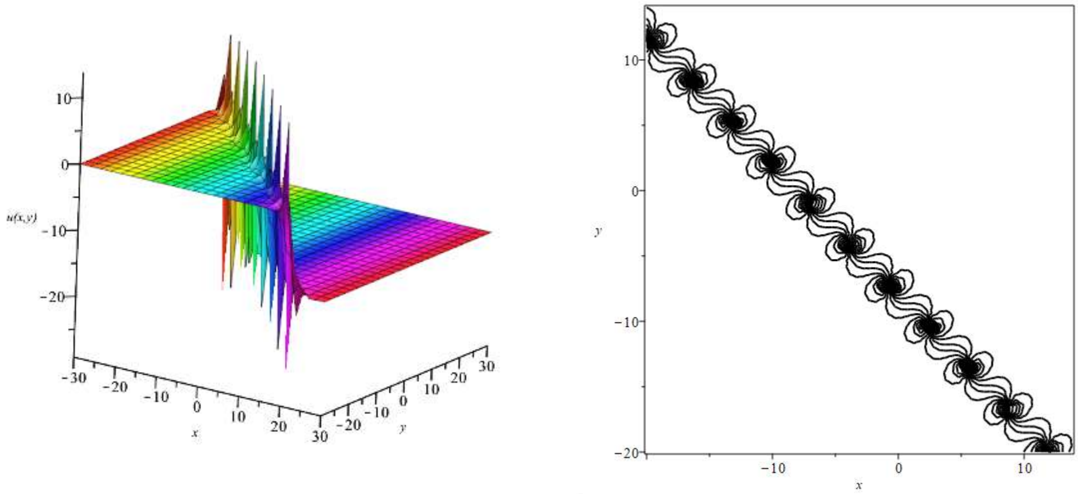

(a) Breather wave solution

(b) Contour plot of breather wave solution

Figure 3.19. 3D plot of Eq. (3.58) drawn by setting $t = 2, \alpha = 2$.

When $N = 3$ as shown in Eq. (3.50), and set the values of parameters as follows

$$k_1 = 1 + i, k_2 = \tfrac{1}{2}, k_3 = 1 - i, l_1 = 1 + 2i, l_2 = 1, l_3 = 1 - 2i, \alpha_1 = \alpha_2 = \alpha_3 = 0, \tag{3.59}$$

and plugging them into Eq. (3.30), the result yields

$$\begin{aligned} f =& 1 + \mathrm{e}^{\frac{x}{2}+y-\left(\frac{3}{8}+\frac{\alpha}{2}\right)t} + \mathrm{e}^{(1-\mathrm{i})x+(1-2\mathrm{i})y+((6+6\mathrm{i})-(1-\mathrm{i})\alpha)t} + \mathrm{e}^{(1+\mathrm{i})x+(1+2\mathrm{i})y+(-1-\mathrm{i})(6\mathrm{i}+\alpha)t} \\ &- 2\mathrm{e}^{2(x+y-(-6+\alpha)t)} + \left(\frac{3}{26} - \frac{11}{26}\mathrm{i}\right)\mathrm{e}^{\left(\frac{3}{2}-\mathrm{i}\right)x+(2-2\mathrm{i})y+\left(\left(\frac{45}{8}+6\mathrm{i}\right)-\left(\frac{3}{2}-\mathrm{i}\right)\alpha\right)t} + \\ &\left(\frac{3}{26} + \frac{11}{26}\mathrm{i}\right)\mathrm{e}^{\left(\frac{3}{2}+\mathrm{i}\right)x+(2+2\mathrm{i})y+\left(\left(\frac{45}{8}-6\mathrm{i}\right)-\left(\frac{3}{2}+\mathrm{i}\right)\alpha\right)t} - \frac{5}{13}\mathrm{e}^{\frac{5x}{2}+3y+\left(\frac{93}{8}-\frac{5}{2}\alpha\right)t}. \end{aligned} \tag{3.60}$$

Plugging Eq. (3.60) into Eq. (3.30), one may get

$$u = \frac{6\left(\frac{1}{2}\mathrm{e}^{\theta_1} + (1-\mathrm{i})\,\mathrm{e}^{\theta_2} + (1+\mathrm{i})\,\mathrm{e}^{\theta_3} - 4\mathrm{e}^{\theta_4} - \left(\frac{1}{4}+\frac{3}{4}\mathrm{i}\right)\mathrm{e}^{\theta_5} - \left(\frac{1}{4}-\frac{3}{4}\mathrm{i}\right)\mathrm{e}^{\theta_6} - \frac{25}{26}\mathrm{e}^{\theta_7}\right)}{1 + \mathrm{e}^{\theta_1} + \mathrm{e}^{\theta_2} + \mathrm{e}^{\theta_3} - 2\mathrm{e}^{\theta_4} + \left(\frac{3}{26}-\frac{11}{26}\mathrm{i}\right)\mathrm{e}^{\theta_5} + \left(\frac{3}{26}+\frac{11\mathrm{i}}{26}\right)\mathrm{e}^{\theta_6} - \frac{5}{13}\mathrm{e}^{\theta_7}}, \tag{3.61}$$

where

$$\begin{aligned}
\theta_1 &= \frac{x}{2} + y - \left(\frac{3}{8} + \frac{\alpha}{2}\right) t, \\
\theta_2 &= (1 - \mathrm{i})\, x + (1 - 2\mathrm{i})\, y + ((6 + 6\mathrm{i}) - (1 - \mathrm{i})\, \alpha)\, t, \\
\theta_3 &= (1 + \mathrm{i})\, x + (1 + 2\mathrm{i})\, y - (1 + \mathrm{i})\, (6\mathrm{i} + \alpha)\, t, \\
\theta_4 &= 2\, (x + y - (-6 + k)\, t)\,, \\
\theta_5 &= \left(\frac{3}{2} - \mathrm{i}\right) x + (2 - 2\mathrm{i})\, y + \left(\left(\frac{45}{8} + 6\mathrm{i}\right) - \left(\frac{3}{2} - \mathrm{i}\right) \alpha\right) t, \\
\theta_6 &= \left(\frac{3}{2} + \mathrm{i}\right) x + (2 + 2\mathrm{i})\, y + \left(\left(\frac{45}{8} - 6\mathrm{i}\right) - \left(\frac{3}{2} + \mathrm{i}\right) \alpha\right) t, \\
\theta_7 &= \frac{5x}{2} + 3y + \left(\frac{93}{8} - \frac{5\alpha}{2}\right) t.
\end{aligned}$$

Eq. (3.61) is an interaction wave solution between breather and one-soliton solutions as presented in Figure 3.20.

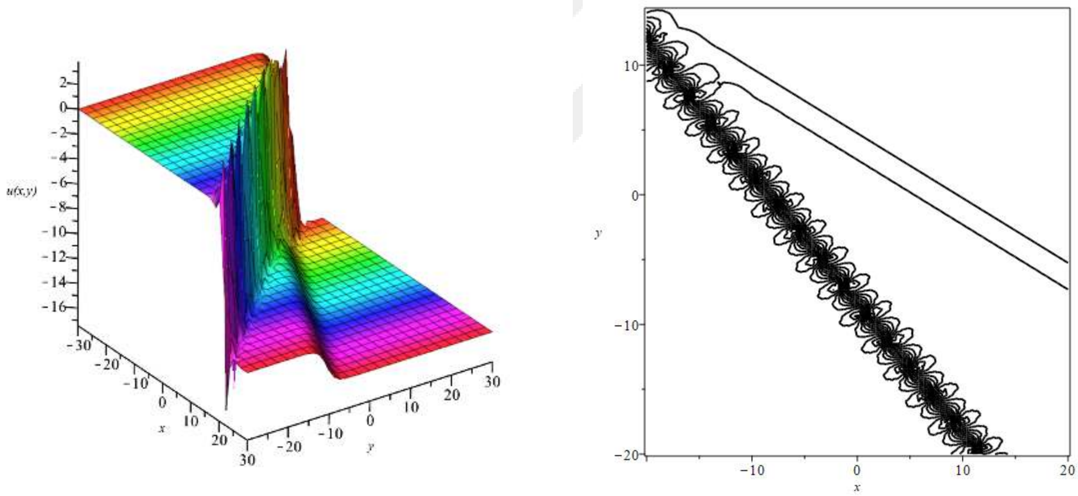

(a) Mixed one-breather-soliton

(b) Contour plot of mixed one-breather-soliton

Figure 3.20. 3D plot of Eq. (3.61) shows an interaction solution between a breather solution and a single-soliton solution drawn by taking $t = 2, \alpha = 2$.

3.2.5. Quadratic function solutions

The rogue wave begins to appear in several natural phenomena and science topics, for example, optical fiber [**58**], the financial market [**59**], internal ocean waves [**60**], and Bose-Einstein condensates [**61**]. In many literature lump solutions of partial differential equations have been addressed, such as lump solutions of partial differential equations have been addressed, such as Ma and Shou [**62**] studied a class of lump solutions of KP equation. Lump wave, mixed lump-stripe, hybrid and rogue wave-stripe solutions of nonlinear wave equation in a generalized (3 + 1)-dimensional in liquid with gas bubbles investigated by Wang et al. [**63**, **64**]. Zhao and He [**65**] constructed multiple lump solutions of the potential Yu-Toda-Sasa-Fukuyama equation. Fokas et al. [**66**] via the inverse spectral problem presented the exact solutions of the Davey-Stewartson II equation that depict the interaction of N-lumps with a line soliton. In this section of paper, we study the lump, mixed kink-lump, and periodic lump solutions to the (2 +1)-dimensional shallow water model.

3.2.6. Real and complex single-lump solutions

To find the single-lump solution, we define the solution of Eq. (3.29) as follows

$$f=(a_1x+a_2y+a_3t+a_4)^2+(b_1x+b_2y+b_3t+b_4)^2+b_5, \tag{3.62}$$

where a_1, a_2, a_3, a_4, b_1, b_2, b_3, b_4 and b_5 all are constants to be determined later. Substituting Eq. (3.62) into Eq. (3.30) as a result, we get a polynomial. Setting the coefficients of polynomial that have the same powers of the independent variables to zero, we gain the system of equations. Solving the obtained system, we can get the following results: **Case 1.** When

$$a_2=-\left(\frac{b_1b_2}{a_1}\right), a_3=-a_1\alpha, b_3=-b_1\alpha,$$

and inserting these values of constants into Eq. (3.62), then putting the outcome result into Eq. (3.30), we get

$$u=-\frac{6\left(2b_1\left(b_4-b_1\alpha t+b_1x+b_2y\right)+2a_1\left(a_4-a_1\alpha t+a_1x-\frac{b_1b_2}{a_1}y\right)\right)}{\left(b_5+\left(b_4-b_1\alpha t+b_1x+b_2y\right)^2+\left(a_4-a_1\alpha t+a_1x-\frac{b_1b_2}{a_1}y\right)^2\right)}. \tag{3.63}$$

Eq. (3.63) is the lump wave solution (see Figure 3.21) that reaches the peaks at the points

$$\left(-\frac{\left(\left({a_1}^2+{b_1}^2\right)\left(a_1a_4+b_1b_4\right)\pm\sqrt{\left({a_1}^2+{b_1}^2\right)^3b_5}\right)}{\left({a_1}^2+{b_1}^2\right)^2}+\alpha t, \frac{a_1\left(a_4b_1-a_1b_4\right)}{\left({a_1}^2+{b_1}^2\right)b_2}\right)$$

in the (x, y) plane. The amplitude of the lump wave solutions is $\pm\frac{6\left({a_1}^2+{b_1}^2\right)^2}{\sqrt{\left({a_1}^2+{b_1}^2\right)^3b_5}}$.

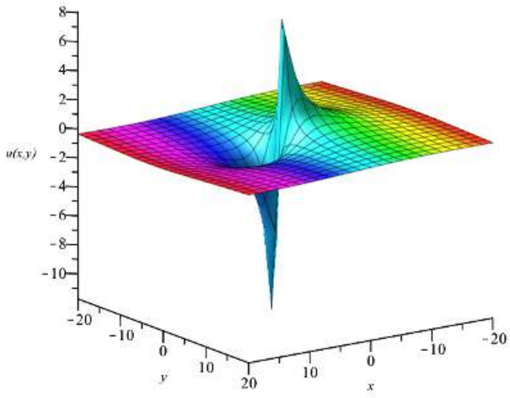

(a) Real solution of Eq. (45)

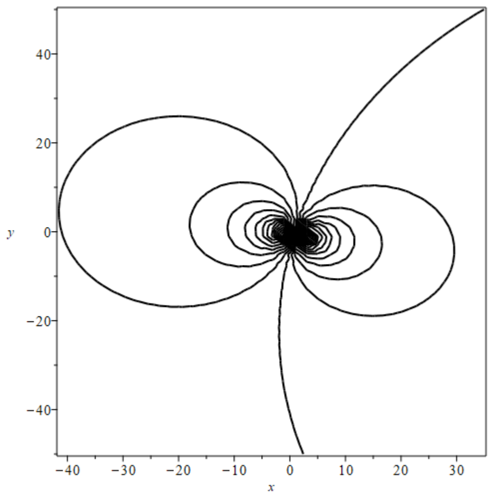

(b) Imaginary solution of Eq. (45)

Figure 3.21. Lump solution drawn by taking $b_1 = 0.5, b_4 = 2, \alpha = 1, b_2 = 2, a_1 = 2, a_4 = 2, b_5 = 1, t = 2.$

Case 2. When

$$a_1 = \mathrm{i}b_1, b_3 = \mathrm{i}a_3 - 2b_1\alpha, b_5 = 0,$$

and putting these values of constants into Eq. (3.62), then substituting the outcome result into Eq. (3.30), we get

$$u(x,y,t) = -\frac{6\begin{pmatrix} 2\mathrm{i}b_1(a_4 + a_3t + \mathrm{i}b_1x + a_2y) + \\ 2b_1(b_4 + (\mathrm{i}a_3 - 2b_1\alpha)t + b_1x + b_2y) \end{pmatrix}}{\begin{pmatrix} (a_4 + a_3t + \mathrm{i}b_1x + a_2y)^2 + \\ (b_4 + (\mathrm{i}a_3 - 2b_1\alpha)t + b_1x + b_2y)^2 \end{pmatrix}}. \tag{3.64}$$

The above equation is the complex 1-lump wave solution as shown in Figure 3.22.

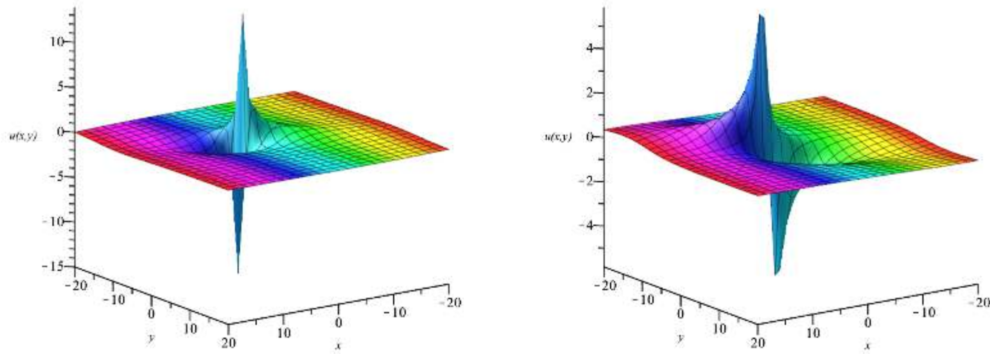

(a) Real solution of Eq. (45)

(b) Imaginary solution of Eq. (45)

Figure 3.22. One-lump solution drawn under Eq. (3.64) by taking $t = 2, a_1 = 1, a_3 = 3, a_4 = 5, b_1 = 1, b_2 = 2, b_4 = 2, \alpha = 0.3$.

Case 3. When

$$b_5 = \frac{9\left(a_1{}^3 a_3 + a_1 a_3 b_1{}^2 + a_1{}^4\alpha + a_1{}^2 b_1{}^2\alpha + \mathrm{i}a_1{}^2 b_1\sqrt{\beta} + \mathrm{i}b_1{}^3\sqrt{\beta}\right)}{\beta}, a_2 = -\frac{\mathrm{i}b_2\sqrt{\beta}}{a_3 + a_1\alpha},$$
$$b_3 = -b_1\alpha - \mathrm{i}\sqrt{\beta},$$

and using these values of constants into Eq. (3.62), then putting the outcome result into Eq. (3.30), we get

$$u = -\frac{6\left(2b_1\left(b_4 - \left(b_1\alpha + \mathrm{i}\sqrt{\beta}\right)t + b_1x + b_2y\right) + 2a_1\left(a_4 + a_3t + a_1x - \frac{\mathrm{i}b_2\sqrt{\beta}y}{a_3 + a_1\alpha}\right)\right)}{\left(b_4 + \left(-b_1\alpha - \mathrm{i}\sqrt{\beta}\right)t + b_1x + b_2y\right)^2 + \left(a_4 + a_3t + a_1x + \frac{\mathrm{i}b_2\sqrt{\beta}y}{-a_3 - a_1\alpha}\right)^2 + b_5}, \tag{3.65}$$

providing that $\beta = a_3{}^2 + 2a_1a_3\alpha + a_1{}^2\alpha^2 > 0$. Eq. (3.65) describes the complex 1-lump wave solution as presented in Figure 3.23.

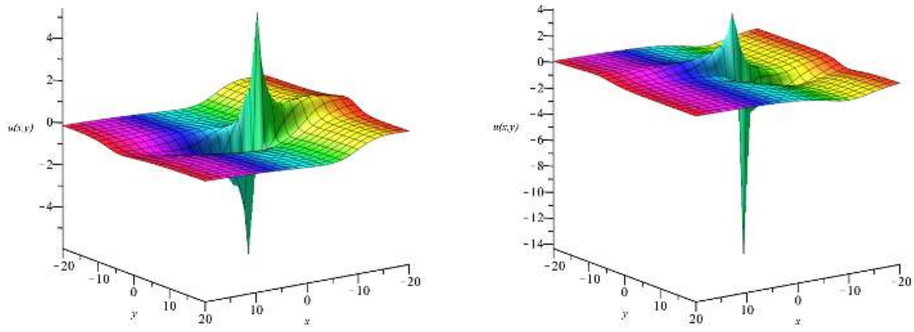

(a) Real solution of Eq. (47) **(b)** Imaginary solution of Eq. (47)

Figure 3.23. One-lump solution drawn by setting $t = 2, a_1 = 1, a_3 = 3, a_4 = 4, b_1 = 1, b_2 = 2, b_4 = 4, b_5 = 5, \alpha = 0.3$.

3.2.7. Interaction between one-lump wave and solitary wave

In this subsection, we derive the collision between the 1-lump wave and kink soliton solution. We assume that the solution of Eq. (3.29) according to Eq. (3.30) has the form

$$f = (a_1x + a_2y + a_3t + a_4)^2 + b_5 + (b_1x + b_2y + b_3t + b_4)^2 + he^{c_1x+c_2y+c_3t}, \tag{3.66}$$

where a_i, b_i, c_i are constants. Inserting Eq. (3.66) into Eq. (3.31), then putting the result into Eq. (3.30), we obtain a polynomial. Taking coefficient of the polynomial, which have the same power of the independent variable to zero, we get the system of equations. Solving the gained system, we have

$$a_4 = b_4 = b_5 = c_2 = 0, a_1 = -\tfrac{b_1b_2}{a_2}, a_3 = \tfrac{b_1b_2\alpha}{a_2}, b_3 = -b_1\alpha, c_3 = -3{c_1}^3 - c_1\alpha. \tag{3.67}$$

Putting Eq. (3.67) into Eq. (3.66), then substituting the outcome result into Eq. (3.30), we acquire

$$u = \frac{6\left(\frac{2b_1b_2}{a_2}\left(\frac{b_1b_2}{a_2}(\alpha t - x) + a_2y\right) - hc_1e^{c_1x-\left(3{c_1}^3+c_1\alpha\right)t} - 2b_1\left(b_1(x-\alpha t) + b_2y\right)\right)}{he^{c_1x-\left(3{c_1}^3+c_1k\right)t} + \left(b_1(x-\alpha)t + b_2y\right)^2 + \left(\frac{b_1b_2}{a_2}(\alpha t - x) + a_2y\right)^2}. \tag{3.68}$$

Eq. (3.68) represents the mixed lump-kink solution of the giving model as shown in Figure 3.24.

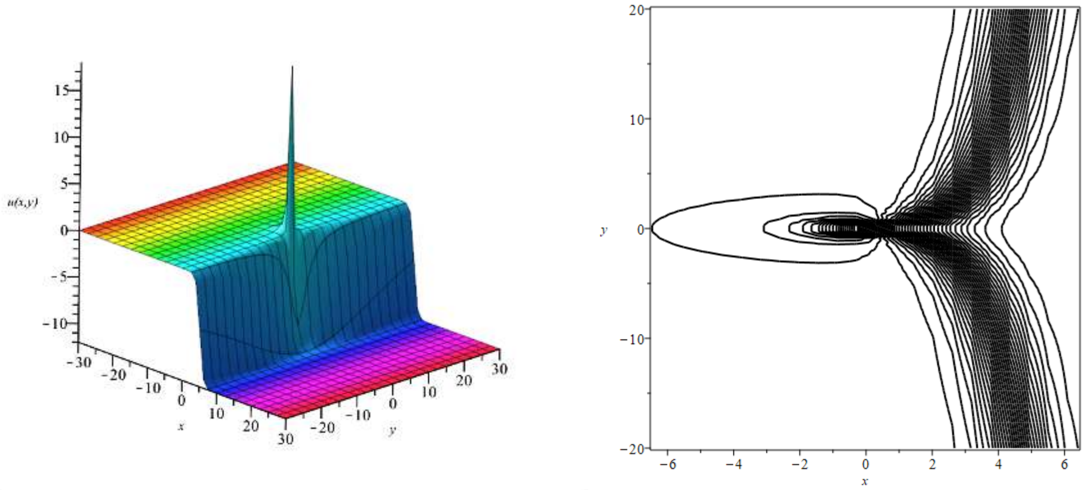

(a) Mixed 1-M-lump-soliton solution

(b) Contour plot of mixed 1-M-lump-soliton solution

Figure 3.24. Interaction solution between 1-lump wave and kink solution drawn when $b_1 = 0.5, \alpha = 1, b_2 = 2, a_1 = 2, a_2 = 1, c_1 = 2, h = 0.2, t = 2$

3.2.8. Periodic lump wave solution

In this subsection, we try to explore the periodic lump solution to the suggested model. For that purpose, we assume

$$f = (a_1x + a_2y + a_3t + a_4)^2 + (b_1x + b_2y + b_3t + b_4)^2 + \varepsilon_1 \sin(c_1x + c_2y + c_3t + c_4) + \varepsilon_2. \tag{3.69}$$

Plugging the trial assumption value of f into Eq. (3.31) and then into Eq. (3.30), we can evaluate the unknown values of parameters $a_i, b_i, c_i, \varepsilon_j; (i = 1,2,3,4; j = 1,2)$ as follows

$$a_1 = -\frac{b_1b_2}{a_2}, a_3 = \frac{b_1b_2\alpha}{a_2}, b_3 = -b_1\alpha, c_2 = 0, c_3 = 3{c_1}^3 - c_1\alpha, c_4 = 0. \tag{3.70}$$

Now, substituting Eq. (3.70) into Eq. (3.69), and putting the outcome result into Eq. (3.30), we get

$$u = \frac{6\left(\frac{2b_1a_4}{a_2}b_2 - \frac{2{b_1}^2{b_2}^2}{{a_2}^2}(x-\alpha t) - 2b_1(b_4 + b_1(x-\alpha t)) - c_1h\cos(\theta_1)\right)}{(b_4 + b_1(x-\alpha t) + b_2y)^2 + h\sin(\theta) + \left(a_4 + \frac{b_1b_2(\alpha t - x) + {a_2}^2y}{a_2}\right)^2 + \varepsilon_2}, \tag{3.71}$$

where $\theta = c_1\left(x + (3{c_1}^2 - \alpha)t\right)$. This equation describes the periodic lump solution to the suggested model as shown in Figure 3.25.

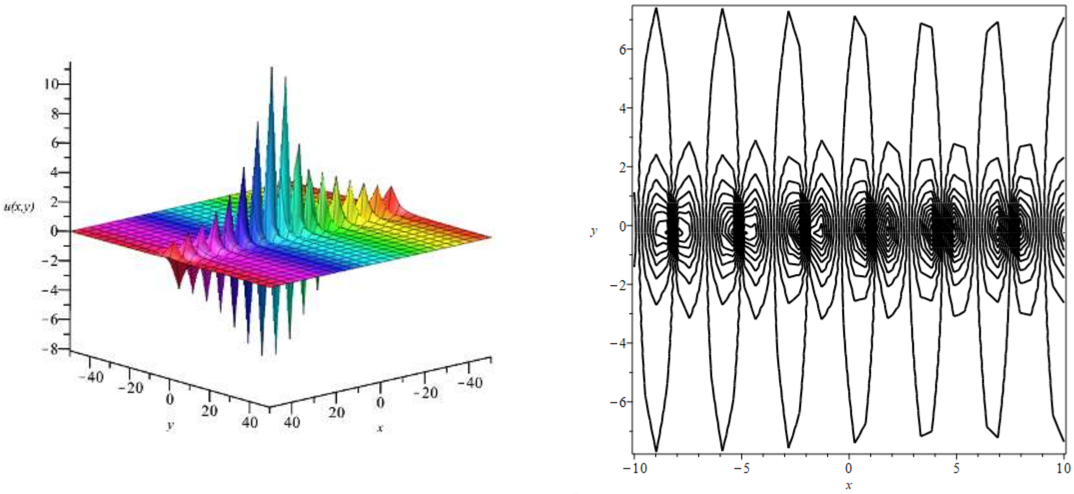

(a) Periodic wave solution

(b) Contour plot for periodic wave solution

Figure 3.25. Periodic wave solution plotted with using $b_1 = 1/10, b_4 = 1/3, \alpha = 2, b_2 = 1/5, a_2 = 2, a_4 = 1/4, t = 2, c_1 = 2, \varepsilon_1 = 4, \varepsilon_2 = 5$.

3.3. The Bogoyavlenskii's generalized breaking soliton equation

Consider the Bogoyavlenskii–Schieff equation [**67**]

$$u_{xt} + u_x u_{xy} + \frac{1}{2} u_{xx} u_y + \frac{1}{4} u_{xxxy} = 0,$$

and the Bogoyavlenskii's generalized breaking soliton equation [**68**] as follows

$$u_{xt} + u_x u_{xy} + \frac{1}{2} u_{xx} u_y + \frac{1}{4} u_{xxxy} = -\alpha^2 \partial_x^{-1} u_{yyy}.$$

The extension of the Bogoyavlenskii's generalized breaking soliton equation introduced by Wazwaz [**69**] by adding $\beta^2 u_{xxx}$ reads

$$u_{xt} + u_x u_{xy} + \frac{1}{2} u_{xx} u_y + \frac{1}{4} u_{xxxy} = -\partial_x^{-1} \left(\alpha^2 u_{yyy} + \beta^2 u_{xxx} \right). \tag{3.72}$$

Several studies have been reported to investigate the Bogoyavlenskii-Schieff equation (BSE). Song-Ju et al. [**50**] explored N-soliton solutions to the BSE equation by disclosing its Lax pair. Wazwaz [**51**] introduced two extensions of the suggested equation and proved that the extension terms do not kill the integration of the standard Bogoyavlenskii–Schieff equation. The Riccati equation expansion method has been used to construct some new solutions to the BSE [**52**]. Ray and Vinita [**53**] have been implemented the Lie group method on BSE to analyze a similarity reduction of the suggested equation. Our purpose for this section of chapter is to explore or study the N-soliton, fusion, rational, and breather solutions for the extension of the Bogoyavlenskii's generalized breaking soliton equation.

3.3.1. N-soliton solutions

In this subsection, we study the N-soliton and fusion solutions to the extension of (2+1)-dimensional Bogoyavlenskii's generalized breaking soliton equation. To start this study, we define a variable transformation for equation that reads

$$u = 2(\log(f(x,y,t)))_x. \tag{3.73}$$

Using Eq. (3.73) and substituting it into Eq. (3.72) gives

$$\begin{aligned}
&8\alpha^2 {f_y}^3 + 4f_x\left(-f_{xy}f_{xx} + f_x\left(2f_t + 2\beta^2 f_x + f_{xxy}\right)\right) - \\
&2f\left(f_{xx}\left(2f_t - f_{xxy}\right) + 2f_x\left(2f_{xt} + 3\beta^2 f_{xx} + f_{xxxy}\right)\right) - \\
&f_y\left(2\left({f_{xx}}^2 - 2f_x f_{xxx}\right) + f\left(12\alpha^2 f_{yy} + f_{xxxx}\right)\right) + \\
&f^2\left(4\left(\alpha^2 f_{yyy} + f_{xxt} + \beta^2 f_{xxx}\right) + f_{xxxxy}\right) = 0,
\end{aligned} \tag{3.74}$$

where $f = f(x,y,t)$. To study the one-soliton solution, we assume that

$$f = 1 + e^{k_1(x + l_1 y + w_1 t)}, \tag{3.75}$$

and $w_1 = -\left(\frac{1}{4}{k_1}^2 l_1 + {l_1}^3\alpha^2 + \beta^2\right)$. Inserting Eq. (3.75) into Eq. (3.73), we get a kink-soliton solution as presented in Figure 3.26 and reads as follows

$$u = \frac{2k_1 \mathrm{e}^{k_1(x+l_1 y)}}{\mathrm{e}^{k_1(x+l_1 y)} + \mathrm{e}^{\frac{1}{4}{k_1}^3 l_1 t + k_1\left({l_1}^3\alpha^2 + \beta^2\right)t}}. \tag{3.76}$$

When $N = 2, 3$, a function f have the following forms, respectively.

$$f = 1 + e^{\psi_1} + e^{\psi_2} + A_{12}e^{\psi_1+\psi_2}, \tag{3.77}$$

$$f = 1 + e^{\psi_1} + e^{\psi_2} + e^{\psi_3} + A_{12}e^{\psi_1+\psi_2} + A_{13}e^{\psi_1+\psi_3} + A_{23}e^{\psi_2+\psi_3} + A_{123}e^{\psi_1+\psi_2+\psi_3}, \tag{3.78}$$

where

$$\psi_i = k_i\left(x + l_i y + w_i t\right) + \alpha_i, \qquad i = 1, 2, ..., N, \tag{3.79}$$

$$A_{ij} = \frac{{k_i}^2 - 2k_i k_j + {k_j}^2 - 4(l_i - l_j)^2\alpha^2}{{k_i}^2 + 2k_i k_j + {k_j}^2 - 4(l_i - l_j)^2\alpha^2}, \qquad 1 \le i < j \le N, \tag{3.80}$$

and

$$A_{123} = A_{12}A_{13}A_{23}. \tag{3.81}$$

Plugging Eq. (3.77) and (3.78) into Eq. (3.73), we gain the double-soliton and triple-soliton solutions as shown in Fig (3.26 (b,c)), respectively.

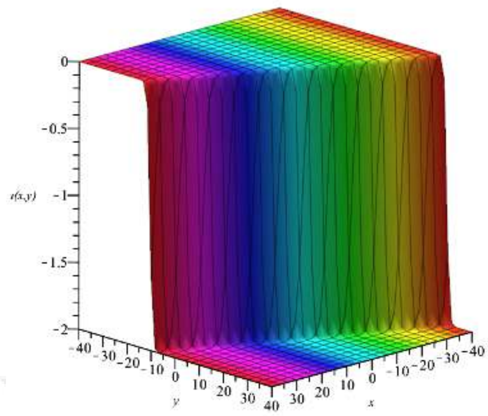

(a) 1-soliton solution

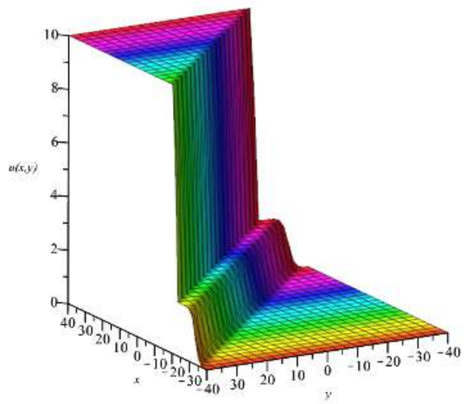

(b) 2-soliton solution

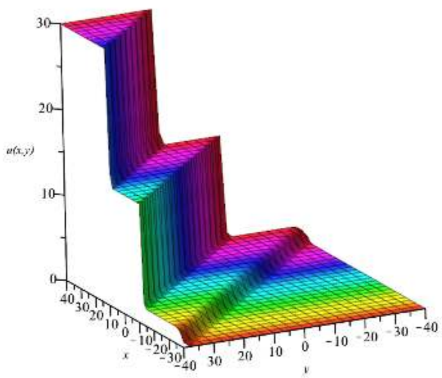

(c) 3-soliton solution

Figure 3.26. 3D figure plotted when (a) $t = 2, k_1 = 1, l_1 = 2, \alpha_1 = 0, \alpha = -1, \beta = 1$ (b) $t = 3, k_1 = 1, k_2 = 4, l_1 = 1, l_2 = 1, \alpha = 1, \beta = 1, \alpha_1 = 0, \alpha_2 = 0$ (c) $t = 3, k_1 = 1, k_2 = 6, k_3 = 8, l_1 = 1, l_2 = 1, l_3 = 1, \alpha_1 = 0, \alpha_2 = 0, \alpha_3 = 0, \alpha = 0.1, \beta = 0.1$.

3.3.2. Fusion Solutions

To study the fusion solution of Eq. (3.72), we let

$$\alpha = \frac{1}{2}, k_1 = -1, k_2 = 2, l_1 = 1, l_2 = 4. \tag{3.82}$$

By using these values in Eq. (3.77) and then into Eq. (3.73), we have

$$u=\frac{4\mathrm{e}^{2\left(x+4y-\left(20+\beta^2\right)t\right)+\alpha 2}-2\mathrm{e}^{-\left(x+y-\frac{1}{4}\left(2+4\beta^2\right)t\right)+\alpha_1}}{1+\left(\mathrm{e}^{-\left(x+y-\frac{1}{4}\left(2+4\beta^2\right)t\right)+\alpha_1}+\mathrm{e}^{2\left(x+4y-\left(20+\beta^2\right)t\right)+\alpha 2}\right)}. \tag{3.83}$$

When we choose $k_1=-1, k_2=2, k_3=3, \alpha=\frac{1}{2}, l_1=1, l_2=4, l_3=5$ and plugging them into Eq. (3.78) then into Eq. (3.73), we can obtain

$$u=\frac{2\left(3\mathrm{e}^{3\left(x+5y-\frac{1}{4}\left(170+4\beta^2\right)t\right)+\alpha_3}+2\mathrm{e}^{2\left(x+4y-\frac{1}{4}\left(80+4\beta^2\right)t\right)+\alpha_2}-\mathrm{e}^{-(x+y)+\frac{1}{4}\left(2+4\beta^2\right)t+\alpha_1}\right)}{1+\left(\mathrm{e}^{-(x+y)+\frac{1}{4}\left(2+4\beta^2\right)t+\alpha_1}+\mathrm{e}^{2\left(x+4y-\frac{1}{4}\left(80+4\beta^2\right)t\right)+\alpha_2}+\mathrm{e}^{3\left(x+5y-\frac{1}{4}\left(170+4\beta^2\right)t\right)+\alpha_3}\right)}. \tag{3.84}$$

Eqs. (3.83) and (3.84) describe the one-fusion and two-fusion solutions of the studied equation as plotted in Figure 3.27.

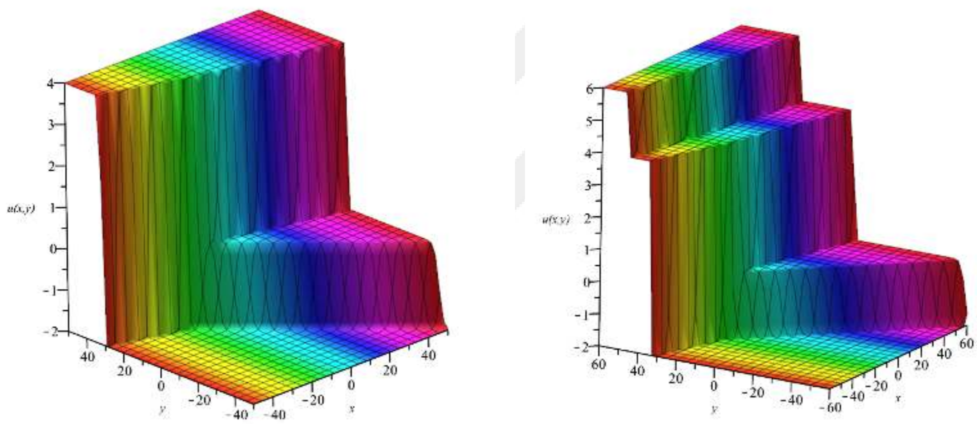

(a) 1-fusion solution

(b) 2-fusion solution

Figure 3.27. 3D figure plotted when (a) $t=3, \beta=1, \alpha_1=0, \alpha_2=0$ (b) $t=3, \alpha_1=\alpha_2=\alpha 3=0, \beta=0.1$.

3.3.3. M-Lump solutions

For investigating 1-M-Lump solution of the Bogoyavlenskii's generalized breaking soliton equation, we let $N=2$ in Eq. (2.1) and apply a long-wave method by taking $k_i\to 0, \alpha_i=-1\ \ (i=1,2)$ with $\frac{k_1}{k_2}=O(1)$, then

$$f_2=\phi_1\phi_2+B_{12}, \tag{3.85}$$

where $B_{12} = \frac{1}{\alpha^2(l_1-l_2)^2}$. Substituting Eq. (3.85) into Eq. (3.73), a 1- M-lump solution (see Figure 3.28) is derived as

$$\begin{aligned} u &= 2\frac{\partial}{\partial x}\log\left(\left(x' + a_1 y'\right)^2 + {b_1}^2 y'^2 - \frac{1}{4{b_1}^2\alpha^2}\right) \\ &= \frac{4\left(x' + a_1 y'\right)}{{b_1}^2 y'^2 + \left(x' + a y'\right)^2 - \frac{1}{4{b_1}^2\alpha^2}}, \end{aligned} \tag{3.86}$$

where

$$\begin{aligned} y' &= y + \alpha^2\left({b_1}^2 - 3{a_1}^2\right)t, \\ x' &= x - \left(\beta^2 - a_1\alpha^2\left(2{b_1}^2 + 2{a_1}^2\right)\right)t. \end{aligned}$$

The rational solution (3.86) is a permanent lump solution that decays as $O\left(\frac{1}{x^2}, \frac{1}{y^2}\right)$ for $|x|, |y| \to \infty$ and move with the speed

$$v_x = \left(\beta^2 - a_1\alpha^2\left(2{b_1}^2 + 2{a_1}^2\right)\right), v_y = \alpha^2\left(3{a_1}^2 - {b_1}^2\right). \tag{3.87}$$

When $N = 4$ in Eq. (2.1) and taking $k_i \to 0, \alpha_i = -1$ $(i = 1, 2, 3, 4)$, then f_4 takes the form below

$$\begin{aligned} f_4 &= \phi_1\phi_2\phi_3\phi_4 + b_{12}\phi_3\phi_4 + b_{13}\phi_2\phi_4 + B_{14}\phi_2\phi_3 + b_{23}\phi_1\phi_4 \\ &\quad + B_{24}\phi_1\phi_3 + B_{34}\phi_1\phi_2 + B_{12}\phi_{34} + B_{13}B_{24} + B_{14}B_{23}, \end{aligned} \tag{3.88}$$

where

$$\begin{aligned} &\phi_i = x + l_i y + \rho_i t, \\ &\rho_i = -\left({l_i}^3\alpha^2 + \beta^2\right), \\ &B_{ij} = \frac{1}{\alpha^2(l_i - l_n)^2}, (i < j), \\ &l_{\frac{N}{2}+i} = l_i^*, \quad \left(i = 1, 2, .., \frac{N}{2}\right). \end{aligned}$$

After inserting Eq. (3.88) into Eq. (3.73) the findings provide us a two-M-lump solution as shown in Figure 3.29.

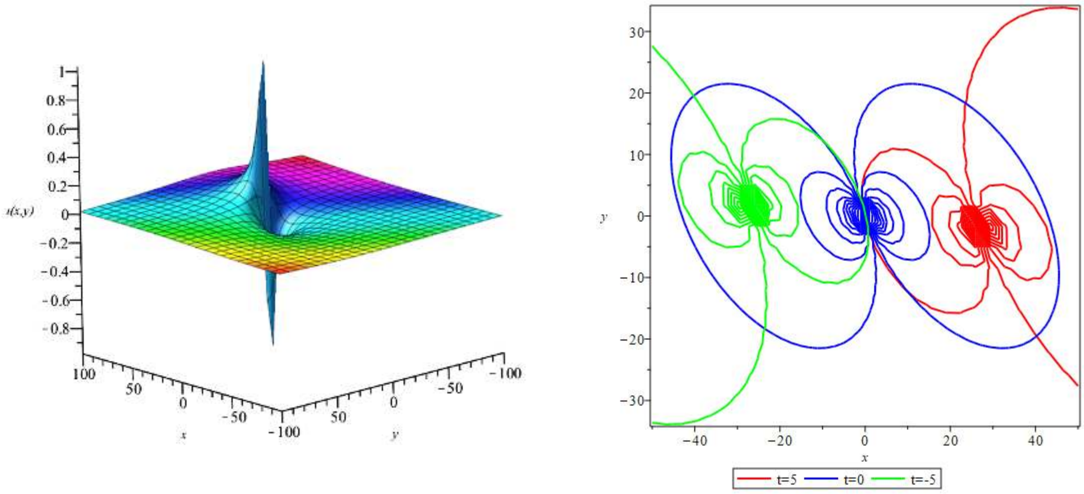

(a) t=10

(b) 1-M-lump in different period of time

Figure 3.28. 3D figure plotted when $k_1 = 1, k_2 = 2, a_1 = 1/2, b_1 = 1, \alpha = 1, \beta = 2$ over different periods of time.

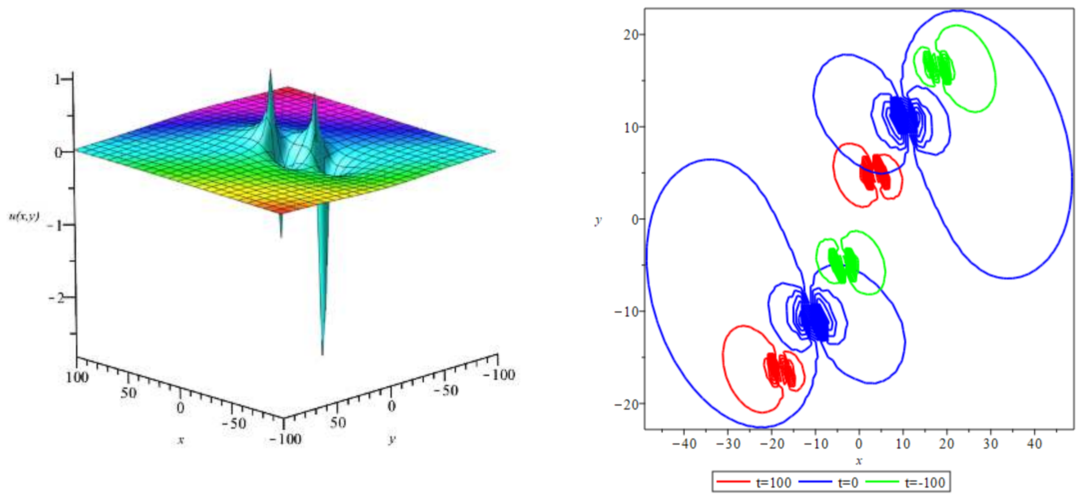

(a) t=100

(b) 2-M-lump in different period of time

Figure 3.29. 3D figure plotted when $a_1 = 1/2, b_1 = 3/2, a_2 = 1/3, b_2 = 4/3, \alpha = 1/5, \beta = 1/20$ over different periods of time.

3.3.4. Interaction between M-Lump and multiple soliton

In this subsection, we try to find the interaction of M-lump solution with soliton solutions of the suggested equation. Assume that $N = 3$ in Eq. (2.1), and using $k_i \to 0, \alpha_i = -1 \ (i = 1, 2)$ with $\frac{k_1}{k_2} = O(1)$, then f_3 can be rewritten as

$$f_3 = \phi_1\phi_2 + B_{12} + (\phi_1\phi_2 + B_{12} + C_{23}\phi_1 + C_{13}\phi_2 + C_{13}C_{23})e^{\psi_3}, \tag{3.89}$$

where the constants $C_{m3}\,(m = 1, 2)$ are defined as

$$C_{m3} = -\frac{4k_3}{{k_3}^2 - 4{l_m}^2\alpha^2 + 8l_ml_3\alpha^2 - 4{l_3}^2\alpha^2}, \qquad m = 1, 2. \tag{3.90}$$

Plugging Eq. (3.89) together with Eq. (3.90) into Eq. (3.73), as a result, we obtain an interaction between M-lump solution with a 1-soliton solution as shown in Figure 3.30. Let, $N = 4$ in Eq. (2.1), and taking $k_i \to 0, \alpha_i = -1 \ (i = 1, 2)$, $\frac{k_1}{k_2} = O(1)$ then

$$\begin{aligned} f_4 =& \phi_1\phi_2 + B_{12} + \Psi_1 e^{\varphi_3} + \Psi_2 e^{\varphi_4} + \\ & A_{34}e^{\varphi_3+\varphi_4}\left(\Psi_1 + \Psi_2 - \phi_1\phi_2 - B_{12} + c_{13}C_{24} + C_{14}C_{23}\right), \end{aligned} \tag{3.91}$$

where

$$\Psi_1 = \phi_1\phi_2 + B_{12} + C_{23}\phi_1 + C_{13}\phi_2 + C_{13}C_{23}.$$

and

$$\Psi_2 = \phi_1\phi_2 + B_{12} + C_{24}\phi_1 + C_{14}\phi_2 + C_{14}C_{24}.$$

The constants $C_{m4}\,(m = 1, 2)$ are defined as

$$C_{m4} = -\frac{4k_4}{{k_4}^2 - 4{l_m}^2\alpha^2 + 8l_ml_4\alpha^2 - 4{l_4}^2\alpha^2}, \qquad m = 1, 2, 3. \tag{3.92}$$

Inserting Eq. (3.91) together with using Eq. (3.92) into Eq. (3.73), the outcomes solution is an interaction between M-lump and 2-soliton solution as seen in Figure 3.31. Moreover, we can investigate the interaction between M-lump solution with fusion solution by making the term A_{34} in Eq. (3.91) to be zero, then f_4 will rewrite as

$$f_4 = \phi_1\phi_2 + B_{12} + \Psi_1 e^{\psi_3} + \Psi_2 e^{\psi_4}. \tag{3.93}$$

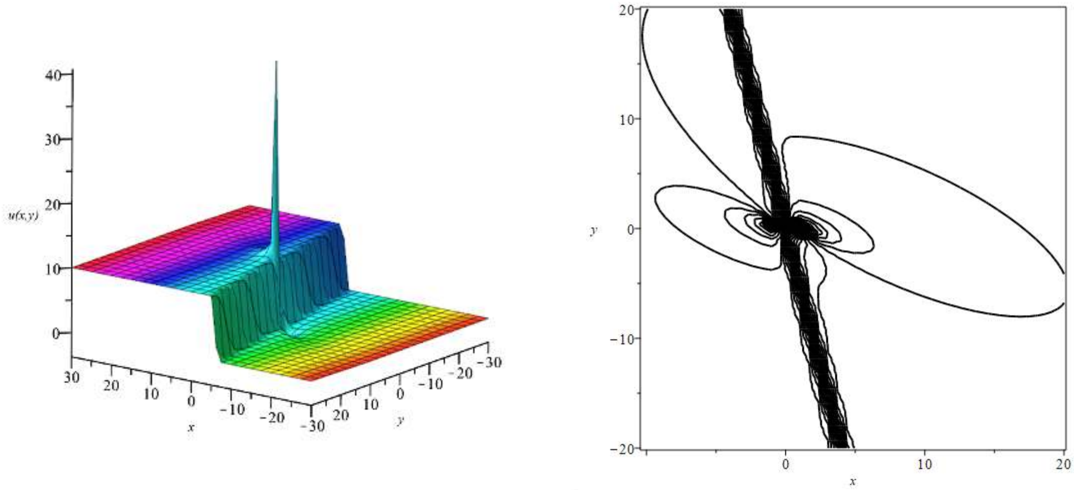

(a) Mixed one-soliton-M-lump wave

(b) Contour plot of mixed one-soliton-M-lump wave

Figure 3.30. 3D figure plotted when $k_3 = 5, a_1 = 1, b_1 = 1, l_3 = 0.2, \alpha = 1, \beta = 0.1, \alpha_1 = 0, \alpha_2 = 0$ and $t = 5$.

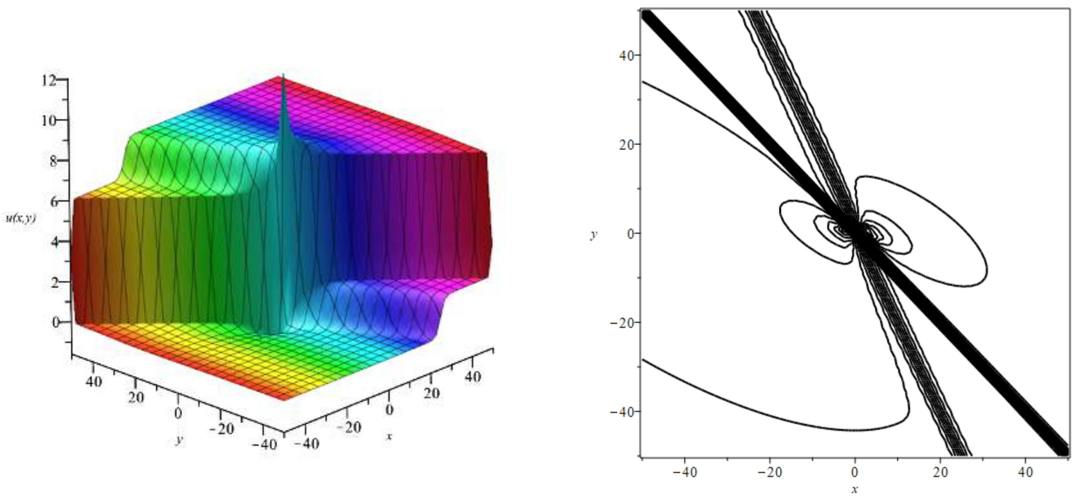

(a) Mixed two-soliton-one-M-lump wave

(b) Contour plot of mixed two-soliton-one-M-lump wave

Figure 3.31. 3D figure plotted when $a_1 = 1, b_1 = 1, l_3 = 1/2, k_3 = 1, l_4 = 1, k_4 = 3, \alpha = 1, \beta = 1$ and $t = 5$.

3.4. The (2+1)-dimensional Date-Jimbo-Kashiwara-Miwa equation

The KP equation was first introduced by Kadomtsev and Petviashvili [**70**] and read as

$$\frac{\partial}{\partial x}\left(u_t + uu_x + u_{xxx}\right) + 3u_{yy} = 0. \tag{3.94}$$

Basic soliton equations, for example, the Kadomtsev-Petviashvili (KP) equation and its Bäcklund transformation formula may well be considered as “atoms” for the construction of different types of soliton equations. Both the unknown equations KP and modified KP hierarchy are fundamental significance not just in the theory of integrable systems, but also play a key role in mathematical physics, too. To investigate that all the KP hierarchy equations are integrable, Dorizzi et al. [**71**] have shown that the higher equations in the KP hierarch, i.e. (3 + 1)-dimensional Jimbo-Miwa equation, can not be integrated without conditional sense. The Date–Jimbo–Kashiwara–Miwa (DJKM) equation is one of the KP hierarch equations that pass integrability. The (2 + 1) dimensional Date-Jimbo-Kashiwara-Miwa (DJKM) equation [**72**] has been written as an integral extension of the KP hierarchy and read

$$u_{xxxxy} + 4u_{xxy}u_x + 2u_{xxx}u_y + 6u_{xy}u_{xx} - \alpha u_{yyy} - 2\beta u_{xxt} = 0. \tag{3.95}$$

A lot of studies have been presented to seek the solutions of Eq. (2). Wang and Hu [**73**] derived the Grammian solutions of the Eq. (2). Guo and Lin [**74**] studied interaction solutions between lump and stripe soliton solutions via a quadratic function. Adem et al. [**75**] used the extended transformed rational function that depends on the Hirota bilinear form to constructed Complexiton solutions of the DJKM equation. Yuan et al.[**76**] studied Wronskian and Grammian solutions to the DJKM equation. Singh and Gupta [**77**] investigated the Painlevé property of the suggested equations and their exact solutions were revealed by Pickering's algorithm. Akram [**78**] was utilized $\exp\left(-\Phi\left(\xi\right)\right)$-expansion method to seek some exact solutions. From the relationship of dispersion to the nonlinearity of the DJKM equation, a logarithmic variable transformation can be written as

$$u = 2\frac{\partial}{\partial x}\left(f\left(x, y, t\right)\right). \tag{3.96}$$

Plugging Eq. (3.96) to Eq. (3.95) a result is

$$\begin{aligned}&2\alpha {f_y}^3 + 4f_x\left(\beta f_t f_x + f_{xy}f_{xx} - f_x f_{xxy}\right) - 2f\left(f_{xx}\left(\beta f_t + f_{xxy}\right) + 2f_x\left(\beta f_{xt} - f_{xxxy}\right)\right) + \\ &f_y\left(2\left({f_{xx}}^2 - 2f_x f_{xxx}\right) + f\left(-3\alpha f_{yy} + f_{xxxx}\right)\right) + f^2\left(\alpha f_{yyy} + 2\beta f_{xxt} - f_{xxxxy}\right) = 0,\end{aligned} \tag{3.97}$$

and can be rewritten as a Hirota bilinear form

$$D_x\left(\left(D_x^3 D_y - 3\beta D_x D_t\right) f.f\right).f^2 + \frac{1}{2}D_y\left(\left(D_x^4 - 3\alpha D_y^2\right) f.f\right).f^2 = 0. \tag{3.98}$$

Where D_x, D_y, D_t are the Hirota's bilinear operators and defined in Eq. 2.2. When f is going to solve Eq. (3.98) or (3.97), then $u = u(x, y, t)$ in Eq. (3.96) describe the solution of Eq. (3.95). In this section of work, we study DJKM equation to reveal their N-soliton waves, fusion solutions, M-lump solutions, and the interactions phenomena that appear between M-lump and N-soliton solutions as well as with fusion solution.

3.4.1. N-soliton solutions

In this section, to ascertain the N-soliton solutions to the DJKM equation in (2+1)-dimensions, we use the logarithmic function defined in Eq. (3.96). First, we use a function $f = f(x, y, t)$ that stated in Eq. (2.1), where

$$\psi_i = k_i \left(x + l_i y + \alpha_i + w_i t\right) + \alpha_i, \tag{3.99}$$

$$A_{ij} = \frac{\left(k_i - k_j\right)^2 + \left(l_i - l_j\right)^2 \alpha}{\left(k_i + k_j\right)^2 + \left(l_i - l_j\right)^2 \alpha}, \tag{3.100}$$

and the dispersion relation is given by

$$w_1 = \frac{{k_1}^2 l_1 - {l_1}^3 \alpha}{2\beta}. \tag{3.101}$$

Let $N = 1$ in Eq. (2.1) and substituting a result with Eqs. (3.99-3.101) into Eq. (3.96), a 1-soliton wave solution can be derived as below

$$u = \frac{2k_1 \mathrm{e}^{k_1\left(x + l_1 y + \frac{\left({k_1}^2 l_1 - {l_1}^3 \alpha\right)}{2\beta} t\right)}}{1 + \mathrm{e}^{k_1\left(x + l_1 y + \frac{\left({k_1}^2 l_1 - {l_1}^3 \alpha\right)}{2\beta} t\right)}}. \tag{3.102}$$

When $N = 2, 3$ in the same way, we can construct 2- and 3-soliton solutions of (2+1)-dimensional DJKM equation as follows

$$u = \frac{2\left(\sum\limits_{i=1}^{2} k_i \mathrm{e}^{k_i\left(x + l_i y + \alpha_i + \frac{l_i\left({k_i}^2 - {l_i}^2 \alpha\right)}{2\beta} t\right)} + \left(k_1 + k_2\right) A_{12} \mathrm{e}^{\sum\limits_{i=1}^{2} k_i\left(x + l_i y + \alpha_i + \frac{l_i\left({k_i}^2 - {l_i}^2 \alpha\right)}{2\beta} t\right)}\right)}{1 + \sum\limits_{i=1}^{2} k_i \mathrm{e}^{k_i\left(x + l_i y + \alpha_i + \frac{l_i\left({k_i}^2 - {l_i}^2 \alpha\right)}{2\beta} t\right)} + \left(k_1 + k_2\right) A_{12} \mathrm{e}^{\sum\limits_{i=1}^{2} k_i\left(x + l_i y + \alpha_i + \frac{l_i\left({k_i}^2 - {l_i}^2 \alpha\right)}{2\beta} t\right)}}, \tag{3.103}$$

and

$$u = \frac{2\left(\sum\limits_{i=1}^{3} k_i \mathrm{e}^{\Psi_i} + \sum\limits_{i<j}^{(3)} \left(k_i + k_j\right) M_{ij} \mathrm{e}^{\Psi_i + \Psi_j} + M_{ijk} e^{\sum\limits_{i=1}^{3} \Psi_i} \sum\limits_{i=1}^{3} k_i\right)}{1 + \sum\limits_{i=1}^{3} k_i \mathrm{e}^{\Psi_i} + \sum\limits_{i<j}^{(3)} \left(k_i + k_j\right) M_{ij} \mathrm{e}^{\Psi_i + \Psi_j} + M_{ijk} e^{\sum\limits_{i=1}^{3} \Psi_i} \sum\limits_{i=1}^{3} k_i}. \tag{3.104}$$

Here we note that $A_{ijk} = A_{ij}A_{ik}A_{jk}$ ($1 \leq i < j < k \leq N$) . Eqs. (3.103) and (3.104) are plotted to better understand their physical phenomena (see Figure 3.32). To study and finding the fusion solutions, we have to choose $A_{ij} = 0$ in Eq. (3.103) and Eq.(3.104). To construct 1-fusion solution, we choose $k_1 = -3, k_2 = -2, l_1 = 1, l_2 = 2, \alpha = -1$ and for 2-fusion solution, we let $k_1 = -3, k_2 = -2, k_3 = -2, l_1 = 1, l_2 = 2, l_3 = 2, \alpha = -1$.

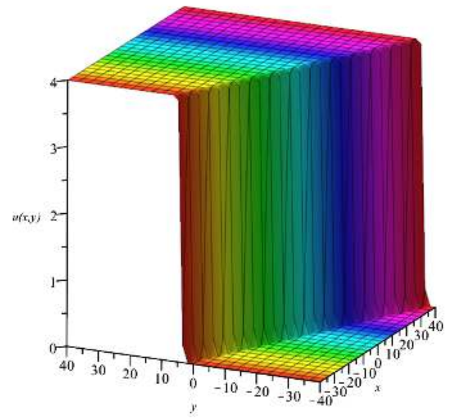

(a) Single-Soliton wave.

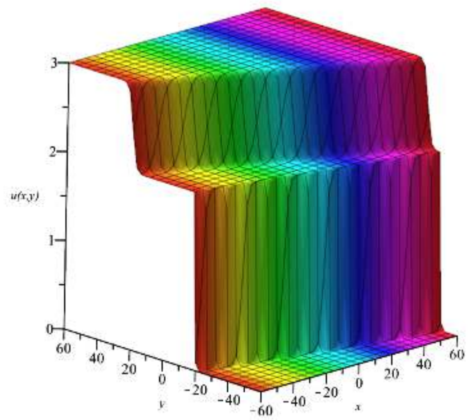

(b) Double-Soliton wave.

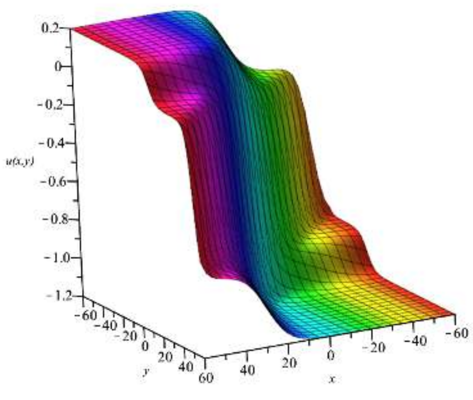

(c) Triple-Soliton wave.

Figure 3.32. 3D sufrace solutions plotted when (a) $t = 4, k_1 = 2, l_1 = 2, \alpha_1 = 0, \alpha = -1, \beta = 1$, (b) $t = 4, k_1 = 0.5, k_2 = 1, l_1 = 2, l_2 = 4, \alpha_1 = 1, \alpha_2 = 1, \alpha = -1, \beta = 1$, (c) $t = 4, k_1 = -0.4, k_2 = -0.2, k_3 = 0.1, l_1 = -1, l_2 = -0.3, l_3 = -3, \alpha_1 = 1, \alpha_2 = 1, \alpha_3 = 1, \alpha = -1, \beta = 1$.

3.4.2. Rational solutions

Lump solutions are a specific type of rational function solutions, observed in all aspects of natural processes, contrary to soliton solutions. In this section of work, we seek M-lump solutions by using long-wave method. When and taking the limit $k_i \to 0$, $\frac{k_1}{k_2} = O(1)$ and $\alpha_i = -1 \ \ (i = 1, 2)$ in Eq. (3.99), we have

$$f_2 = \phi_1\phi_2 + B_{12}, \tag{3.105}$$

where

$$\phi_i = x + l_i y + \rho_i t, \tag{3.106}$$

$$\rho_i = -\frac{\alpha}{2\beta} {l_i}^3, \tag{3.107}$$

and

$$B_{ij} = -\frac{4}{\left(l_i - l_j\right)^2 \alpha}. \tag{3.108}$$

Putting Eq. (13) into Eq. (3) and using $l_1 = a_1 + b_1 \mathrm{i}$, $l_2 = {l_1}^*$, we obtain a 1-M-lump solution as shown in Figure 3.33 and read as follows

$$\begin{aligned} u &= 2\frac{\partial}{\partial x} \log\left(\left(x' + a_1 y'\right)^2 + {b_1}^2 {y'}^2 + \frac{1}{{b_1}^2 \alpha}\right) \\ &= \frac{4\left(x' + a_1 y'\right)}{\left(x' + a_1 y'\right)^2 + {b_1}^2 {y'}^2 + \frac{1}{{b_1}^2 \alpha}}, \end{aligned} \tag{3.109}$$

where

$$\begin{aligned} x' &= x + \frac{\alpha a_1}{\beta}\left(\frac{{a_1}^2}{2} + {b_1}^2\right) t, \\ y' &= y + \frac{\alpha}{2\beta}\left({b_1}^2 - 3{a_1}^2\right) t. \end{aligned}$$

The rational solution (3.109) is a permanent lump solution that decays as $O\left(\frac{1}{x^2}, \frac{1}{y^2}\right)$ for $|x|, |y| \to \infty$ and to move with the velocity

$$\begin{aligned} v_x &= -\frac{\alpha a_1}{\beta}\left(\frac{{a_1}^2}{2} + {b_1}^2\right), \\ v_y &= \frac{\alpha}{2\beta}\left(3{a_1}^2 - {b_1}^2\right). \end{aligned}$$

From 4-soliton solutions, we can derive a 2-M-lump solution by taking a limit $k_i \to 0$ and $\alpha_i = -1$ $(i = 1, 2, 3, 4)$, then f_4 is equivalent to

$$\begin{aligned} f_4 = {} & \phi_1\phi_2\phi_3\phi_4 + B_{12}\phi_3\phi_4 + B_{13}\phi_2\phi_4 + B_{14}\phi_2\phi_3 + B_{23}\phi_1\phi_4 \\ & + B_{24}\phi_1\phi_3 + B_{34}\phi_1\phi_2 + B_{12}B_{34} + B_{13}B_{24} + B_{14}B_{23}, \end{aligned} \tag{3.110}$$

where $\phi_i (i = 1, 2, 3, 4)$, $\rho_i (i = 1, 2, 3, 4)$ and $B_{ij}, i < j$ are defined in Eqs. (3.106), (3.107) and (3.108), respectively. Eq. (3.110) gives us a singular solution at some position, to find a non-singular 2-M-lump solution we choose $l_{\frac{N}{2}+i} = l_i^*$, $\left(i = 1, 2, .., \frac{N}{2}\right)$. Substituting Eq. (3.110) with related equations leads a two-M-lump solution to the studied equation as shown in Figure 3.34.

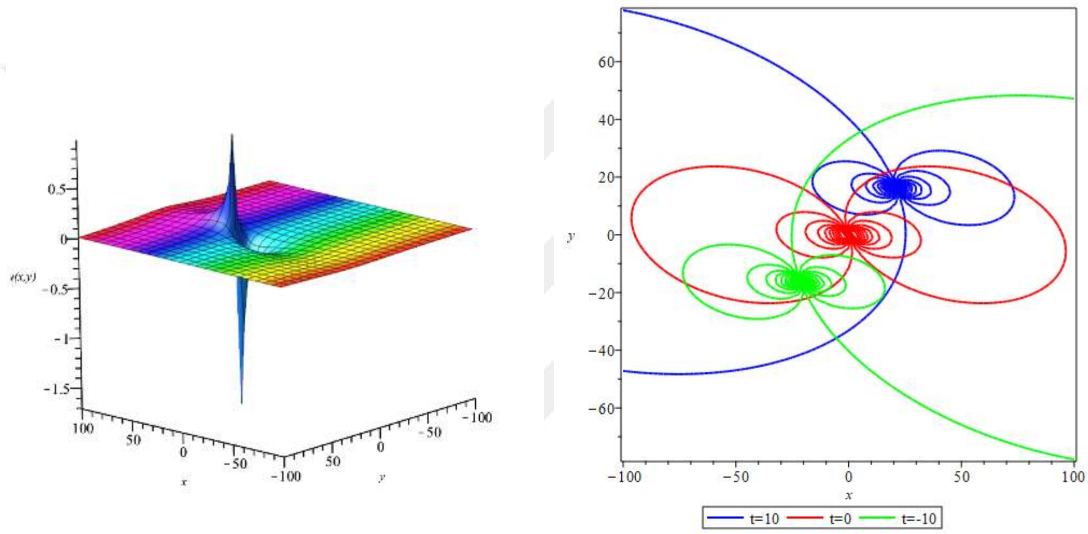

(a) Single-M-lump wave

(b) Contour plot for single-M-lump wave in different period of time

Figure 3.33. 3D surface solution plotted when $t = 4, a = 1/2, b = 2, \alpha = -1, \beta = 1$.

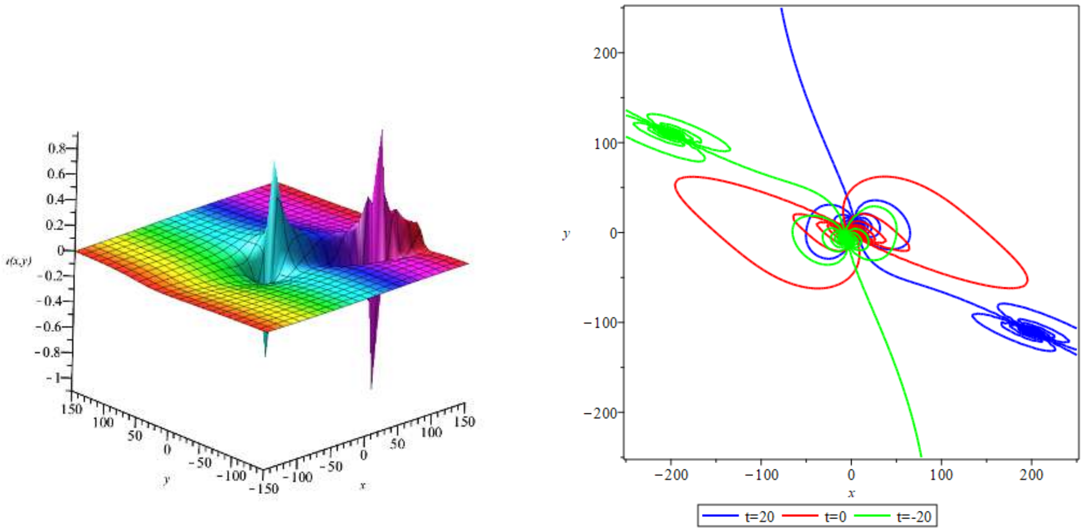

(a) Double-M-lump solution

(b) Contour plot for double-M-lump solution in different period of time

Figure 3.34. 3D surface solution plotted when $t = 4, a = 2, b = 1, d = 1, c = 1/4, \alpha = -1, \beta = 1$.

3.4.3. Interactions phenomena between 1-M-lump and soliton solutions

The interaction physical phenomena between M-lump wave and 1-, 2-soliton solutions as well as with fusion solution will construct in this section of the work. To study the interaction between M-lump and 1-soliton solution, we let $N = 3$ in Eq. (2.1), taking the limit $k_i \to 0, (i = 1, 2)$ and $\frac{k_1}{k_2} = O(1)$, then f_3 can set up as

$$f_3 = \phi_1\phi_2 + B_{12} + (\phi_1\phi_2 + B_{12} + C_{23}\phi_1 + C_{13}\phi_2 + C_{13}C_{23})e^{\psi_3}, \tag{3.111}$$

where ψ_3 is stated in Eq. (3.99), $\phi_i\,(i = 1, 2)$ are stated in Eq. (3.106), B_{12} is given in Eq. (3.108). The constants $C_{m3}\,(m = 1, 2)$ are defined as below

$$C_{m3} = -\frac{4k_3}{{k_3}^2 + {l_m}^2\alpha - 2l_m l_3\alpha + {l_3}^2\alpha}, \qquad m = 1, 2. \tag{3.112}$$

As a result of substituting Eq. (3.111) together with its related equations into Eq. (3.96), we obtain an equation that presents a collision between a 1-M-lump solution and a 1-soliton solution (see Figure 3.35).

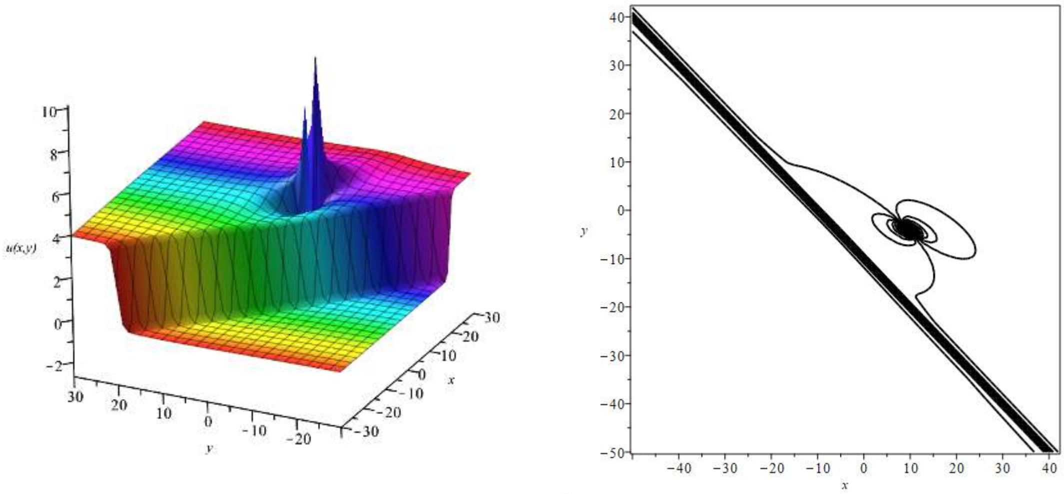

(a) Mixed single-M-lump-soliton solution

(b) Corresponding contour plot to mixed single-M-lump-soliton solution

Figure 3.35. 3D surface solution plotted when $a = 1, b = 1, k_3 = 2, l_3 = 1, \alpha = -1, \beta = 1, t = 4$.

The collision physical phenomena between single-M-lump and 2-soliton solution can be derived by choosing $N = 4$ in Eq. (2.1), and taking the limit $k_i \to 0, \alpha_i = -1$ $(i = 1, 2)$ and letting $\frac{k_1}{k_2} = O(1)$, f_4 will be equivalent to

$$
\begin{aligned}
f_4 =& \phi_1\phi_2 + B_{12} + \Psi_1 e^{\psi_3} + \Psi_2 e^{\psi_4} + \\
& A_{34} e^{\psi_3+\psi_4} \left(\Psi_1 + \Psi_2 - \phi_1\phi_2 - B_{12} + C_{13}C_{24} + C_{14}C_{23}\right),
\end{aligned}
\tag{3.113}
$$

$$\Psi_1 = \phi_1\phi_2 + B_{12} + C_{23}\phi_1 + C_{13}\phi_2 + C_{13}C_{23}.$$

$$\Psi_2 = \phi_1\phi_2 + B_{12} + C_{24}\phi_1 + C_{14}\phi_2 + C_{14}C_{24}.$$

Here ψ_3, ψ_4 are stated in Eq. (3.99), ϕ_1, ϕ_2 are stated in Eq. (3.106), B_{12} is given from Eq. (3.108) and A_{34} is defined in Eq. (3.100). The $C_{m4}\,(m = 1, 2)$ are constants and defined as

$$C_{m4} = -\frac{4k_4}{{k_4}^2 + {l_m}^2\alpha - 2l_m l_4\alpha + {l_4}^2\alpha}. \tag{3.114}$$

As a result of replacing Eq. (3.113) with their related equations into Eq. (3.96), an equation that describes a collision phenomenon between single-M-lump and a two-soliton solution is revealed (see Figure 3.36).

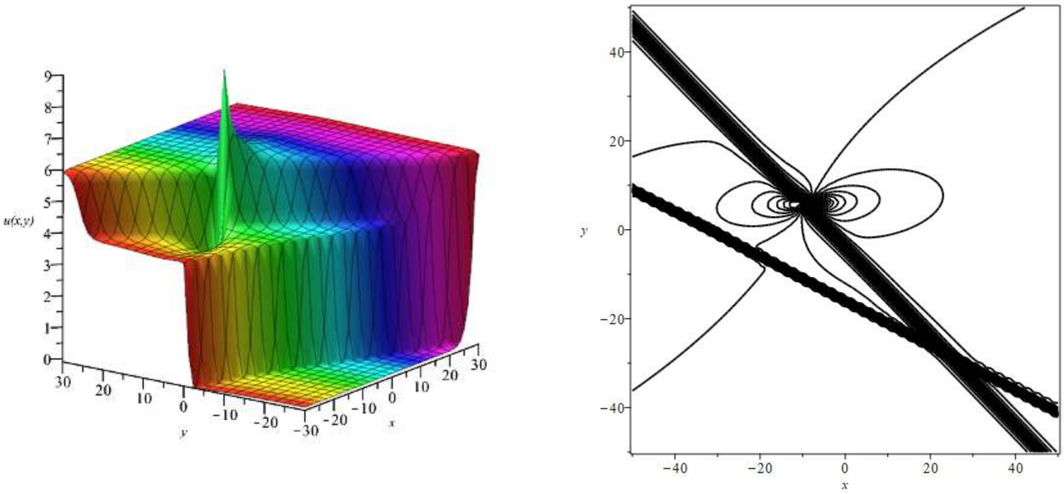

(a) Mixed 1-M-lump-2-soliton solution

(b) Corresponding contour plot to mixed 1-M-lump-2-soliton solution

Figure 3.36. 3D surface solution plotted when $a = -1/2, b = 2, k_3 = 1, k_4 = 2, l_3 = 1, l_4 = 2, \alpha = -1, \beta = 1, t = 4$.

In the case, a value of $A_{34} = 0$ in Eq. (3.113), f_4 will be rewritten as

$$f_4 = \phi_1\phi_2 + B_{12} + \Psi_1 e^{\psi_3} + \Psi_2 e^{\psi_4}. \tag{3.115}$$

This equation describes interaction phenomena that appear between 1-M-lump solution and 1-fusion solution as shown in Figure 3.37.

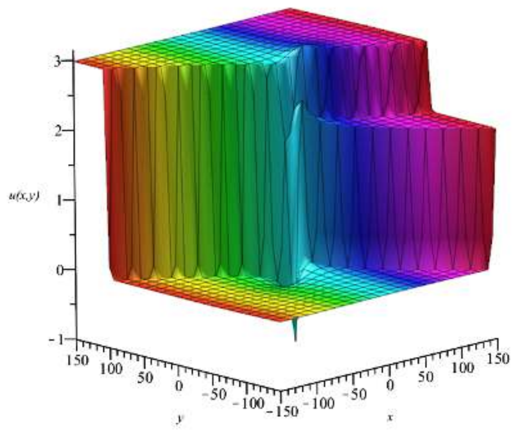

(a) Mixed 1-M-lump-fusion solution

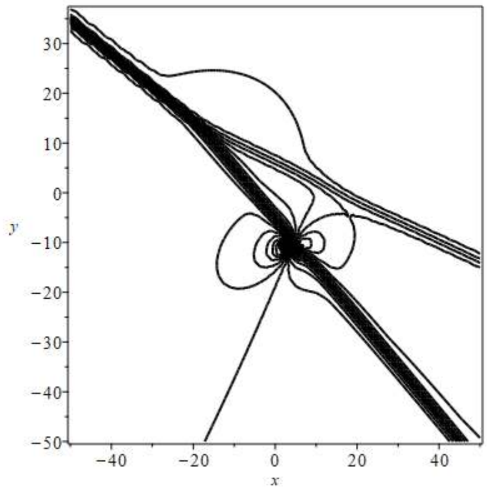

(b) Corresponding contour plot to mixed 1-M-lump-fusion solution

Figure 3.37. 3D surface solution plotted when $a_1 = 1, b_1 = 3, k_3 = -1, k_4 = 1, l_3 = 1, l_4 = 3, \alpha = -1, \beta = 1$.

3.5. The (2+1)-dimensional Bogoyavlensky-Konopelchenko equation

Let us consider the (2+1)-dimensional Bogoyavlensky-Konopelchenko (BK) equation

$$u_{tx} + \alpha \left(6u_x u_{xx} + u_{xxxx}\right) + \beta \left(u_{xxxy} + 3u_x u_{xy} + 3u_{xx} u_y\right) = 0 \tag{3.116}$$

that was introduced as a special case of a (2+1)-dimensional version of the KdV equation in [**79**] and described as the interaction of a long wave propagating along the x-axis and a Riemann wave propagating along the y-axis [**44**]. In this paper, we study the (2+1)-dimensional generalized Bogoyavlensky-Konopelchenko (gBK) equation

$$u_{tx} + \alpha \left(6u_x u_{xx} + u_{xxxx}\right) + \beta \left(u_{xxxy} + 3u_x u_{xy} + 3u_{xx} u_y\right) + \gamma_1 u_{xx} + \gamma_2 u_{xy} + \gamma_3 u_{yy} = 0, \tag{3.117}$$

which is a generalization of Eq. (3.116). Chen and Ma [**80**] have studied lower-order lump to the suggested equation. In Ref. [**81**] a few classes of exact and explicit solutions have been reported from different ansatze on solution forms, for example, traveling wave, 2-wave solutions, and polynomial solutions. To investigate Eq. (3.117), we use the link between u and f:

$$u = 2(\ln f\,(x, y, t))_x. \tag{3.118}$$

Insert Eq. (3.118) into Eq. (3.117), we get

$$2f\left(\gamma_3 f_{yy}+f_{xt}+\gamma_2 f_{xy}+\gamma_1 f_{xx}+\beta f_{xxxy}+\alpha f_{xxxx}\right)-2\gamma_3 {f_y}^2-2f_y\left(\gamma_2 f_x+\beta f_{xxx}\right)-$$
$$2\left(f_t f_x+\gamma_1 {f_x}^2-3f_{xx}\left(\beta f_{xy}+\alpha f_{xx}\right)+f_x\left(3\beta f_{xxy}+4\alpha f_{xxx}\right)\right)=0. \tag{3.119}$$

The logarithmic variable transformation (3.118) is also a characteristic one in establishing Bell polynomial theories of soliton equations [**37**]. Eq. (3.119) can be rewritten as a Hirota bilinear form as follows

$$\left(D_x D_t+\alpha {D_x}^4+\beta {D_x}^3 D_y+\gamma_1 {D_x}^2+\gamma_2 D_x D_y+\gamma_3 {D_y}^2\right) f.f=0. \tag{3.120}$$

It's obvious that when $f=f(x,y,t)$ in Eqs. (3.120) is a solution of Eq. (3.118), then $u=2(\ln f\,(x,y,t))_x$ will solve Eq. (3.117).

3.5.1. Complex one-, two, and three-soliton solutions

In this section, we try to construct special complex one-, two-, and three-soliton solutions to the introduced equation. The N-soliton wave solutions to the gBK equation has been reported in Ref. [**81**]. To find complex soliton solutions, we require

$$w_i=-\left(\alpha {k_i}^2+\beta {k_i}^2 l_i+\gamma_1+l_i\gamma_2+{l_i}^2\gamma_3\right), \qquad i=1,2,3. \tag{3.121}$$

To determine special complex one-, two-, three-soliton solutions, we take

$$f{=}\mathrm{i}{+}\mathrm{e}^{\psi}, \tag{3.122}$$

$$f=\mathrm{i}+e^{\psi_1}+e^{\psi_2}+\xi_{12}e^{\psi_1+\psi_2}, \tag{3.123}$$

$$f=\mathrm{i}+e^{\psi_1}+e^{\psi_2}+e^{\psi_3}+\xi_{12}e^{\psi_1+\psi_2}+\xi_{13}e^{\psi_1+\psi_3}+\xi_{23}e^{\psi_2+\psi_3}+\xi_{123}e^{\psi_1+\psi_2+\psi_3}, \tag{3.124}$$

where

$$\psi_i=k_i\left(x+l_i y+w_i t\right)+\alpha_i, \quad (i=1,2,...,N) \tag{3.125}$$

$$\xi_{ij}=\frac{\mathrm{i}(l_i-l_j)^2\gamma_3-\mathrm{i}\left(k_i-k_j\right)\left(3\left(k_i-k_j\right)\alpha+k_i\left(2l_i+l_j\right)\beta-k_2\left(l_i+2l_j\right)\beta\right)}{\left(k_i+k_j\right)\left(3\left(k_i+k_j\right)\alpha+k_i\left(2l_i+l_j\right)\beta+k_j\left(l_i+2l_j\right)\beta\right)-\left(l_i-l_j\right)^2\gamma_3}, \tag{3.126}$$

and

$$\xi_{123}=\xi_{12}\xi_{13}\xi_{23}. \tag{3.127}$$

Plugging Eq. (3.122) into Eq. (3.118), we get

$$u = \frac{2k_1 \mathrm{e}^{k_1\left(x+l_1y-\left({k_1}^2\alpha+{k_1}^2l_1\beta+\gamma_1+l_1\gamma_2+{l_1}^2\gamma_3\right)t+\alpha_0\right)}}{\mathrm{i}+\mathrm{e}^{k_1\left(x+l_1y-\left({k_1}^2\alpha+{k_1}^2l_1\beta+\gamma_1+l_1\gamma_2+{l_1}^2\gamma_3\right)t+\alpha_0\right)}}. \tag{3.128}$$

This is a complex 1-soliton solution as shown in Figure 3.38.

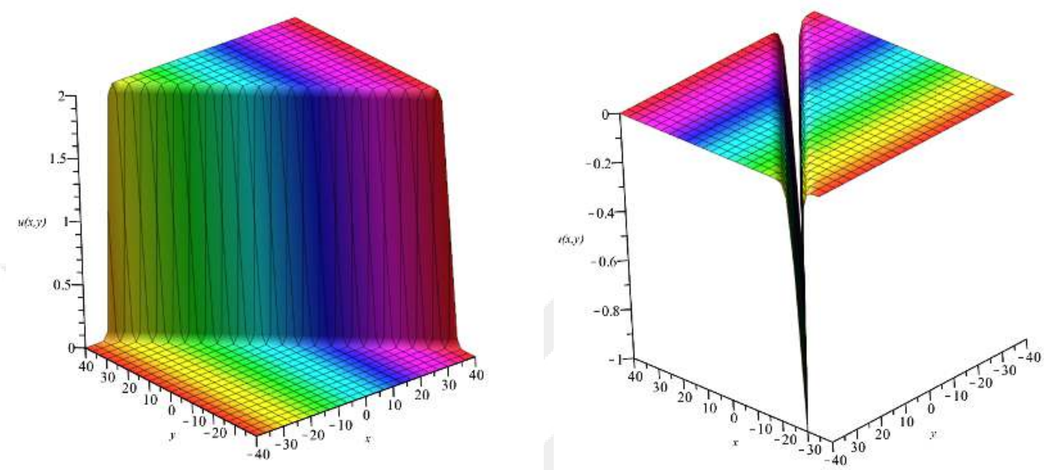

(a) Real solution **(b)** Imaginary solution

Figure 3.38. 3D surface of 1-soliton solution plotted when $t = 2, l_1 = 1, k_1 = 1, \alpha_1 = 0, \alpha = 1, \beta = 1, \gamma_1 = 1, \gamma_2 = 1, \gamma_3 = 1$.

By inserting Eq. (3.123) into Eq. (3.118), we have a complex two-soliton wave solution to the considered equation (see Figure 3.39)

$$u = \frac{2\left(k_1\mathrm{e}^{\psi_1}+k_2\mathrm{e}^{\psi_2}+\xi_{12}\left(k_1+k_2\right)\mathrm{e}^{\psi_1+\psi_2}\right)}{\mathrm{i}+\mathrm{e}^{\psi_1}+\mathrm{e}^{\psi_2}+\xi_{12}\mathrm{e}^{\psi_1+\psi_2}}. \tag{3.129}$$

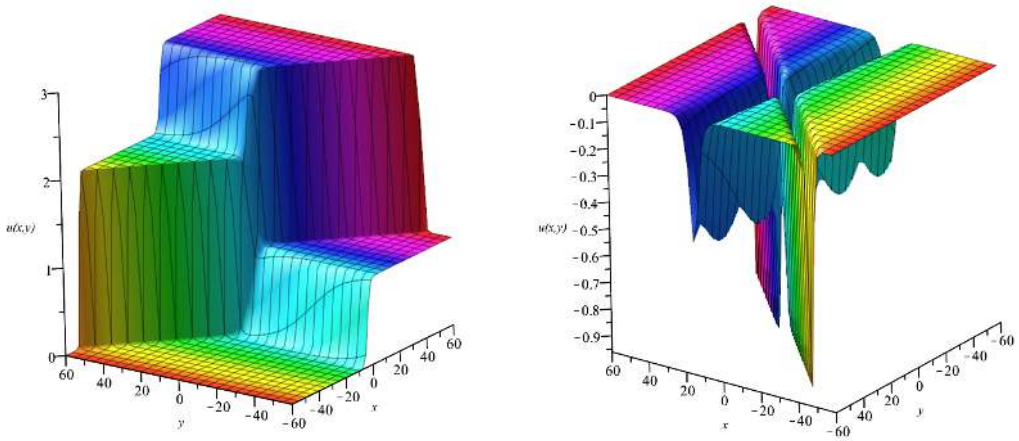

(a) Real solution **(b)** Imaginary solution

Figure 3.39. 3D surface of 2-soliton solution plotted when $t = 2, l_1 = -0.1, l_2 = 1, k_1 = 0.5, k_2 = 1, \alpha_1 = 0, \alpha_2 = 0, \alpha = 2, \beta = 1, \gamma_1 = 1, \gamma_2 = 1, \gamma_3 = 1$.

Substituting Eq. (3.124) into Eq. (3.118), we get

$$u = \frac{2\begin{pmatrix} \mathrm{e}^{\psi_1}k_1 + \mathrm{e}^{\psi_2}k_2 + \xi_{12}\left(k_1+k_2\right)\mathrm{e}^{\psi_1+\psi_2} + \mathrm{e}^{\psi_3}k_3 + \xi_{13}\left(k_1+k_3\right)\mathrm{e}^{\psi_1+\psi_2} + \\ \xi_{23}\left(k_2+k_3\right)\mathrm{e}^{\psi_2+\psi_3} + \xi_{123}\left(k_1+k_2+k_3\right)\mathrm{e}^{\psi_1+\psi_2+\psi_3} \end{pmatrix}}{\mathrm{i} + \mathrm{e}^{\psi_1} + \mathrm{e}^{\psi_2} + \xi_{12}\mathrm{e}^{\psi_1+\psi_2} + \mathrm{e}^{\psi_3} + \xi_{13}\mathrm{e}^{\psi_1+\psi_3} + \xi_{23}\mathrm{e}^{\psi_2+\psi_3} + \xi_{123}\mathrm{e}^{\psi_1+\psi_2+\psi_3}}. \tag{3.130}$$

This is a complex 3-soliton solution as seen in Figure 3.40.

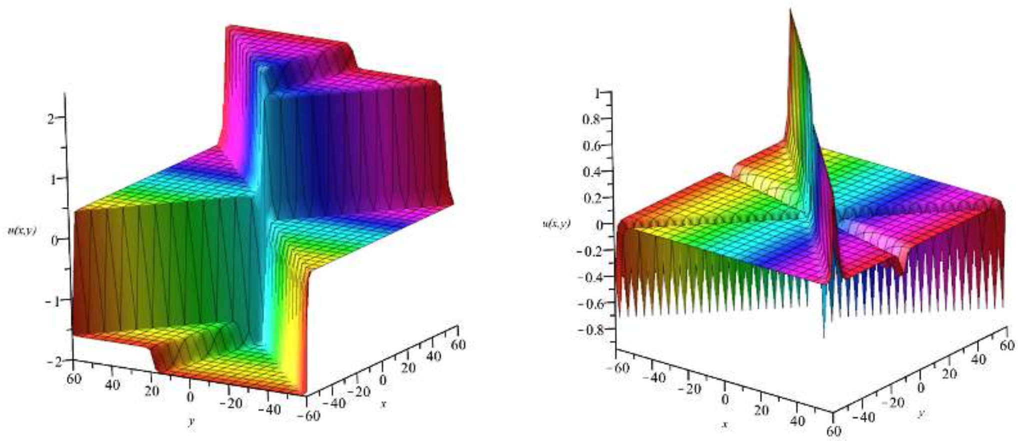

(a) Real solution **(b)** Imaginary solution

Figure 3.40. 3D surface of 3-soliton solution plotted when $t = 2, l_1 = 1, l_2 = -1, l_3 = 4, k_1 = -1, k_2 = 1, k_3 = 0.3, \alpha_1 = 0, \alpha_2 = -2, \alpha_3 = 5, \alpha = -1, \beta = -1, \gamma_1 = 1, \gamma_2 = 1, \gamma_3 = 1.$

3.5.2. M-lump solutions

Lump solutions are analytical rational function solutions located in all directions in space. In this portion of the paper, we use a long-wave limit method to construct a rational solution to a gBK equation. Consider Eq. (2.1) and using the long-wave limit method by taking the limit $k_i \to 0$, $\frac{k_1}{k_2} = O(1)$, and $e^{\alpha_i} = -1 \ (i = 1, 2)$, we get

$$f_2 = \phi_1\phi_2 + B_{12}, \tag{3.131}$$

where

$$\phi_i = x + l_i y + \rho_i t, \tag{3.132}$$

$$\rho_i = -\left(\gamma_1 + l_i\gamma_2 + {l_i}^2\gamma_3\right), \tag{3.133}$$

$$B_{ij} = \frac{6\left(2\alpha + (l_i + l_j)\beta\right)}{(l_i - l_j)^2\gamma_3}, \qquad (i < j) \tag{3.134}$$

and

$$l_{\frac{N}{2}+i} = l_i^*, \quad \left(i = 1, 2, .., \frac{N}{2}\right). \tag{3.135}$$

Plugging Eq. (3.132-3.135) into Eq. (3.131) then into Eq. (3.118), we can construct a one-M-lump solution (see Figure 3.41) Here, $l_1 = a_1 + \mathrm{i}b_1$, $l_2 = a_2 + \mathrm{i}b_2$, $l_3 = a_1 + \mathrm{i}b_1$ and $l_4 = a_2 - \mathrm{i}b_2$.

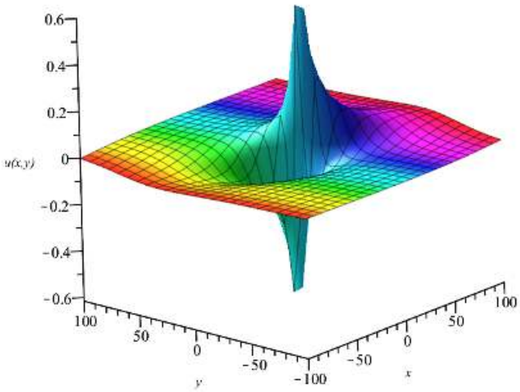

(a) One-M-lump solution

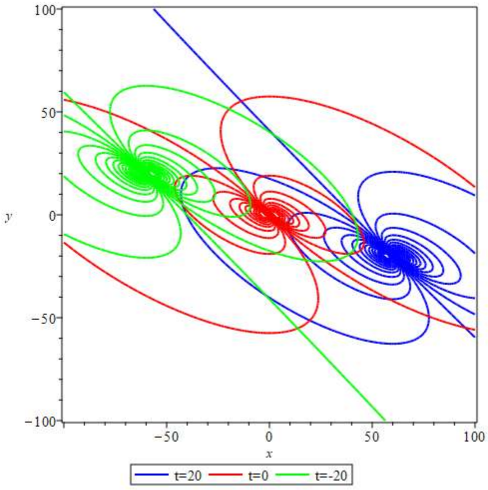

(b) Corresponding contour plot of one-M-lump solution

Figure 3.41. 3D surface and contour plot plotted when $t = 2, a_1 = 1, b_1 = 1, l_1 = 1, l_2 = 3, \alpha = 1, \beta = 1, \gamma_1 = 1, \gamma_2 = 1, \gamma_3 = -1$.

$$
\begin{aligned}
u &= 2\frac{\partial}{\partial x}\log\left(\left(x' + ay'\right)^2 + b^2y'^2 - \frac{3\left(\alpha + a\beta\right)}{b^2\gamma_3}\right) \\
&= \frac{4\left(x' + ay'\right)}{\left(x' + ay'\right)^2 + b^2y'^2 - \frac{3(\alpha+a\beta)}{b^2\gamma_3}}, \\
&= \frac{4\left(x - t\gamma_1 + a\left(y - t\gamma_2\right) - a^2t\gamma_3 + b^2t\gamma_3\right)}{\left(\begin{array}{l}\left(x - \gamma_1 t - (a - \mathrm{i}b)\left(\left(\gamma_2 + a\gamma_3 - \mathrm{i}b\gamma_3\right)t - y\right)\right) \\ \left(x - \gamma_1 t - (a + \mathrm{i}b)\left(\left(\gamma_2 + a\gamma_3 + \mathrm{i}b\gamma_3\right)t - y\right)\right) - \dfrac{3\left(\alpha + a\beta\right)}{b^2\gamma_3}\end{array}\right)},
\end{aligned}
\tag{3.136}
$$

where

$$
\begin{aligned}
y' &= \text{y-2a}\gamma_3\text{t - }\gamma_2\text{t }, \\
x' &= x + b^2\gamma_3 t - \gamma_1 t.
\end{aligned}
\tag{3.137}
$$

The rational solution (3.137) is a permanent lump solution that decays as $O\left(\frac{1}{x^2}, \frac{1}{y^2}\right)$ for $|x| \to \infty$, $|y| \to \infty$ and moves with the velocity

$$
\begin{aligned}
v_x &= 2a\gamma_3 - \gamma_2, \\
v_y &= \gamma_1 - b^2\gamma_3.
\end{aligned}
\tag{3.138}
$$

To study and reveal a 2-M-lump solution to a gBK equation, consider Eq. (2.1) and taking

$e^{\alpha_i} = -1 \ (i = 1, 2, 3, 4)$ and taking a limit $k_i \to 0$, we get

$$f_4 = \phi_1\phi_2\phi_3\phi_4 + B_{12}\phi_3\phi_4 + B_{13}\phi_2\phi_4 + B_{14}\phi_2\phi_3 + B_{23}\phi_1\phi_4 \\ + B_{24}\phi_1\phi_3 + B_{34}\phi_1\phi_2 + B_{12}B_{34} + B_{13}B_{24} + B_{14}B_{23}. \tag{3.139}$$

Here $\phi_1, \phi_2, \phi_3, \phi_4$, ρ_i, $B_{ij} \ (i < j)$, and $l_{\frac{N}{2}+i}$ are given by Eqs. (3.132-3.135), respectively. Plugging Eq. (3.139) into Eq. (3.118), as a result, we can obtain a double-M-lump solution to the suggested equation as shown in Figure 3.42.

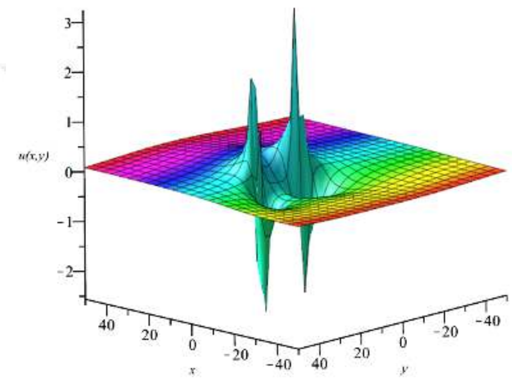

(a) Two-M-lump solution

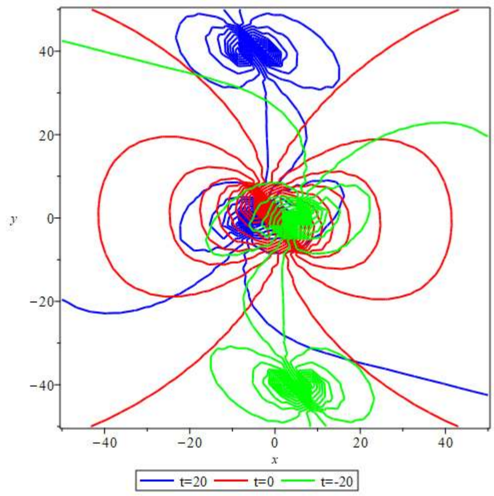

(b) Corresponding contour plot of two-M-lump solution

Figure 3.42. 3D surface and contour plot are drawn when $t = 10, a = 1/2, b = 1, c = -1/2, d = 1, l_1 = 0.1, l_2 = 1, l_3 = 2, \alpha = 1, \beta = 1, \gamma_1 = 1, \gamma_2 = 1, \gamma_3 = 1$.

3.5.3. Physical interactions between M-lump solution and soliton wave

In this section, we study the interaction physical phenomena between the 1-M-lump solution and the one-soliton solution. For this purpose, we consider Eq. (1.6), and take the limit $k_i \to 0, (i = 1, 2)$ and $\frac{k_1}{k_2} = O(1)$. As a result, f_3 could be rewritten as follows

$$f_3 = \phi_1\phi_2 + B_{12} + (\phi_1\phi_2 + B_{12} + C_{23}\phi_1 + C_{13}\phi_2 + C_{13}C_{23})e^{\psi_3}, \tag{3.140}$$

Here ψ_3 is defined in Eq. (3.125), $\phi_i \ (i = 1, 2)$ are defined in Eq. (3.132), B_{12} is given in Eq. (3.134) and $\alpha = \frac{(l_1-l_3)(l_3-l_2)\gamma_3}{{k_3}^2} - \frac{\beta}{2}(l_1 + l_2)$. The constants C_{13}, C_{23} are stated as follows

$$C_{13} = \frac{12\,(l_3 - l_2)}{k_3\,(l_1 + 3l_2 - 4l_3)}, C_{23} = \frac{12\,(l_3 - l_1)}{k_3\,(3l_1 + l_2 - 4l_3)}, \tag{3.141}$$

or

$$\alpha = \frac{(l_1 - l_3)(l_3 - l_2)\gamma_3}{{k_3}^2} - l_3\beta, C_{13} = -\frac{6\left({k_3}^2\beta + 2(l_3 - l_2)\gamma_3\right)}{{k_3}^3\beta - k_3(l_1 + 3l_2 - 4l_3)\gamma_3},$$
$$C_{23} = -\frac{6\left({k_3}^2\beta + 2(l_3 - l_1)\gamma_3\right)}{{k_3}^3\beta - k_3(3l_1 + l_2 - 4l_3)\gamma_3}. \tag{3.142}$$

Substituting Eqs. (3.140) and (3.141) into Eq. (3.118), we get an equation that presents a collision between the 1-M-lump solution and the 1-soliton solution as seen in Figure 3.43.

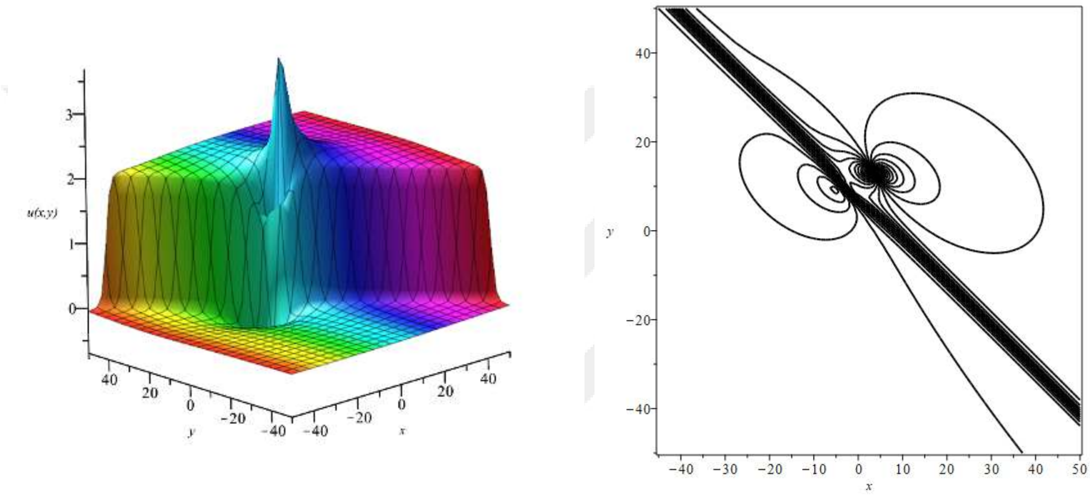

(a) Mixed 1-M-lump-soliton solution

(b) Corresponding contour plot of mixed 1-M-lump-soliton solution

Figure 3.43. 3D surface of interaction between a one-M-lump solution and soliton wave solution drawn when $t = 5, a = 1/2, b = 1, l_3 = 1, k_3 = 2, \alpha_1 = 0, \alpha_2 = 1, \beta = 1, \gamma_1 = 1, \gamma_2 = 1, \gamma_3 = 1$.

We can also choose

$$\beta = \frac{(l_1 - l_3)(l_3 - l_2)\gamma_3 - {k_3}^2\alpha}{{k_3}^2 l_3}, C_{13} = -\frac{6\left({k_3}^2\alpha + (l_2 - l_3)(l_1 + l_3)\gamma_3\right)}{k_3\left({k_3}^2\alpha + l_1 l_2\gamma_3 + (2l_2 - 3l_3)l_3\gamma_3\right)},$$
$$C_{23} = -\frac{6\left({k_3}^2\alpha + (l_1 - l_3)(l_2 + l_3)\gamma_3\right)}{k_3\left({k_3}^2\alpha - 3{l_3}^2\gamma_3 + l_1(l_2 + 2l_3)\gamma_3\right)}, \tag{3.143}$$

or

$$\beta = -\frac{2\left(k_3{}^2\alpha + (l_1 - l_3)(l_2 - l_3)\gamma_3\right)}{k_3{}^2(l_1 + l_2)}, C_{13} = -\frac{12(l_2 - l_3)}{k_3(l_1 + 3l_2 - 4l_3)}, \\ C_{23} = -\frac{12(l_1 - l_3)}{k_3(3l_1 + l_2 - 4l_3)}. \tag{3.144}$$

Putting Eqs. (3.143), (3.140) into Eq. (3.118), we can construct another solution that describe the interaction between 1-M-lump solution and 1-soliton wave solution as shown in Figure 3.44.

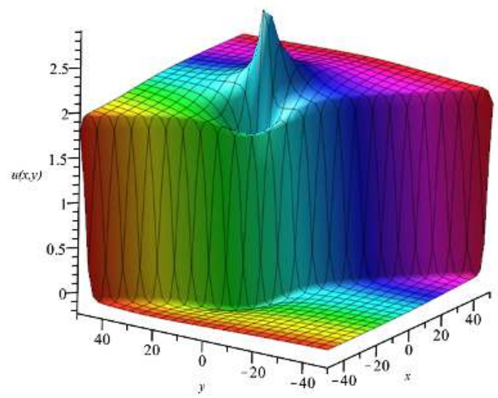

(a) Mixed 1-M-lump-soliton solution

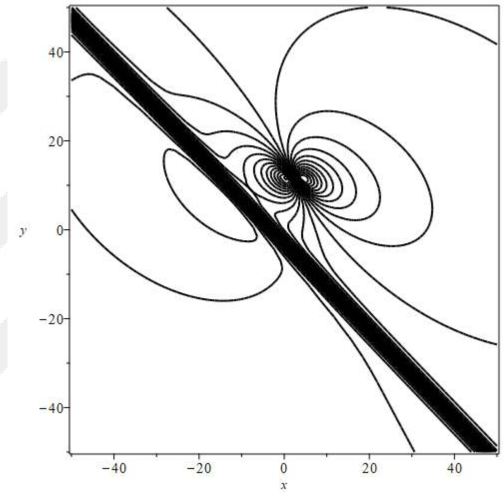

(b) Corresponding contour plot of mixed 1-M-lump-soliton

Figure 3.44. 3D surface of interaction between a one-lump solution and soliton wave solution drawn when $t = 5, a = 1/2, b = 1, l_3 = 1, k_3 = 1, \alpha_1 = 0, \alpha_2 = 1, \alpha = 1, \gamma_1 = 1, \gamma_2 = 1, \gamma_3 = 1$.

3.5.4. Quadratic Solutions

In this portion of the paper, we investigate single-lump solution via a quadratic function. The quadratic function solutions and symbolic computation method can be use to construct different kinds of exact solutions to many classes of PDEs. Now, we define the solution of Eq. (3.118) as follows

$$f(x, y, t) = (a_1x + a_2y + a_3t + a_4)^2 + (b_1x + b_2y + b_3t + b_4)^2 + c_1, \tag{3.145}$$

where a_i, b_i and c_1 are constants to be determined later. Plugging Eq. (3.145) into Eq. (3.118), as a result, we gain a polynomial. Setting the coefficients of the polynomial with the same powers of the independent variables to zero, one can obtain the following cases of solutions: **Case 1:** When we have

$$a_1 = b_1, a_3 = \frac{\left({b_2}^2 - {a_2}^2 - 2a_2b_2\right)\gamma 3}{2b_1} - b_1\gamma_1 - a_2\gamma_2,$$
$$b_3 = \frac{\left({a_2}^2 - 2a_2b_2 - {b_2}^2\right)\gamma_3}{2b_1} - b_1\gamma_1 - b_2\gamma_2, c_1 = -\frac{12{b_1}^3\left(2b_1\alpha + (a_2+b_2)\beta\right)}{(a_2-b_2)^2\gamma_3}, \tag{3.146}$$

and plugging them into Eq. (3.145), then into Eq. (3.118), one can obtain

$$u = \frac{4b_1\left(2b_1x + (a_2+b_2)y + (a_3+b_3)t + a_4 + b_4\right)}{(a_4 + a_3t + b_1x + a_2y)^2 + (b_4 + b_3t + b_1x + b_2y)^2 - \frac{12{b_1}^3(2b_1\alpha + (a_2+b_2)\beta)}{(a_2-b_2)^2\gamma_3}}. \tag{3.147}$$

Eq. (3.147) is a lump solution as shown in Figure 3.45.

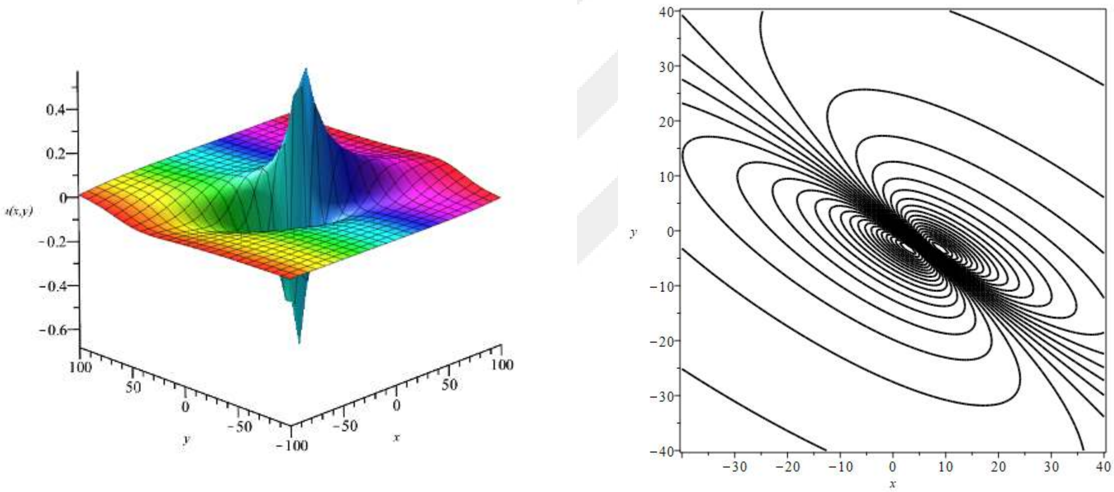

(a) Lump solution

(b) Corresponding contour plot of lump solution

Figure 3.45. 3D surface and contour plot plotted when $t = 2, a_1 = 0.01, a_2 = 1, a_3 = 0.1, a_4 = 0.5, b_1 = 0.5, b_2 = 0.2, b_4 = 0.2, c_1 = 1, \gamma_1 = 1, \gamma_2 = 1, \gamma_3 = -1, \alpha = 0.5, \beta = 1$.

Case 2: In case

$$a_2 = -\frac{a_1\gamma_2 + i\sqrt{a_1\left(4a_3\gamma_3 + 4a_1\gamma_1\gamma_3 - a_1{\gamma_2}^2\right)}}{2\gamma_3}, b_1 = \mathrm{i}a_1, b_3 = \mathrm{i}a_3,$$
$$b_2 = \frac{\sqrt{a_1\left(4a_3\gamma_3 + 4a_1\gamma_1\gamma_3 - a_1{\gamma_2}^2\right)} - \mathrm{i}a_1\gamma_2}{2\gamma_3}, \tag{3.148}$$

and using them into Eq. (3.145), then into Eq. (3.118), a result yields

$$u = \frac{4a_1(a_4 + \mathrm{i}b_4)\gamma_3}{\left({a_4}^2 + {b_4}^2 + c_1 + (2a_3a_4 + 2\mathrm{i}a_3b_4)t\right)\gamma_3 - a_1(a_4 + \mathrm{i}b_4)(\gamma_2y - 2\gamma_3x) + (b_4 - \mathrm{i}a_4)\sqrt{\Phi}y}, \tag{3.149}$$

where $\Phi = a_1 \left(4a_3\gamma_3 + 4a_1\gamma_1\gamma_3 - a_1{\gamma_2}^2\right) > 0$. The above equation is a complex single-soliton solution to a gBK equation as seen in Figure 3.46.

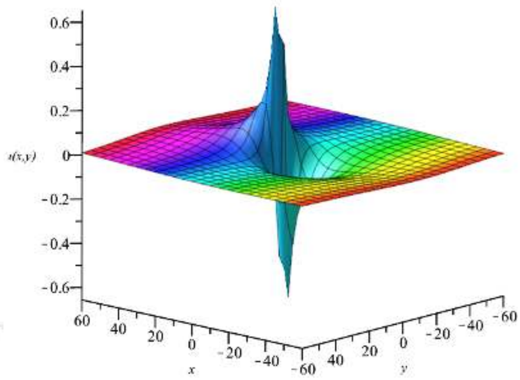

(a) Real solution of lump wave

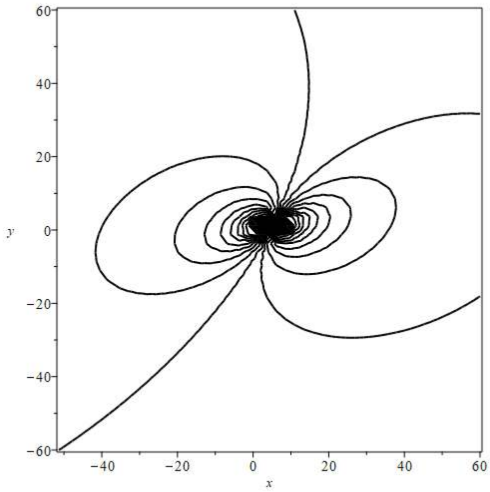

(b) Corresponding contour plot of real lump solution

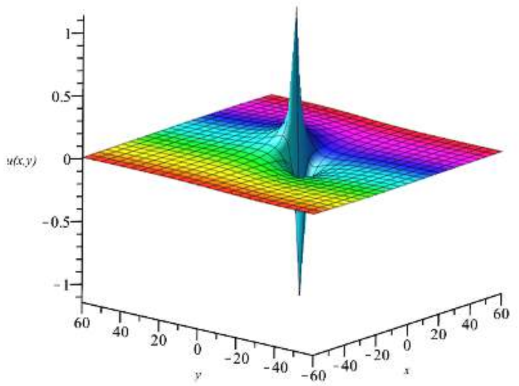

(c) Imaginary solution of lump wave

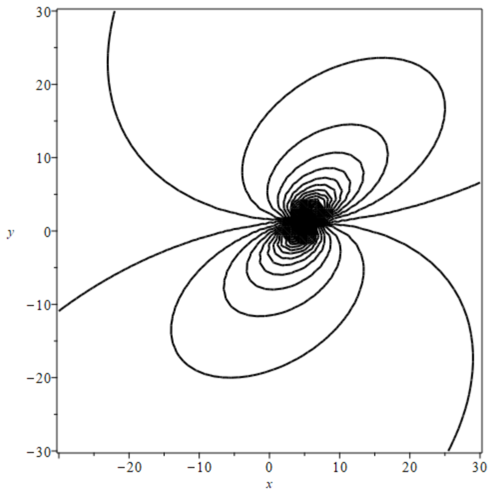

(d) Corresponding contour plot of imaginary lump solution

Figure 3.46. 3D surface and contour plot of Eq. (3.149) plotted when $t = 2, a_1 = -0.3, a_2 = 1, a_3 = 0.1, a_4 = 0.5, b_1 = 0.5, b_2 = 0.2, b_4 = 0.2, c_1 = 1, \gamma_1 = 2, \gamma_2 = 1, \gamma_3 = 1, \alpha = 1, \beta = 1$.

3.6. The (2+1)-dimensional KdV equation including time-variable coefficients

Different types of KdV equations have been studied, for example, the simplified

Hirota's method has been used to investigate three extended higher-order KdV-type equations [**82**]. A variety of techniques have been applied on a new integrable nonlocal modified KdV equation to construct various solutions with distinct physical structures [**83**, **84**]. The geophysical KdV equation has been studied via the homotopy perturbation method [**85**]. In Ref. [**86**], multiple soliton solutions have been offered for modified Korteweg–de-Vries equations. The family of the KdV type equation has been investigated in Ref. [**87**]. A third-order KdV equation has been numerically investigated in Ref. [**88**].

Consider the (2+1)-dimensional KdV equation below

$$v_t + v_{xxx} + 3\left(v\partial_y^{-1}v_x\right)_x = 0. \tag{3.150}$$

Boiti et al. [**89**] was first introduced this equation by apply the conception of the weak Lax pair. This equation is also known as the Boiti-Leon-Manna-Pempinelli equation and showed that it possesses Lax pair test. Also, conservation laws, integrability characteristics, and multi-soliton solutions were offered. Moreover, in the case of $y = x$, Eq. (3.150) will change to the standard KdV equation in (1+1)-dimensions.

Wazwaz [**90**] introduced a new extension of the (2+1)-dimensional KdV equation with constant coefficients, as below

$$u_{ty} + u_{xxxy} + \alpha(u_y u_x)_x + \beta u_{xx} + \gamma u_{yy} = 0, \tag{3.151}$$

that gained upon utilizing the potential

$$v\left(x, y, t\right) = u_y\left(x, y, t\right).$$

Also, derived KdV equation including time-variable coefficients

$$u_{ty} + h\left(t\right) u_{xxxy} + h\left(t\right) \left(u_y u_x\right)_x + h\left(t\right) u_{xx} + k\left(t\right) u_{yy} = 0. \tag{3.152}$$

It is well-known that in some real-world problems nonlinear evolution equations with variable coefficients provide more realistic aspects in the inhomogeneities of media and non-uniformities of boundaries in comparison to their constant coefficients and has several applications in various area such as optical fibers, propagation of wave, rogue waves, and a variety of other physical systems.

In this section of chapter, we study the KdV equation with time-variable coefficients. Firstly, we first aim to use a symbolic computational method to seek lump and periodic wave solutions to Eq. (3.152). The second aim is to obtain M-lump waves, a collision of M-lump wave with soliton solutions, as well as complex multi-soliton solutions via using the simplified Hirota method and a long-wave method.

3.6.1. Lump wave Solutions

In this portion, we consider the KdV equation with time-variable coefficients and defining its logarithmic variable transform as below

$$u\left(x,y,t\right)=\frac{6f\left(x,y,t\right)_x}{f\left(x,y,t\right)}. \tag{3.153}$$

Motivated by early research [**91**], lump solution to the suggested equation including variable-coefficients can be derived from the below assumption

$$f\left(x,y,t\right)=\left(a_1x+a_2y+\int a_3\left(t\right)dt+a_4\right)^2+\left(b_1x+b_2y+\int b_3\left(t\right)dt+b_4\right)^2+c_1. \tag{3.154}$$

Here, both functions $a_3\left(t\right)$, $b_3\left(t\right)$ are differentiable, and $a_i, b_i(i=1,2,3,4)$ defines as real constants. Putting Eq. (3.154) into (3.153), then into (3.152), and make the coefficients of $x^2, y^2, xy, xy, ...$ equal to zero, we obtain

$$\begin{aligned}
a_3\left(t\right)&=\frac{\left(a_2{b_1}^2-2a_1b_1b_2-{a_1}^2a_2\right)h\left(t\right)}{{a_2}^2+{b_2}^2}-a_2k\left(t\right),\\
b_3\left(t\right)&=\frac{\left({a_1}^2b_2-{b_1}^2b_2-2a_1a_2b_1\right)h\left(t\right)}{{a_2}^2+{b_2}^2}-b_2k\left(t\right),\\
c_1&=-\frac{3\left({a_1}^2+{b_1}^2\right)\left(a_1a_2+b_1b_2\right)\left({a_2}^2+{b_2}^2\right)}{\left(a_2b_1-a_1b_2\right)^2}.
\end{aligned} \tag{3.155}$$

Substitutting Eq. (3.155) into Eq. (3.153), we get

$$u=\frac{6\left(2a_1\left(a_4+a_1x+a_2y+\eta_1\right)+2b_1\left(b_4+b_1x+b_2y+\eta_2\right)\right)}{\left(a_4+a_1x+a_2y+\eta_1\right)^2+\left(b_4+b_1x+b_2y+\eta_2\right)^2-\frac{3\left({a_1}^2+{b_1}^2\right)\left(a_1a_2+b_1b_2\right)\left({a_2}^2+{b_2}^2\right)}{\left(a_2b_1-a_1b_2\right)^2}}, \tag{3.156}$$

where

$$\eta_1=\int\left(\frac{\left(a_2{b_1}^2-2a_1b_1b_2-{a_1}^2a_2\right)h\left(t\right)}{{a_2}^2+{b_2}^2}-a_2k\left(t\right)\right)\mathrm{d}t, \tag{3.157}$$

and

$$\eta_2=\int\left(\frac{\left({a_1}^2b_2-{b_1}^2b_2-2a_1a_2b_1\right)h\left(t\right)}{{a_2}^2+{b_2}^2}-b_2k\left(t\right)\right)\mathrm{d}t. \tag{3.158}$$

providing that $a_1a_2+b_1b_2<0$. This solution resembles a lump wave solution as seen in Figure 3.47.

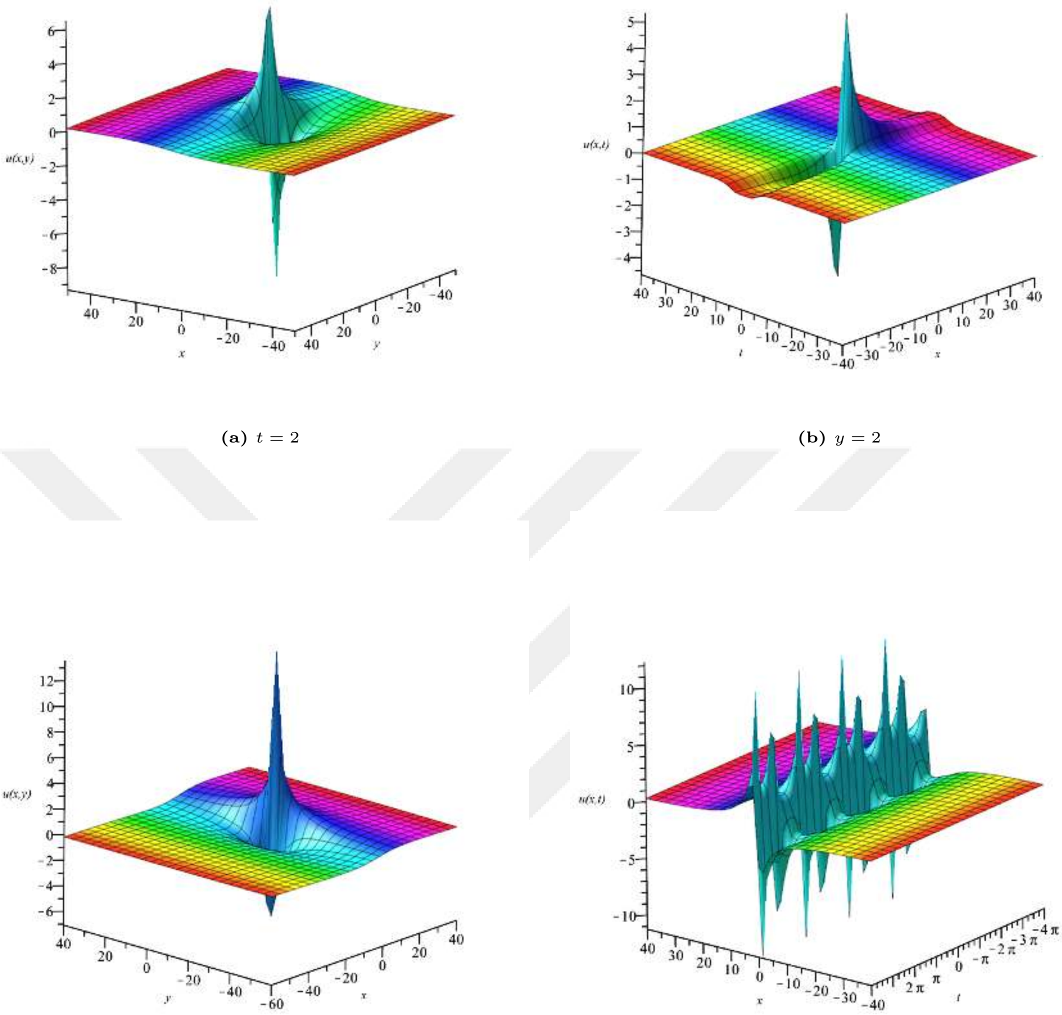

(a) $t = 2$

(b) $y = 2$

(c) $t = \pi/4$

(d) $y = 2$

Figure 3.47. 3-D surfaces of Eq. 3.156 are plotted in case $a_1 = -3, a_2 = \frac{1}{2}, a_3 = 1, a_4 = 2, b_1 = 1, b_2 = 1, b_4 = 1/2, c_1 = 1$. In a, b, c, $h(t) = k(t) = t$, and in d, e, f, $h(t) = cos(t), k(t) = sin(t)$.

When we have

$$a_1 = \mathrm{i}b_1, a_2 = \mathrm{i}b_2, a_3\left(t\right) = -\frac{\mathrm{i}\left({b_1}^2 h\left(t\right) + {b_2}^2 k\left(t\right)\right)}{b_2}, b_3\left(t\right) = -\frac{{b_1}^2 h\left(t\right)}{b_2} - b_2 k\left(t\right), \tag{3.159}$$

and applying this case of solution on Eq. (3.153), we get

$$u = \frac{12b_1\left(b_2\left(\mathrm{i}a_4 + b_4 - \int \eta_3 \mathrm{d}t\right) + b_2 \int \eta_3 \mathrm{d}t\right)}{b_2\left(c_1 + \left(b_1 x + b_2 y - \int \eta_3 \mathrm{d}t + b_4\right)^2 + \left(\mathrm{i}\left(b_1 x + b_2 y\right) - i\int \eta_3 \mathrm{d}t\right)^2 + a4\right)}, \tag{3.160}$$

$$\eta_3 = \frac{{b_1}^2 h\left(t\right)}{b_2} + b_2 k\left(t\right).$$

This solution resembles a complex lump wave of the KdV equation.

3.6.2. M-lump waves

This section of research focuses on constructing rational solutions that can be addressed by using a long-wave method. The multi-soliton solutions of the KdV equation including time-dependent variables have been reported in Ref. [**90**]. Usually, the soliton solutions of differential equations can be derived by employing Hirota's method on Eq. (2.1) , where

$$A_{ij} = \frac{{l_i}^2\left(3{k_i}^2 l_j - 3k_i k_j l_j - 1\right) + l_i l_j\left(2 - 3k_i k_j l_j + 3{k_j}^2 l_j\right) - {l_j}^2}{{l_i}^2\left(3{k_i}^2 l_j + 3k_i k_j l_j - 1\right) + l_i l_j\left(2 + 3k_i k_j l_j + 3{k_j}^2 l_j\right) - {l_j}^2}, \qquad i < j \tag{3.161}$$

$$\psi_i = k_i\left(x + l_i y + w_i\left(t\right)\right) + \alpha_i, \tag{3.162}$$

$$w_i\left(t\right) = -\frac{1}{l_i}\int\left(h\left(t\right) + {k_i}^2 l_i h\left(t\right) + {l_i}^2 k\left(t\right)\right)\mathrm{d}t. \tag{3.163}$$

Here $w_i\left(t\right)$ are differentiable functions and k_i, l_i are real scalars. By using a long-wave method, using $N = 2$ in Eq. (2.1), taking $k_i \to 0$, $e^{\alpha_i} = -1 \ \ (i = 1, 2)$ and $\frac{k_1}{k_2} = O\left(1\right)$, we have

$$f = \phi_1 \phi_2 + B_{12}, \tag{3.164}$$

where

$$\phi_i = x + l_i y + \rho_i t,\ \rho_i\left(t\right) = -\frac{1}{l_1}\int\left(h\left(t\right) + {l_1}^2 k\left(t\right)\right)\mathrm{d}t, \tag{3.165}$$

and

$$B_{ij} = \frac{6 l_i l_j\left(l_i + l_j\right)}{\left(l_i - l_j\right)^2},\ l_{\frac{N}{2}+i} = l_i^*,\ \ \left(i = 1, 2, .., \frac{N}{2}\right) \text{ and } i < j. \tag{3.166}$$

Here $l_1 = a_1 + \mathrm{i}b_1$ and $l_2 = a_1 - \mathrm{i}b_1$. By plugging Eq. (3.164) into logarithmic variable transform, we obtain

$$u = \frac{6\left(2x + \left(l_1 + l_2\right)y - \frac{1}{l_1}\int\left(h\left(t\right) + {l_1}^2 k\left(t\right)\right)\mathrm{d}t - \frac{1}{l_2}\int\left(h\left(t\right) + {l_2}^2 k\left(t\right)\right)\mathrm{d}t\right)}{\frac{6 l_1 l_2\left(l_1 + l_2\right)}{\left(l_1 - l_2\right)^2} + \left(x + l_1 y - \frac{1}{l_1}\int\left(h\left(t\right) + {l_1}^2 k\left(t\right)\right)\mathrm{d}t\right)\left(x + l_2 y - \frac{1}{l_2}\int\left(h\left(t\right) + {l_2}^2 k\left(t\right)\right)\mathrm{d}t\right)}. \tag{3.167}$$

Eq. (3.167) is a one-M-lump solution to Eq. (3.152), and it is shown in Figure 3.48.

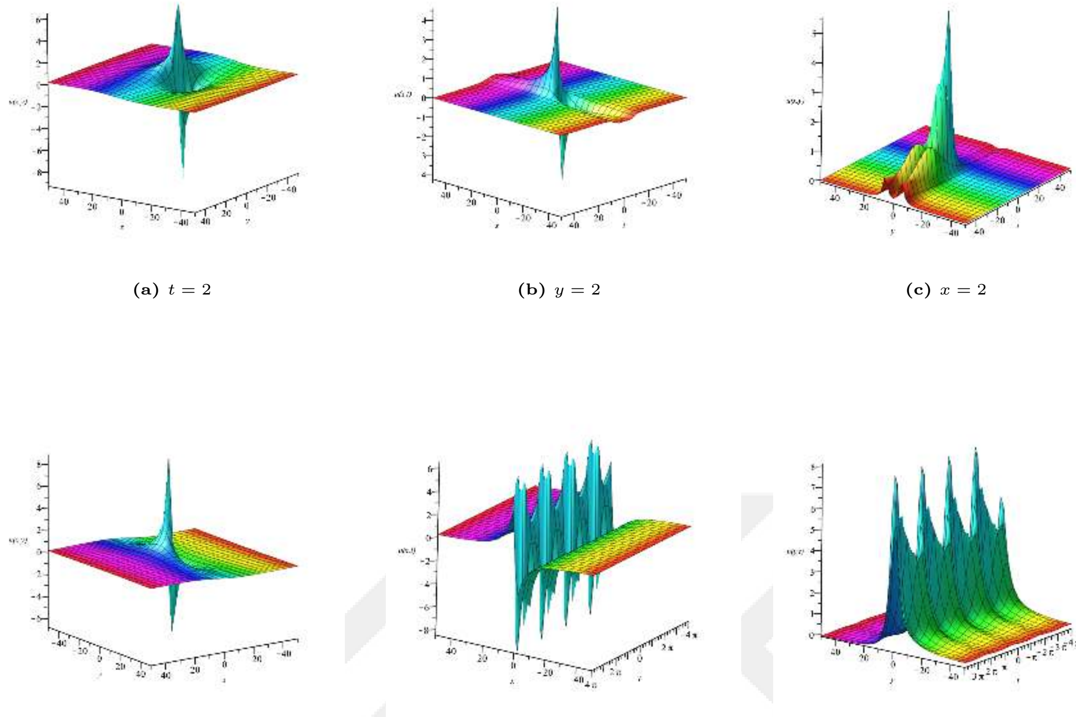

(a) $t = 2$ (b) $y = 2$ (c) $x = 2$

(d) $t = \pi/2$ (e) $y = 2$ (f) $x = 2$

Figure 3.48. 3-D surfaces of Eq. 3.167 are plotted in case $a = -1/10, b = 1/2$. In a, b, c, $h(t) = k(t) = t$, and in d, e, f, $h(t) = sin(t)$ while $k(t) = cos(t)$

To derive 2-M-lump solution to the extended KdV equation, we choose $N = 4$ in Eq. (2.1), $e^{\alpha_i} = -1$ $(i = 1, 2, 3, 4)$ and taking $k_i \to 0$. Thus we find

$$\begin{aligned} f = {} & \phi_1\phi_2\phi_3\phi_4 + B_{12}\phi_3\phi_4 + B_{13}\phi_2\phi_4 + B_{14}\phi_2\phi_3 + B_{23}\phi_1\phi_4 \\ & + B_{24}\phi_1\phi_3 + B_{34}\phi_1\phi_2 + B_{12}\phi_{34} + B_{13}B_{24} + B_{14}B_{23}. \end{aligned} \tag{3.168}$$

Where ϕ_1, ϕ_2, ϕ_3, ϕ_4, ρ_i, B_{ij} $(i < j)$, and $l_{\frac{N}{2}+i}, (i = 1, 2, .., N)$ are determined in Eqs. (3.165) and (3.166), respectively. We use $l_1 = a_1 + ib_1$, $l_2 = a_3 + ib_3$, $l_3 = l_1^*$ and $l_4 = l_2^*$, where $*$ is a notation for the complex conjugate. Substitutting Eq. (3.168) into Eq. (3.153), a result gives double-M-lump solution to the KdV equation as reported in Figure 3.49.

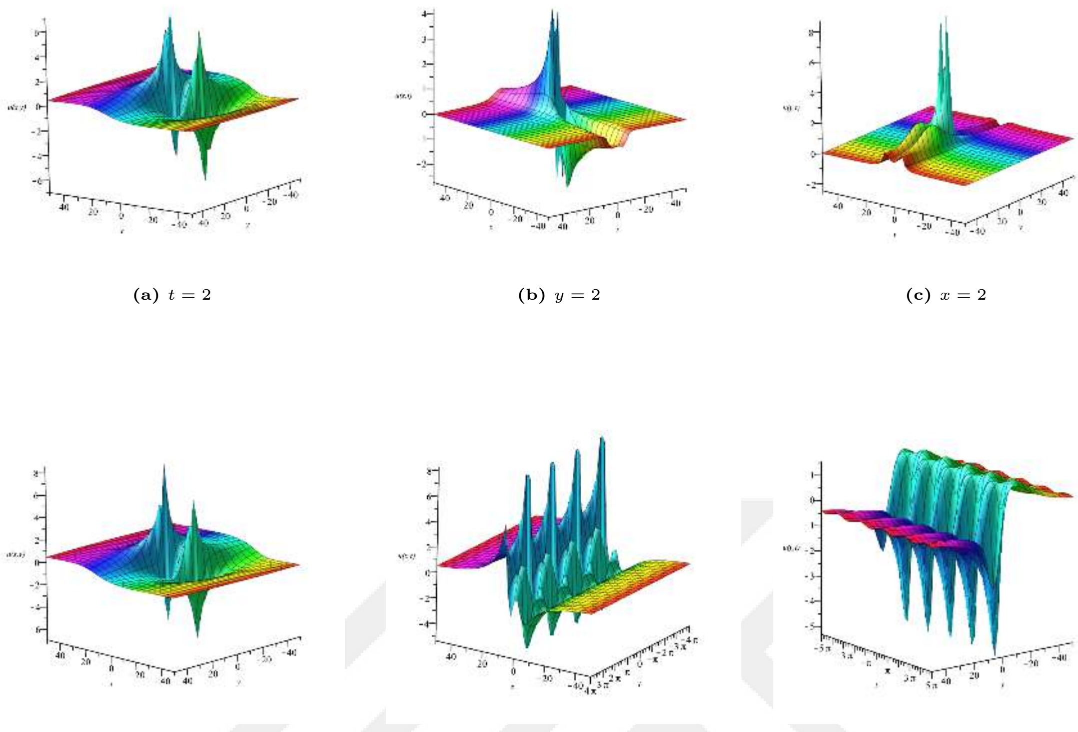

(a) $t = 2$ **(b)** $y = 2$ **(c)** $x = 2$

(d) $t = \pi/4$ **(e)** $y = 2$ **(f)** $x = 2$

Figure 3.49. 3-D surfaces of two-M-lump wave are plotted in case $a_1 = -\frac{1}{10}, b_1 = \frac{1}{2}, a_2 = -1/4, b_2 = \frac{1}{3}$. In (a,b,c), $h(t) = k(t) = t$, and in (d,e,f), $h(t) = \sin(t)$ while $k(t) = \cos(t)$

To construct 3-M-lump solution to the extended KdV equation, we choose $N = 6$ in Eq. (2.1), $e^{\alpha_i} = -1$ $(i = 1, 2, 3, 4, 5, 6)$ and taking $k_i \to 0$. A result gives f_6 that have 306 terms. Putting f_6 into Eq. (3.153) and letting $l_2 = l_4^* = a_1 + \mathrm{i}b_1$, $l_3 = l_1^* = a_2 + \mathrm{i}b_2$ and $l_6 = l_5^* = a_3 + \mathrm{i}b_3$, we get a three-M-lump wave solution and its features are presented in Figure 3.50.

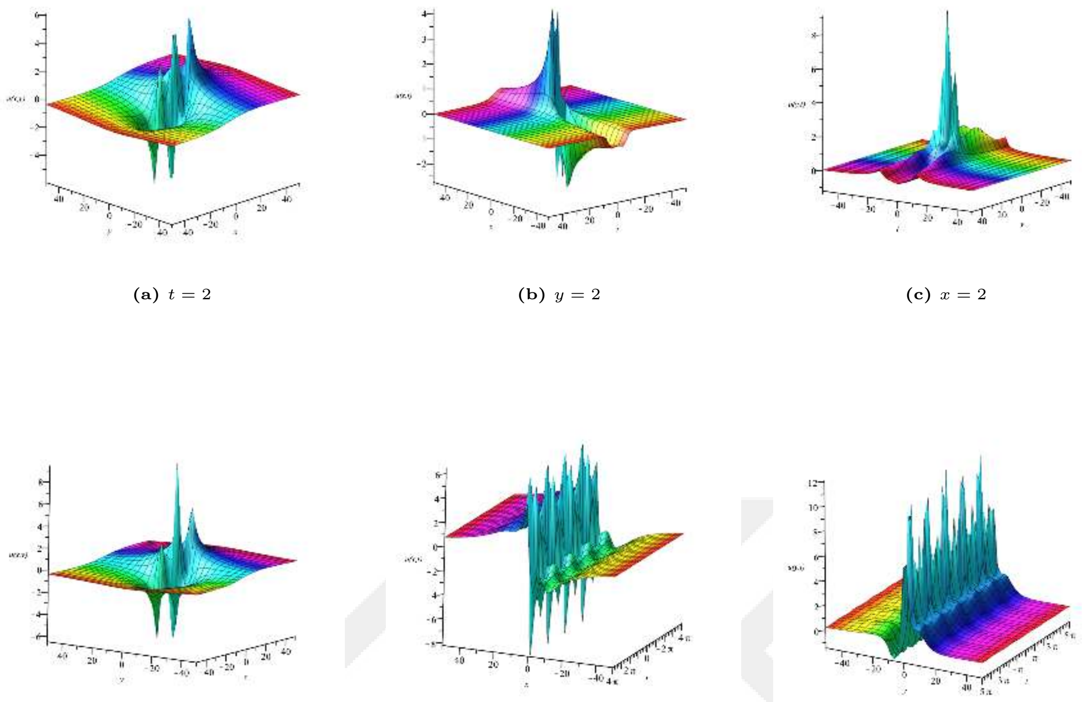

(a) $t = 2$ **(b)** $y = 2$ **(c)** $x = 2$

(d) $t = \pi/4$ **(e)** $y = 2$ **(f)** $x = 2$

Figure 3.50. 3-D surfaces of three-M-lump wave are plotted in case $a_1 = -\frac{1}{2}, b_1 = \frac{3}{2}, a_2 = -\frac{1}{3}, b_2 = 1, a_3 = -\frac{1}{9}, b_3 = \frac{1}{2}$. In (a,b,c), $h(t) = k(t) = t$, and in (d,e,f), $h(t) = \sin(t)$ while $k(t) = \cos(t)$

3.6.3. Physical Interaction Phenomena

This section of research focuses on constructing the physical interaction wave solutions to the KdV equation. We begin by constructing a solution that appears of collision of 1-M-lump with 1-soliton solutions. In order to achieve this, let $N = 3$ in Eq. (2.1), taking $k_i \to 0, (i = 1, 2)$ and $\frac{k_1}{k_2} = O(1)$, as a result, Eq. (19) can be formulated as follows

$$f = \phi_1\phi_2 + B_{12} + (\phi_1\phi_2 + B_{12} + C_{23}\phi_1 + C_{13}\phi_2 + C_{13}C_{23})e^{\psi_3}. \tag{3.169}$$

Where ψ_3 is defined in Eq. (3.162), $\phi_i\,(i = 1, 2)$ are determined in Eq. (3.165) and B_{12} is specified in Eq. (3.166). The constants C_{13}, C_{23} are stated as below

$$C_{mn} = -\frac{6k_n l_n \left({l_m}^2 + l_m l_n\right)}{2l_m l_n - {l_n}^2 + 3{k_n}^2 l_m {l_n}^2 - {l_m}^2}, \;\; m < n. \tag{3.170}$$

Substituting Eqs. (3.170) and (3.169) into Eq. (3.153), the result yields a solution that represents a collision of 1-M-lump with 1-soliton wave solutions, as presented in Figure 3.51.

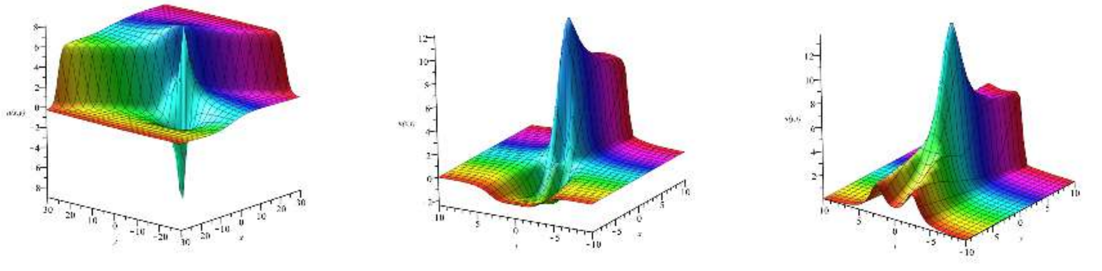

(a) $t = 2$ **(b)** $y = 2$ **(c)** $x = 2$

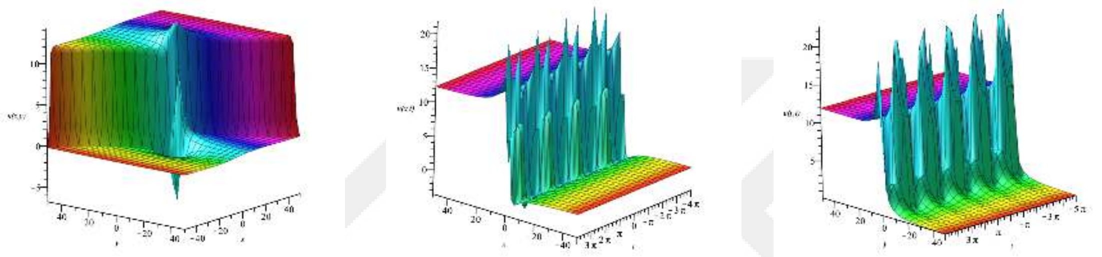

(d) $t = \pi/4$ **(e)** $y = 2$ **(f)** $x = 2$

Figure 3.51. 3-D surfaces of collision between M-lump and one-soliton waves are plotted in case $a = -1/10, b = 1/2, l_3 = 1, k_3 = 1$. In (a,b,c), $h(t) = k(t) = t$, and in (d,e,f), $h(t) = \sin(t)$ while $k(t) = \cos(t)$

To construct interaction between two-soliton and one-M-lump wave, we have

$$\begin{aligned} f =&\phi_1\phi_2 + B_{12} + \Psi_1 \mathrm{e}^{\phi_3} + \Psi_2 \mathrm{e}^{\psi_4} - \\ &A_{34}\mathrm{e}^{\psi_3+\psi_4}\left(\phi_1\phi_2 + B_{12} - C_{14}C_{23} - C_{13}C_{24} - \Psi_1 - \Psi_2\right), \end{aligned} \tag{3.171}$$

where

$$\Psi_1 = \phi_1\phi_2 + B_{12} + C_{23}\phi_1 + C_{13}\phi_2 + C_{13}C_{23},$$

$$\Psi_2 = \phi_1\phi_2 + B_{12} + C_{24}\phi_1 + C_{14}\phi_2 + C_{14}C_{24}.$$

The constants B_{ij} and C_{mn} are defined in Eq. (3.166) and Eq. (3.170). The functions ψ_i and ϕ_i are defined in Eq. (3.162) and Eq. (3.165). Substituting Eq. (3.171) into Eq. (3.153), gives a solution that represents interaction phenomena of a one-M-lump with a two-soliton wave solutions as seen in Figure 3.52.

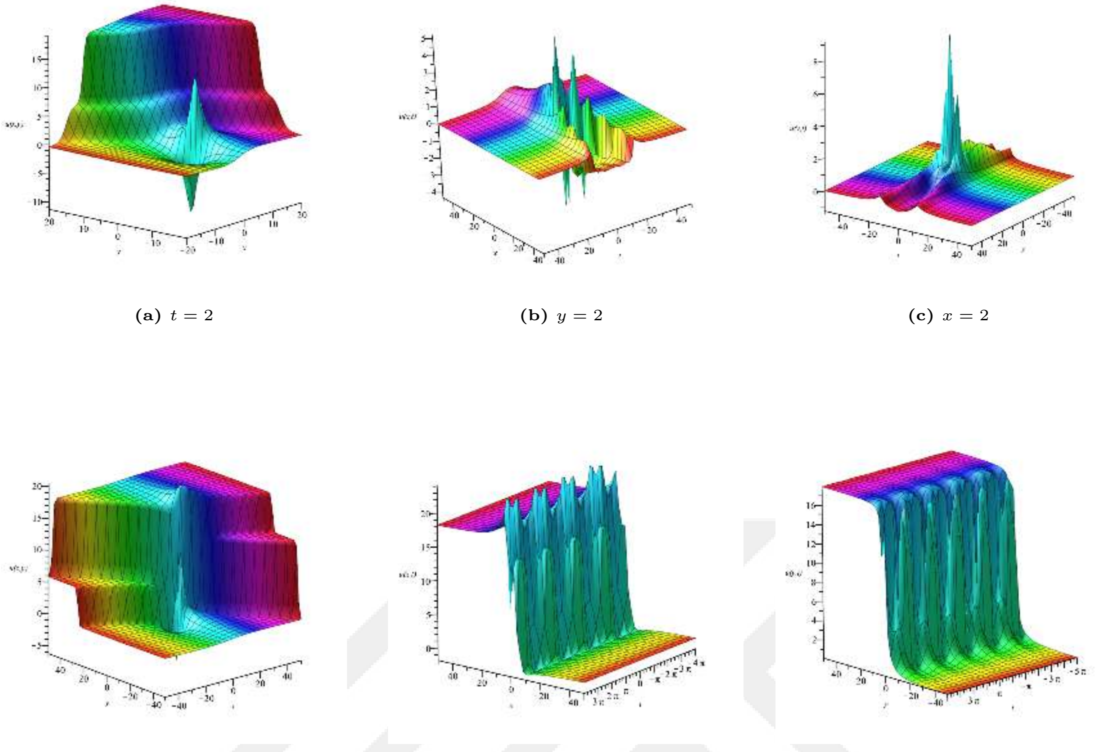

(a) $t = 2$ **(b)** $y = 2$ **(c)** $x = 2$

(d) $t = \pi/4$ **(e)** $y = 2$ **(f)** $x = 2$

Figure 3.52. 3-D surfaces are plotted for a collision of a M-lump wave with a two-soliton wave in case $a = -1/20, b = 1/2, l_3 = 1, k_3 = 1, l_4 = 1, k_4 = 2$. In a, b, c, $h(t) = k(t) = t$, and in d, e, f, $h(t) = sin(t)$ while $k(t) = cos(t)$

Motivated by Ref. [**63**] and taking $N = 5$ in Eq (2.1), an assumption that use to derive a collision of two-M-lump wave with one-soliton solution can be formulated as follows

$$\begin{aligned} f = {} & \phi_1\phi_2\phi_3\phi_4 + B_{34}\phi_1\phi_2 + B_{24}\phi_1\phi_3 + B_{23}\phi_1\phi_4 + B_{14}\phi_2\phi_3 + B_{13}\phi_2\phi_4 \\ & + B_{12}\phi_3\phi_4 + Q_1 e^{k_5(x+l_5y+w_5+\alpha_5(t))} + B_{14}B_{23} + B_{13}B_{24} + B_{12}B_{34}, \end{aligned} \tag{3.172}$$

where

$$\begin{aligned} Q_1 = {} & \phi_1\phi_2\phi_3\phi_4 + C_{45}\phi_1\phi_2\phi_3 + C_{15}\phi_2\phi_3\phi_4 + C_{25}\phi_1\phi_3\phi_4 + C_{35}\phi_1\phi_2\phi_4 + \\ & (B_{34} + C_{35}C_{45})\,\phi_1\phi_2 + (B_{24} + C_{25}C_{45})\,\phi_1\phi_3 + (B_{14} + C_{15}C_{45})\,\phi_2\phi_3 + \\ & (B_{23} + C_{25}C_{35})\,\phi_1\phi_4 + (B_{13} + C_{15}C_{35})\,\phi_2\phi_4 + (B_{12} + C_{15}C_{25})\,\phi_3\phi_4 + \\ & (B_{34}C_{25} + B_{24}C_{35} + B_{23}C_{45} + C_{25}C_{35}C_{45})\,\phi_1 + (B_{34}C_{15} + B_{14}C_{35})\,\phi_2 + \\ & (B_{13}C_{45} + C_{15}C_{35}C_{45})\,\phi_2 + (B_{24}C_{15} + B_{14}C_{25} + B_{12}C_{45} + C_{15}C_{25}C_{45})\,\phi_3 \\ & + (B_{23}C_{15} + B_{13}C_{25} + B_{12}C_{35} + C_{15}C_{25}C_{35})\,\phi_4 + B_{14}B_{23} + B_{13}B_{24} + \\ & B_{12}B_{34} + B_{34}C_{15}C_{25} + B_{24}C_{15}C_{35} + B_{14}C_{25}C_{35} + B_{23}C_{15}C_{45} + B_{13}C_{25}C_{45} \\ & + B_{12}C_{35}C_{45} + C_{15}C_{25}C_{35}C_{45} \end{aligned}$$

All necessary constants and functions are defined in this paper. Now, to construct a collision of two-M-lump wave with one-soliton wave, we put Eq. (3.172) into Eq. (3.153), a result gives an interaction physical phenomenon as presented in Figure 3.53.

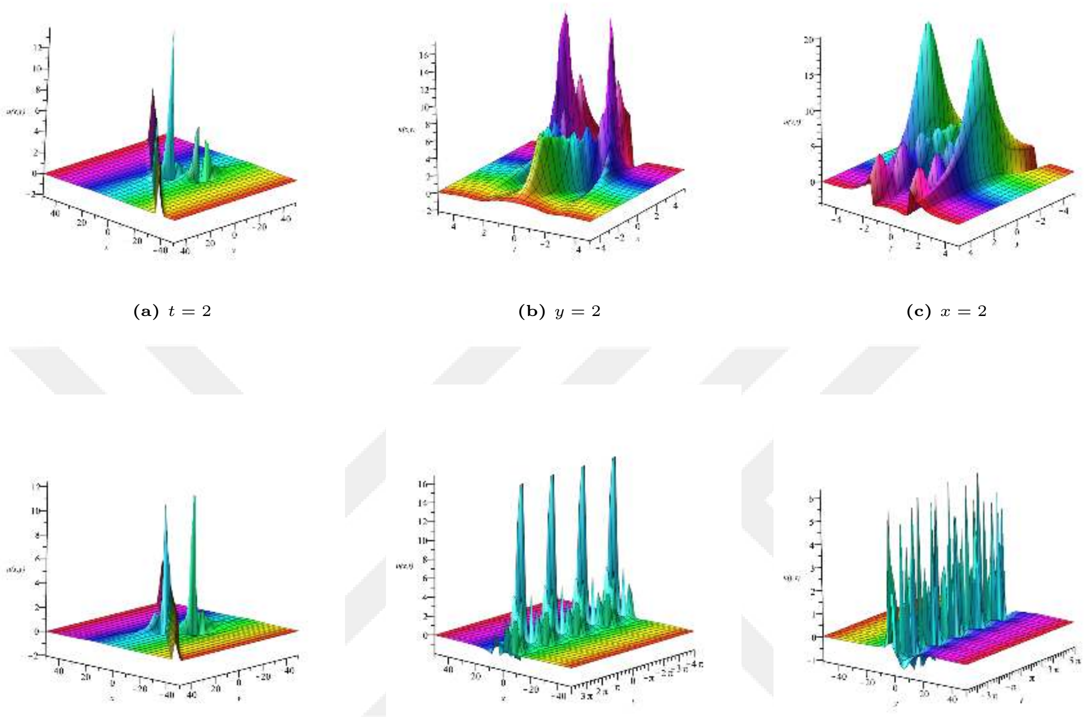

(a) $t = 2$ **(b)** $y = 2$ **(c)** $x = 2$

(d) $t = \pi/4$ **(e)** $y = 2$ **(f)** $x = 2$

Figure 3.53. 3-D surfaces are plotted for a collision of a two-M-lump wave with a one-soliton wave in case $a = -1/10, b = -1/2, c = -1/4, d = 1/3, l_5 = 1, k_5 = 2$. In (a,b,c), $h(t) = k(t) = t$, and in (d,e,f), $h(t) = \sin(t)$ while $k(t) = \cos(t)$.

3.6.4. Complex soliton waves

In this section, we aim to obtain complex multi-soliton solutions to a KdV equation by using Mathematica symbolic computations. Let,

$$f = \mathrm{i} + \mathrm{e}^{\psi_1}, \tag{3.173}$$

$$f = \mathrm{i} + e^{\psi_1} + e^{\psi_2} + \xi_{12} e^{\psi_1+\psi_2}, \tag{3.174}$$

$$f = \mathrm{i} + e^{\psi_1} + e^{\psi_2} + e^{\psi_3} + \xi_{12} e^{\psi_1+\psi_2} + \xi_{13} e^{\psi_1+\psi_3} + \xi_{23} e^{\psi_2+\psi_3} + \mathrm{i}\xi_{123} e^{\psi_1+\psi_2+\psi_3}, \tag{3.175}$$

where $\psi_i (i = 1, 2, ..., N)$ are defined in Eq. (3.162) and

$$\xi_{ij} = \frac{\mathrm{i}\left({l_i}^2\left(1-3{k_i}^2 l_j+3k_i k_j l_j\right)+l_i l_j\left(-2+3k_i k_j l_j-3{k_j}^2 l_j\right)+{l_j}^2\right)}{{l_i}^2\left(3{k_i}^2 l_j+3k_i k_j l_j-1\right)+l_i l_j\left(2+3k_i k_j l_j+3{k_j}^2 l_j\right)-{l_j}^2}, \qquad i<j. \tag{3.176}$$

Plugging (3.173) into (3.153), a result is

$$u\left(x,y,t\right) = 6k_1 + \frac{6k_1}{\mathrm{i}e^{k_1\left(x+l_1 y-\frac{\int\left(\left(1+{k_1}^2 l_1\right)h(t)+{l_1}^2 k(t)\right)\mathrm{d}t}{l_1}\right)+\alpha_1}-1}. \tag{3.177}$$

This equation represents a complex one-soliton wave and its features are showed in Figure 3.54.

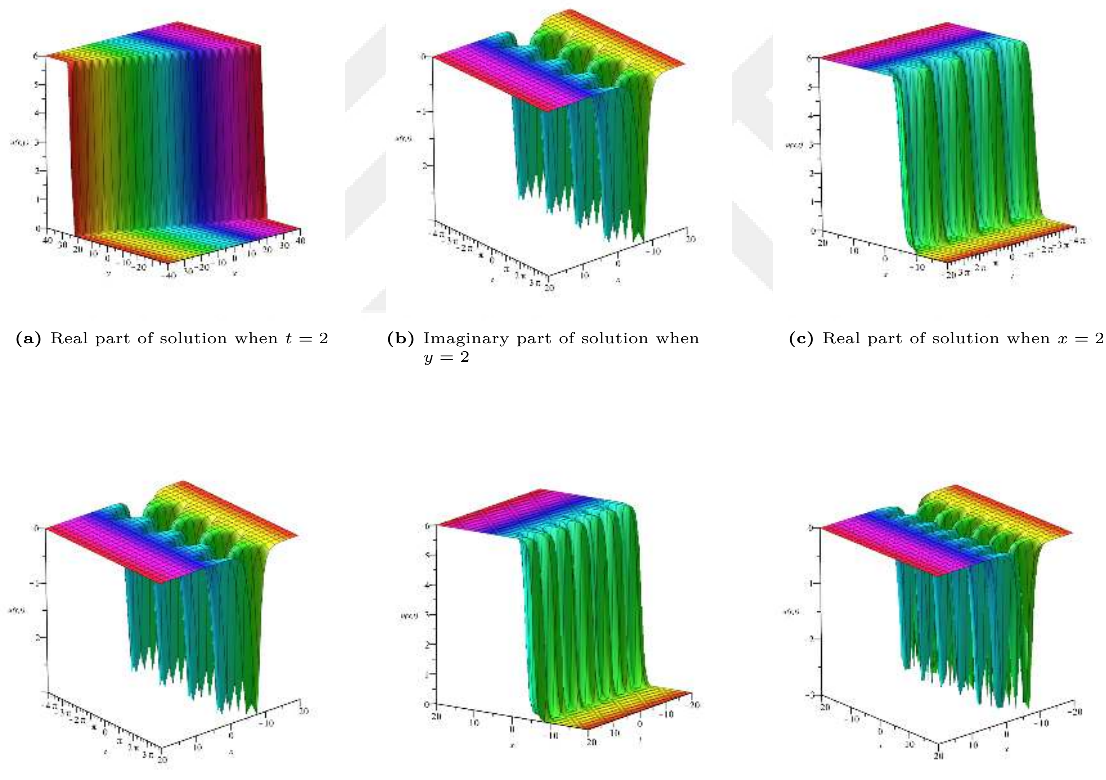

(a) Real part of solution when $t = 2$

(b) Imaginary part of solution when $y = 2$

(c) Real part of solution when $x = 2$

(d) Imaginary part of solution when $t = \pi/4$

(e) Real part of solution when $y = 2$

(f) Imaginary part of solution when $x = 2$

Figure 3.54. 3-D surfaces of a complex single-soliton wave solution plotted in case $k_1 = 1, l_1 = 2, \alpha_1 = 0$. In (a,b,c), $h(t) = k(t) = t$ and in (d,e,f), $h(t) = \sin(t)$ while $k(t) = \cos(t)$.

By substituting Eq. (3.174) into a variable transform equation, we obtain a complex double-soliton wave (see Figure 3.55). Moreover, by inserting Eq. (3.175) into Eq. (3.153), a complex triple-soliton solution is constructed and a result is presented graphically as seen in Figure 3.56.

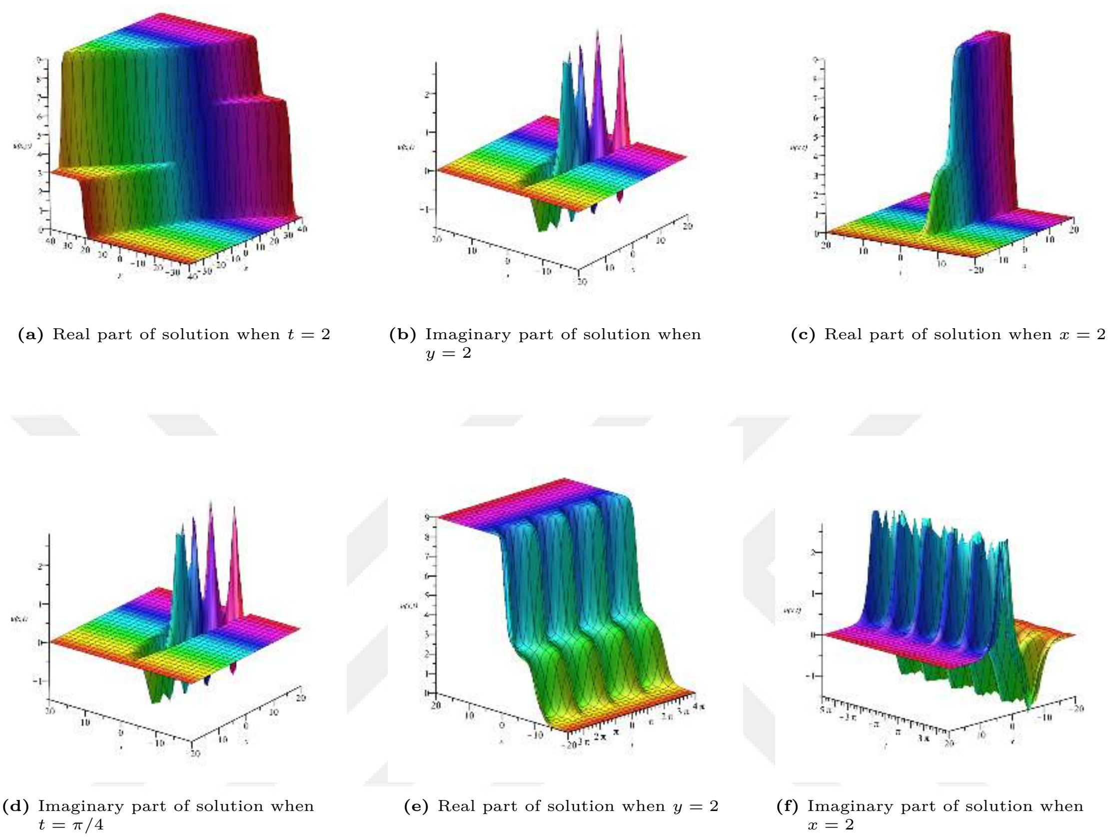

(a) Real part of solution when $t = 2$

(b) Imaginary part of solution when $y = 2$

(c) Real part of solution when $x = 2$

(d) Imaginary part of solution when $t = \pi/4$

(e) Real part of solution when $y = 2$

(f) Imaginary part of solution when $x = 2$

Figure 3.55. 3-D surfaces of a complex double-soliton wave solution plotted in case $k_1 = 1, l_1 = 1, k_2 = \frac{1}{2}, l_2 = 2, \alpha_1 = 0, \alpha_2 = 2$. In (a,b,c), $h(t) = k(t) = t$, and in (d,e,f), $h(t) = \sin(t)$ while $k(t) = \cos(t)$.

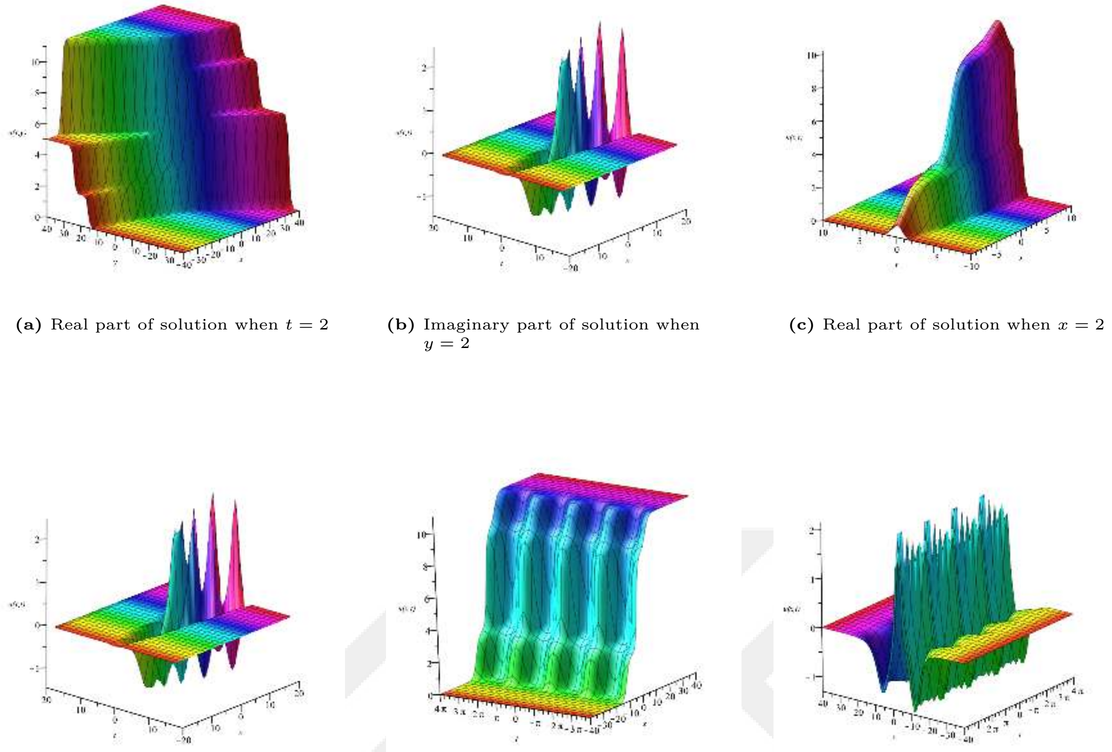

(a) Real part of solution when $t = 2$ **(b)** Imaginary part of solution when $y = 2$ **(c)** Real part of solution when $x = 2$

(d) Imaginary part of solution when $t = \pi/4$ **(e)** Real part of solution when $y = 2$ **(f)** Imaginary part of solution when $x = 2$

Figure 3.56. 3-D surfaces of a complex triple-soliton wave solution plotted in case $k_1 = 1, l_1 = 1, k_2 = \frac{1}{2}, l_2 = 2, k_3 = \frac{1}{3}, l_3 = 3, \alpha_1 = 0, \alpha_2 = 2, \alpha_3 = 0$. In (a,b,c), $h(t) = k(t) = t$, and in (d,e,f), $h(t) = \sin(t)$ while $k(t) = \cos(t)$.

3.7. The (3+1)-dimensional generalized Kadomtsev-Petviashvili equation

The goal of this study is to investigate rational solutions and their interaction with soliton solution to the new (3+1)-dimensional generalized Kadomtsev-Petviashvili (gKP) equation

$$u_{tx} + u_{ty} + u_{tz} - u_{zz} + 3(u_x u_y)_x + u_{xxxy} = 0. \tag{3.178}$$

Authors in Ref. [**92**] reported some new exact periodic solitary-wave solutions. Liu et al. [**93**] offered interaction solutions of the rational function include trigonometric, exponential, and hyperbolic functions. To our knowledge, no literature addressed M-lump wave and their interaction with one-, and two-soliton solutions.

This section of thesis is organized as follows: In subsection one, single-M-lump, double-M-lump and triple-M-lump wave solutions for a gKP equation are revealed. The interaction solutions of single-M-lump waves with one, and two-soliton solutions, also an interaction between double-M-lump wave and single-soliton solutions are presented in subsection 2.

3.7.1. M-lump wave solutions

Consider the variable transform

$$u\left(x,y,z,t\right)=2(\log f\left(x,y,z,t\right))_{x}, \tag{3.179}$$

and using it on Eq. (3.179), we have

$$\left(D_tD_x+D_tD_y+D_tD_z+{D_x}^3D_y-{D_z}^2\right)f.f=0.$$

Usually, soliton solutions are constructed by using Eq. (2.1). Here, we let the dispersion variable ψ_i is defined as

$$\psi_i=k_i\left(x+l_iy+(l_i-1)z+w_it\right)+\alpha_i, \tag{3.180}$$

where the dispersion relation is

$$w_i=\frac{1}{2}\left(\frac{1}{l_i}+l_i-{k_i}^2-2\right), \tag{3.181}$$

and the phase shift A_{ij} is

$$A_{ij}=\frac{{l_j}^2+{l_i}^2\left(1+3k_i\left(k_i-k_j\right)l_j\right)+l_il_j\left(3k_j\left(k_j-k_i\right)l_j-2\right)}{{l_n}^2+{l_i}^2\left(1+3k_i\left(k_i+k_j\right)l_j\right)+l_il_j\left(3k_j\left(k_i+k_j\right)l_j-2\right)}. \tag{3.182}$$

In Ref. [**94**], Wazwaz examined the multi-soliton solutions of Eq. (3.178).

Now, we use the long-wave method on Eq. (2.1) by taking $N=2$, $k_i\to 0$, $e^{\alpha_i}=-1\ \ (i=1,2)$ and $\frac{k_1}{k_2}=O\left(1\right)$, then Eq. (2.1) and Eqs. (3.180-3.182), respectively becomes

$$f=\phi_1\phi_2+B_{12}. \tag{3.183}$$

Here

$$\phi_i=x+l_iy+(l_i-1)z+\rho_it,\quad \rho_i=\frac{\left(-1+l_i\right)^2}{2l_i}, \tag{3.184}$$

and

$$B_{ij}=-\frac{6l_il_j\left(l_i+l_j\right)}{\left(l_i-l_j\right)^2},\ l_{\frac{N}{2}+i}=l_i^*,\ \ \left(i=1,2,...,\frac{N}{2}\right)\text{ and } i<j. \tag{3.185}$$

By plugging Eqs. (3.184-3.186) into Eq. (3.183), then into Eq. (3.179), we get

$$
\begin{aligned}
u &= 2\log\left(\left(x' + a_1 y' + (a_1-1)\,z'\right)^2 + {b_1}^2 (y'+z')^2 + \frac{3a_1\left({a_1}^2+{b_1}^2\right)}{{b_1}^2}\right)_x \\
&= \frac{4\left(x' + a_1 y' + (a_1-1)\,z'\right)}{\left(x' + a_1 y' + (a_1-1)\,z'\right)^2 + {b_1}^2 (y'+z')^2 + \frac{3a_1\left({a_1}^2+{b_1}^2\right)}{{b_1}^2}},
\end{aligned}
\tag{3.186}
$$

where

$$x' = x + \left(\frac{a_1}{\left({a_1}^2+{b_1}^2\right)} - \frac{1}{2}\right)t,$$

$$y' = y - \frac{1}{2\left({b_1}^2+{a_1}^2\right)}t,$$

and

$$z' = z + \frac{1}{2}t.$$

This is a one-M-lump wave for a gKP equation as stated in Figure 3.57. This rational solution is a permanent wave solution decaying as $O\left(\frac{1}{x^2}, \frac{1}{y^2}, \frac{1}{z^2}\right)$ for $|x|, |y|, |z| \to \infty$ and moving with the velocity

$$v_x = \frac{1}{2} - \frac{a_1}{\left({a_1}^2+{b_1}^2\right)}, \qquad v_y = \frac{1}{2\left({b_1}^2+{a_1}^2\right)}, \qquad v_z = -\frac{1}{2}.$$

It is interesting to know that this wave is travel along the following straight line

$$y = \frac{\left({a_1}^2+{b_1}^2-1\right)\left(\sqrt{3\left(a_1{b_1}^2\left({a_1}^2+{b_1}^2\right)^5\right)} + {b_1}^2\left({a_1}^2+{b_1}^2\right)^2(z-x)\right)}{2{b_1}^2\left((a_1-1)\,a_1+{b_1}^2\right)\left({a_1}^2+{b_1}^2\right)^2} - z.$$

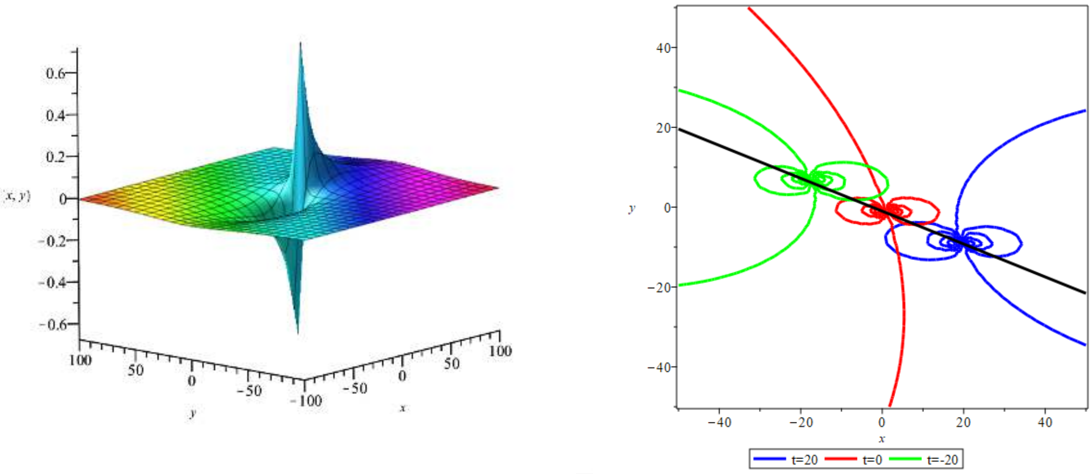

(a) $z = 1, t = 5$

(b) 1-M-lump solution at different period of time

Figure 3.57. M-lump wave of Eq. (3.187) when $a_1 = \frac{1}{3}, b_1 = 2$.

To offer a 2-M-lump solution to a g KP equation, we let $N = 4$ in Eq. (2.1), taking $e^{\alpha_i} = -1$ $(i = 1, 2, 3, 4)$, and $k_i \to 0$, we get

$$\begin{aligned} f = {} & \phi_1\phi_2\phi_3\phi_4 + B_{12}\phi_3\phi_4 + B_{13}\phi_2\phi_4 + B_{14}\phi_2\phi_3 + B_{23}\phi_1\phi_4 \\ & + B_{24}\phi_1\phi_3 + B_{34}\phi_1\phi_2 + B_{12}\phi_{34} + B_{13}\phi_{24} + B_{14}B_{23}. \end{aligned} \tag{3.187}$$

Where $\phi_1, \phi_2, \phi_3, \phi_4$, ρ_i, B_{ij} $(i < j)$ and $l_{\frac{N}{2}+m}$ are defined in Eqs. (3.184) and (3.185), respectively. By putting Eq. (3.187) into Eq. (3.179), an outcome is a double-M-lump solution to the studied equation as shown in Figure 3.58. The two-M-lump wave travels along two different lines

$$y_1 = \frac{\left(a_1{}^2 + b_1{}^2 - 1\right)\left(\sqrt{3\left(a_1 b_1{}^2\left(a_1{}^2 + b_1{}^2\right)^5\right)} + b_1{}^2\left(a_1{}^2 + b_1{}^2\right)^2 (z - x)\right)}{2b_1{}^2\left(\left(a_1 - 1\right)a_1 + b_1{}^2\right)\left(a_1{}^2 + b_1{}^2\right)^2} - z,$$

and

$$y_2 = \frac{\left(a_2{}^2 + b_2{}^2 - 1\right)\left(\sqrt{3\left(a_2 b_2{}^2\left(a_2{}^2 + b_2{}^2\right)^5\right)} + b_2{}^2\left(a_2{}^2 + b_2{}^2\right)^2 (z - x)\right)}{2b_2{}^2\left(\left(a_2 - 1\right)a_2 + b_2{}^2\right)\left(a_2{}^2 + b_2{}^2\right)^2} - z.$$

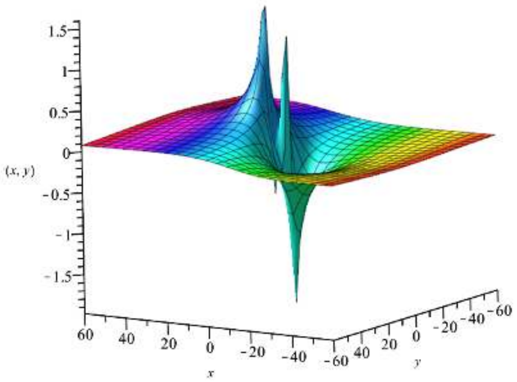

(a) $z = 1, t = 5$

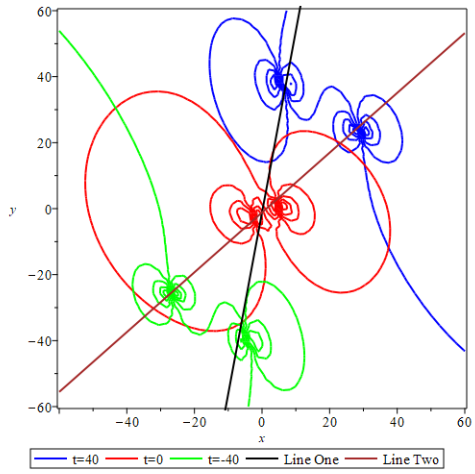

(b) 2-M-lump solution at different period of time

Figure 3.58. Two-M-lump wave when $a_1 = \frac{1}{4}, b_1 = \frac{1}{2}, a_2 = \frac{1}{5}, b_1 = \frac{2}{3}$.

To construct a 3-M-lump solution of Eq. (3.179), we use $k_i \to 0$, $e^{\alpha_i} = -1$, $(i = 1, 2, 3, 4, 5, 6)$ and taking $N = 6$ in Eq. (2.1), we have

$$\begin{aligned}
f_6 = {} & \phi_1\phi_2\phi_3\phi_4\phi_5\phi_6 + B_{12}B_{34}B_{56} + B_{12}B_{35}B_{46} + B_{12}B_{45}B_{36} + B_{13}B_{24}B_{56} + \\
& B_{13}B_{25}B_{46} + B_{13}B_{45}B_{26} + B_{23}B_{14}B_{56} + B_{14}B_{25}B_{36} + B_{14}B_{35}B_{26} + B_{24}B_{15}B_{36} + \\
& B_{34}B_{15}B_{26} + B_{23}B_{15}B_{46} + B_{23}B_{45}B_{16} + B_{24}B_{35}B_{16} + B_{34}B_{25}B_{16} + \phi_2\phi_3\phi_4\phi_5B_{16} + \\
& \phi_2\phi_3\phi_5\phi_6B_{14} + \phi_2\phi_3\phi_4\phi_6B_{15} + \phi_3\phi_4\phi_5\phi_6B_{12} + \phi_2\phi_4\phi_5\phi_6B_{13} + \phi_1\phi_2\phi_4\phi_6B_{35} + \\
& \phi_1\phi_2\phi_4\phi_5B_{36} + \phi_1\phi_4\phi_5\phi_6B_{23} + \phi_1\phi_3\phi_5\phi_6B_{24} + \phi_1\phi_3\phi_4\phi_6B_{25} + \phi_1\phi_3\phi_4\phi_5B_{26} + \\
& \phi_1\phi_2\phi_3\phi_4B_{56} + \phi_1\phi_2\phi_3\phi_6B_{45} + \phi_1\phi_2\phi_3\phi_5B_{46} + \phi_1\phi_2\phi_5\phi_6B_{34} + \phi_1\phi_2B_{34}B_{56} + \\
& \phi_1\phi_2B_{35}B_{46} + \phi_1\phi_2B_{45}B_{36} + \phi_1B_{23}\phi_4B_{56} + \phi_1B_{23}B_{45}\phi_6 + \phi_1B_{23}\phi_5B_{46} + \\
& \phi_1\phi_3B_{24}B_{56} + \phi_1\phi_6B_{24}B_{35} + \phi_1\phi_5B_{24}B_{36} + \phi_1\phi_3B_{25}B_{46} + \phi_1\phi_6B_{34}B_{25} + \\
& \phi_1\phi_4B_{25}B_{36} + \phi_1\phi_3B_{45}B_{26} + \phi_1\phi_5B_{34}B_{26} + \phi_1\phi_4B_{35}B_{26} + \phi_4\phi_5B_{12}B_{36} + \\
& \phi_3\phi_4B_{12}B_{56} + \phi_3\phi_6B_{12}B_{45} + \phi_3\phi_5B_{12}B_{46} + \phi_5\phi_6B_{12}B_{34} + \phi_4\phi_6B_{12}B_{35} + \\
& \phi_5\phi_6B_{13}B_{24} + \phi_4\phi_6B_{13}B_{25} + \phi_4\phi_5B_{13}B_{26} + \phi_2\phi_4B_{13}B_{56} + \phi_2\phi_6B_{13}B_{45} + \\
& \phi_2\phi_5B_{13}B_{46} + \phi_2\phi_3B_{14}B_{56} + \phi_2\phi_6B_{14}B_{35} + \phi_2\phi_5B_{14}B_{36} + \phi_5\phi_6B_{23}B_{14} + \\
& \phi_3\phi_6B_{14}B_{25} + \phi_3\phi_5B_{14}B_{26} + \phi_4\phi_6B_{23}B_{15} + \phi_3\phi_6B_{24}B_{15} + \phi_3\phi_4B_{15}B_{26} + \\
& \phi_2\phi_3B_{15}B_{46} + \phi_2\phi_6B_{34}B_{15} + \phi_2\phi_4B_{15}B_{36} + \phi_2\phi_4B_{35}B_{16} + \phi_4\phi_5B_{23}B_{16} + \\
& \phi_3\phi_5B_{24}B_{16} + \phi_3\phi_4B_{25}B_{16} + \phi_2\phi_3B_{45}B_{16} + \phi_2\phi_5B_{34}B_{16}.
\end{aligned} \tag{3.188}$$

We note that $\phi_1, \phi_2, \phi_3, \phi_4, \phi_5, \phi_6$, B_{ij} and $l_{\frac{N}{2}+i}$ are defined in Eq. (3.184) and Eq. (3.185), respectively. As a result of substituting Eq. (3.188) with its related equations into Eq. (3.179), a triple-M-lump solution is obtained as seen in Figure 3.59. We note that $l_1 = a_1 + \mathrm{i}b_1$, $l_2 = a_2 + \mathrm{i}b_2$, $l_3 = a_3 + \mathrm{i}b_3$, $l_4 = l_1{}^*$, $l_5 = l_2{}^*$ and $l_6 = l_3{}^*$. It is interesting to know that a three-M-lump wave travels along the following straight lines

$$y_1 = \frac{\left({a_1}^2 + {b_1}^2 - 1\right)\left(\sqrt{3\left(a_1{b_1}^2\left({a_1}^2 + {b_1}^2\right)^5\right)} + {b_1}^2\left({a_1}^2 + {b_1}^2\right)^2(z - x)\right)}{2{b_1}^2\left((a_1 - 1)\,a_1 + {b_1}^2\right)\left({a_1}^2 + {b_1}^2\right)^2} - z,$$

$$y_2 = \frac{\left({a_2}^2 + {b_2}^2 - 1\right)\left(\sqrt{3\left(a_2{b_2}^2\left({a_2}^2 + {b_2}^2\right)^5\right)} + {b_2}^2\left({a_2}^2 + {b_2}^2\right)^2(z - x)\right)}{2{b_2}^2\left((a_2 - 1)\,a_2 + {b_2}^2\right)\left({a_2}^2 + {b_2}^2\right)^2} - z,$$

and

$$y_3 = \frac{\left({a_3}^2 + {b_3}^2 - 1\right)\left(\sqrt{3\left(a_3{b_3}^2\left({a_3}^2 + {b_3}^2\right)^5\right)} + {b_3}^2\left({a_3}^2 + {b_3}^2\right)^2(z - x)\right)}{2{b_3}^2\left((a_3 - 1)\,a_3 + {b_3}^2\right)\left({a_3}^2 + {b_3}^2\right)^2} - z.$$

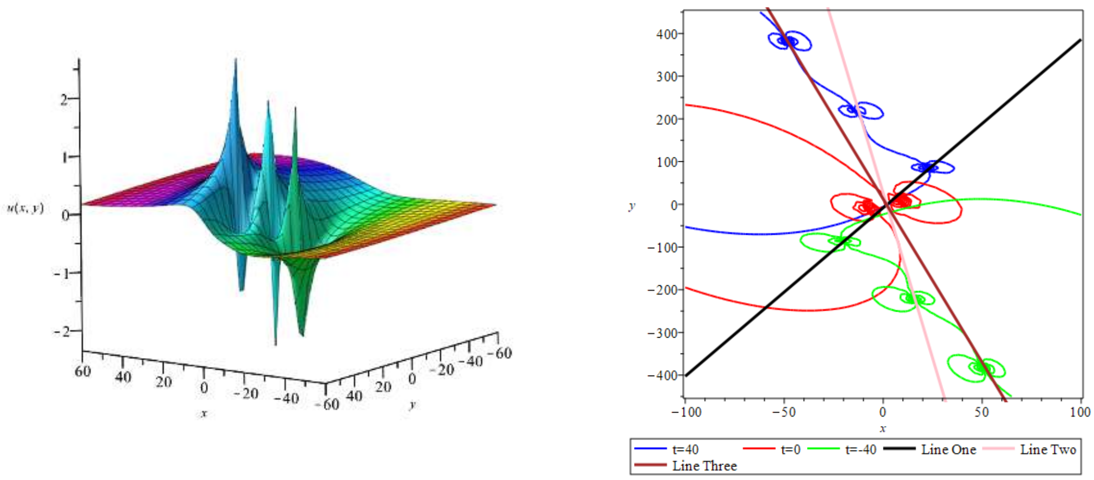

(a) $z = 1, t = 5$

(b) 1-M-lump solution at different period of time

Figure 3.59. Three-M-lump wave when $a_1 = \frac{1}{5}, b_1 = \frac{1}{2}, a_2 = \frac{1}{6}, b_2 = \frac{1}{3}, a_3 = \frac{1}{7}, b_2 = \frac{1}{4}$.

3.7.2. Physical Interaction Phenomena

The goal of this section is to construct the collision between a 1-M-lump solution with one-soliton and two-soliton solutions, as well as between a 2-M-lump wave and one-soliton solution. Firstly, we let $N = 3$ in Eq. (2.1), taking the limit $k_i \to 0, (i = 1, 2)$ and $\frac{k_1}{k_2} = O(1)$, an outcome is

$$f = \phi_1\phi_2 + B_{12} + (\phi_1\phi_2 + B_{12} + C_{23}\phi_1 + C_{13}\phi_2 + C_{13}C_{23})e^{\psi_3}. \tag{3.189}$$

Where ψ_3 is defined in Eq. (3.180), $\phi_i\,(i = 1, 2)$ are defined in Eq. (3.184), B_{12} is given in Eq. (3.185). The constants C_{13}, C_{23} are derived as follows

$$C_{mn} = -\frac{6l_m l_n k_n\,(l_m + l_n)}{{l_m}^2 + {l_n}^2 + l_m l_n \left(3{k_n}^2 l_n - 2\right)},\ \ m < n. \tag{3.190}$$

By substituting Eq. (3.190) into Eq. (3.189), and then into Eq. (3.179) a gained result is a solution that characterize a collision between 1-M-lump solution and 1-soliton solution as seen in Figure 3.60.

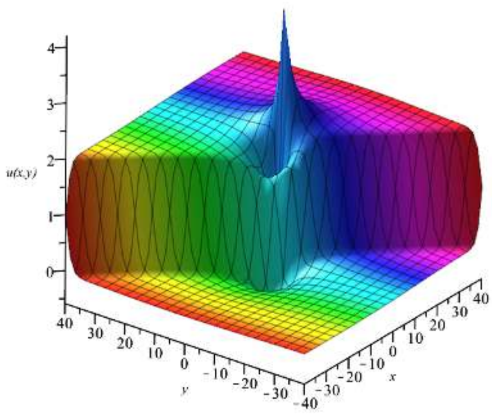

(a) $z = 1, t = 2$

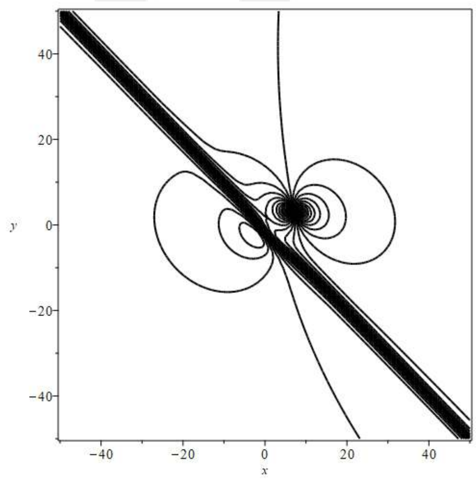

(b) Contour plot for mixed 1-M-lump-soliton solution

Figure 3.60. One-M-lump-soliton solution when $a_1 = \frac{1}{5}, b_1 = 1, k_3 = 1,\ l_3 = 1,\ \alpha_3 = 1.$

To find an interaction of two-soliton with M-lump wave, we assume that

$$\begin{aligned} f =& B_{12} + \Psi_1 e^{\varphi_3} + \Psi_2 e^{\varphi_4} + \phi_1\phi_2 - \\ & A_{34}e^{\varphi_3+\varphi_4}\left(\phi_1\phi_2 + B_{12} - C_{14}C_{23} - C_{13}C_{24} - \Psi_1 - \Psi_2\right), \end{aligned} \tag{3.191}$$

where

$$\Psi_1 = \phi_1\phi_2 + B_{12} + C_{23}\phi_1 + C_{13}\phi_2 + C_{13}C_{23},$$

and

$$\Psi_2 = \phi_1\phi_2 + B_{12} + C_{24}\phi_1 + C_{14}\phi_2 + C_{14}C_{24}.$$

The constants B_{ij} and C_{mn} are defined in Eq. (3.185) and Eq. (3.190). The functions ψ_i and ϕ_i are defined in Eq. (3.180) and Eq. (3.184). By substituting Eq. (3.191) into Eq. (3.179), an outcome is a solution that represents an interaction between a one-M-lump wave and a two-soliton solution as seen in Figure 3.61.

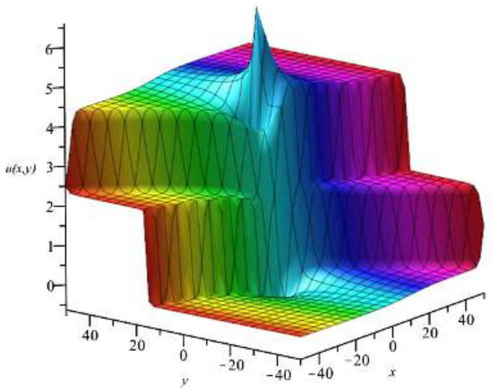

(a) $z = 1, t = 2$

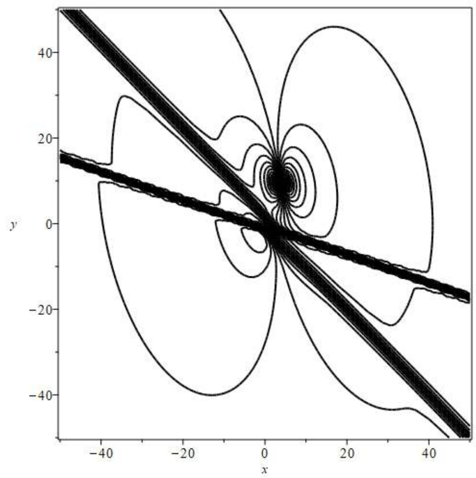

(b) Contour plot for mixed 1-M-lump-2-soliton solution

Figure 3.61. 1-M-lump-two-soliton solution when $a = \frac{1}{7}, b = \frac{1}{2}, l_3 = 1, k_3 = 1, l_4 = 3$, $k_4 = \frac{6}{5}$, $\alpha_3 = 1$, $\alpha_4 = 2$.

Motivated by Ref. [**63**], when $N = 5$ in Eq. (2.1), the interaction between two-M-lump wave and one-soliton solution can be formulated as follows

$$\begin{aligned} f = {} & \phi_1\phi_2\phi_3\phi_4 + B_{34}\phi_1\phi_2 + B_{24}\phi_1\phi_3 + B_{23}\phi_1\phi_4 + B_{14}\phi_2\phi_3 + B_{13}\phi_2\phi_4 \\ & + B_{12}\phi_3\phi_4 + Q\mathrm{e}^{k_5(x+l_5y+(l_5-1)z+w_5t)+\alpha_5} + B_{14}B_{23} + B_{13}B_{24} + B_{12}B_{34}, \end{aligned} \tag{3.192}$$

where

$$
\begin{aligned}
Q = {} & \phi_1\phi_2\phi_3\phi_4 + C_{45}\phi_1\phi_2\phi_3 + C_{15}\phi_2\phi_3\phi_4 + C_{25}\phi_1\phi_3\phi_4 + C_{35}\phi_1\phi_2\phi_4 \\
& + (B_{34} + C_{35}C_{45})\,\phi_1\phi_2 + (B_{24} + C_{25}C_{45})\,\phi_1\phi_3 + (B_{14} + C_{15}C_{45})\,\phi_2\phi_3 \\
& + (B_{23} + C_{25}C_{35})\,\phi_1\phi_4 + (B_{13} + C_{15}C_{35})\,\phi_2\phi_4 + (B_{12} + C_{15}C_{25})\,\phi_3\phi_4 \\
& + (B_{34}C_{25} + B_{24}C_{35} + B_{23}C_{45} + C_{25}C_{35}C_{45})\,\phi_1 + B_{14}B_{23} + B_{13}B_{24} \\
& + (B_{34}C_{15} + B_{14}C_{35} + B_{13}C_{45} + C_{15}C_{35}C_{45})\,\phi_2 + B_{12}B_{34} + B_{34}C_{15}C_{25} \\
& + (B_{24}C_{15} + B_{14}C_{25} + B_{12}C_{45} + C_{15}C_{25}C_{45})\,\phi_3 + B_{24}C_{15}C_{35} + B_{14}C_{25}C_{35} \\
& + (B_{23}C_{15} + B_{13}C_{25} + B_{12}C_{35} + C_{15}C_{25}C_{35})\,\phi_4 + B_{23}C_{15}C_{45} + B_{13}C_{25}C_{45} \\
& + B_{12}C_{35}C_{45} + C_{15}C_{25}C_{35}C_{45}.
\end{aligned} \tag{3.193}
$$

All used constants and functions are stated in this paper. Now to offer an interaction between a two-M-lump and a one-soliton solutions, we plug Eq. (3.193) into Eq. (3.179), as a result, we get a phenomenon that happens between two-M-lump and one-soliton solution as presented in Figure 3.62.

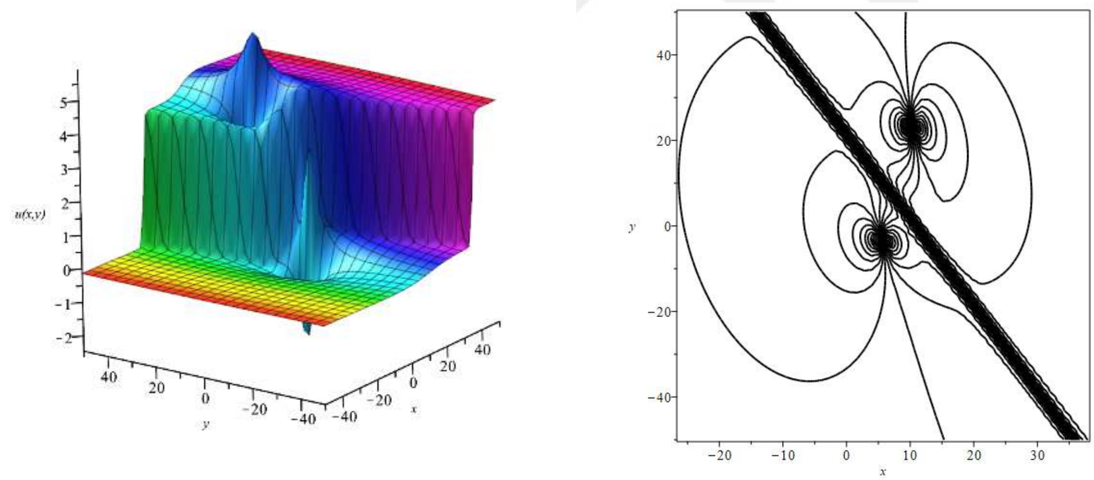

(a) $z = t = 5$

(b) Contour plot for mixed 2-M-lump-1-soliton solution

Figure 3.62. 2-M-lump-1-soliton when $a_1 = \frac{1}{7}, b_1 = \frac{1}{2}, a_2 = \frac{1}{20}, b_2 = \frac{1}{3}, l_5 = \frac{1}{2}$, $k_5 = 2$, $\alpha_5 = 1$.

4. Newly modified method and its application

Peregrin [**95**] first reported the Boussinesq equations for variable water depth, which are efficient for shallow water, as well as linked to it as a normal Boussinesq equation. Boussinesq equations are the most common nonlinear partial differential equations developed to describe water dynamics with both a low amplitude as well as a long wave. Such equations are one of the most important equations for forecasting wave changes in coastal regions, as well as commonly used in coastal and ocean engineering. In this research, we use the newly MEFM to find new solutions for the Boussinesq-type equations and the Adomian decomposition method to studies numerical solutions to the suggested equations. Moreover, the instability modulation of models is also presented.

The Boussinesq equations in (1+1)-dimensions [**96**] are read

$$\begin{aligned} &v_t + w_x + v v_x = 0, \\ &w_t + (wv)_x + v_{xxx} = 0. \end{aligned} \tag{4.1}$$

This paired Boussinesq equation also appears in shallow water waves for two layers of fluid flow. This scenario occurs at a time when accidental oil spills from a vessel, resulting in a layer of oil floating above the water surface.

4.1. General structures of the method

Suppose there is a nonlinear partial differential equation

$$P\left(\varphi, \varphi_x, \varphi\varphi_x, \varphi_t, \varphi_{tt},\ \ldots\right) = 0. \tag{4.2}$$

To reveal the exact solutions of equation (4.2), the below transformation may be use

$$\varphi\left(x,t\right) = \phi\left(\xi\right), \qquad \xi = x - v\,t, \tag{4.3}$$

where ν is an arbitrary scalar and ξ describe the wave variable. Plugging Eq. (4.3) to the Eq. (4.2), the result could be written as follows

$$N\left(\phi, \phi^2, \phi\phi', \phi'',\ \ldots\right) = 0. \tag{4.4}$$

Now, let a new trial solution to the Eq. (4.4) be as follows

$$\begin{aligned}\phi(\xi) &= \frac{\sum\limits_{i=0}^{n} a_i\left(a^{-i\,\phi(\xi)}\right)^i}{\sum\limits_{j=0}^{m} b_j\left(a^{-j\,\phi(\xi)}\right)^j} + \frac{\sum\limits_{i=0}^{n} c_i\left(a^{i\,\phi(\xi)}\right)^i}{\sum\limits_{j=0}^{m} d_j\left(a^{j\phi(\xi)}\right)^j} \\ &= \frac{a_0 + a_1 a^{-\phi(\xi)} + a_2 a^{-2\phi(\xi)} + \ldots + a_n a^{-n\phi(\xi)}}{b_0 + b_1 a^{-\phi(\xi)} + b_2 a^{-2\phi(\xi)} + \ldots + b_n a^{-m\phi(\xi)}} + \\ &\quad \frac{c_0 + c_1 a^{\phi(\xi)} + c_2 a^{2\phi(\xi)} + \ldots + c_n a^{n\phi(\xi)}}{d_0 + d_1 a^{\phi(\xi)} + d_2 a^{2\phi(\xi)} + \ldots + d_n a^{m\phi(\xi)}},\end{aligned} \tag{4.5}$$

where a_i, b_j, c_i and d_j, $(0 \leq i \leq n,\ 0 \leq j \leq m)$ are constants and $\phi(\xi)$ is the auxiliary ODE defined by

$$\phi'(\xi) = \frac{a^{-\phi(\xi)} + \mu\, a^{\phi(\xi)} + \lambda}{\ln(a)}, \tag{4.6}$$

where μ, λ are scalars, and $a > 0$, $a \neq 1$. The general solution of the auxiliary ODE is as follows:

I. When $\lambda^2 - 4\mu > 0$, then $\phi(\xi) = \log_a\left(-\lambda - \sqrt{\lambda^2 - 4\mu}\tanh\left(\frac{1}{2}\sqrt{\lambda^2 - 4\mu}\,(\xi + \epsilon)\right)\right)$.

II. When $\lambda^2 - 4\mu < 0$, then $\phi(\xi) = \log_a\left(-\lambda + \sqrt{-\lambda^2 + 4\mu}\tan\left(\frac{1}{2}\sqrt{-\lambda^2 + 4\mu}\,(\xi + \epsilon)\right)\right)$.

III. When $\lambda^2 - 4\mu > 0$ and $\mu = 0$, then$\phi(\xi) = \log_a\left(\frac{\lambda}{-1+\cosh(\lambda(\xi+\epsilon))+\sinh(\lambda(\xi+\epsilon))}\right)$.

IV. When $\lambda^2 - 4\mu = 0, \lambda \neq 0$ and $\mu \neq 0$, then$\phi(\xi) = \log_a\left(\frac{-2-\lambda(\xi+\epsilon)}{2\mu(\xi+\epsilon)}\right)$.

V. When $\lambda^2 - 4\mu = 0, \lambda = 0$ and $\mu = 0$, then $\phi(\xi) = \log_a(\xi + \epsilon)$.

4.2. Implement on the coupled BE via newly MEFM

Consider Eq. (4.1) that describe the Boussinesq equations in (1+1)-dimension. By plugging the wave transform

$$v(x,t) = V(\xi), \quad w(x,t) = W(\xi), \quad \xi = x - kt, \tag{4.7}$$

to the Eq. (4.1), we have

$$VV' - kV' + W' = 0, \tag{4.8}$$

$$WV' - kW' + VW' + V''' = 0. \tag{4.9}$$

Once integrating Eq. (4.8) with respect to ξ and setting the integration constant to zero, we get

$$W = \frac{2kV - V^2}{2}. \tag{4.10}$$

Replacing Eq. (4.10) into Eq. (4.9), we get

$$2V'' - V^3 + 3kV^2 - 2k^2V = 0, \tag{4.11}$$

according to the balanced relationship between V'' and V^3, we get $n = m + 1$, choosing $m = 1$ gives $n = 2$. Substituting the value of n and m into Eq. (4.5) yields

$$V(\xi) = \frac{a_0 + a_1 a^{-\phi(\xi)} + a_2 a^{-2\phi(\xi)}}{b_0 + b_1 a^{-\phi(\xi)}} + \frac{c_0 + c_1 a^{\phi(\xi)} + c_2 a^{2\phi(\xi)}}{d_0 + d_1 a^{\phi(\xi)}}. \tag{4.12}$$

Using Eq. (4.12) and its second derivative with Eq. (4.11), we gain the polynomial equation of $a^{\phi(\xi)}$. After that, we obtain a set of algebraic equations from this polynomial by matching the sum of the $a^{\phi(\xi)}$ coefficients with the same power to zero. By solving the system of equations, we can obtain and study the following solutions.

Case 1. When $a_0 = b_0\left(-\lambda + \sqrt{\Delta}\right), a_1 = -\frac{b_0 c_0}{d_1} + b_1\left(-\lambda + \sqrt{\Delta}\right), a_2 = -\frac{b_1 c_0}{d_1}, c_2 = -2d_1\mu, k = \sqrt{\Delta}, d_0 = 0, c_1 = 0$, we get the following solutions:

$$v(x,t) = \sqrt{\Delta}\left(1 + \tanh\left(\frac{1}{2}\left(x + \epsilon - t\sqrt{\Delta}\right)\sqrt{\Delta}\right)\right), \tag{4.13}$$

$$w(x,t) = \frac{\Delta}{1 + \cosh\left(\left(x + \epsilon - t\sqrt{\Delta}\right)\sqrt{\Delta}\right)}, \tag{4.14}$$

providing that $\Delta = \lambda^2 - 4\mu > 0$, $\lambda \neq 0, \mu \neq 0$. Eqs. (4.13) and (4.14) are the kink type and soliton surfaces as seen in Figure 4.1.

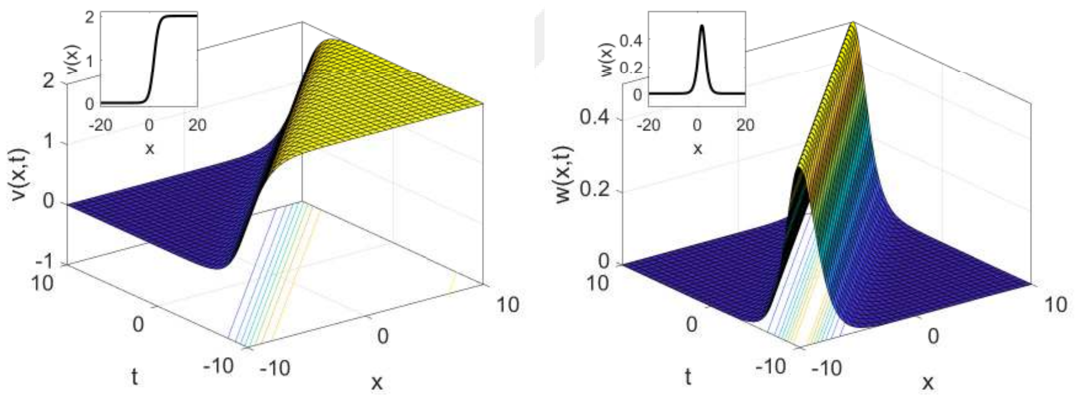

(a) The kink-type wave

(b) The soliton surface

Figure 4.1. 3D and 2D graph of Eqs. (4.13) and (4.14) drawn when $\lambda = 3, \mu = 2, \epsilon = 0.1$.

Case 2. When $a_0 = b_0\left(\lambda + 2\sqrt{\Delta}\right)$, $a_1 = b_0\left(-2 - \frac{c_0}{d_1} + \frac{\lambda(\lambda+\sqrt{\Delta})}{\mu}\right)$, $a_2 = -\frac{b_0 c_0 \lambda}{2d_1\mu}$, $c_2 = 2d_1\mu$, $b_1 = \frac{b_0\lambda}{2\mu}$, $k = 2\sqrt{\Delta}$, $d_0 = 0$, $c_1 = 0$, we get the following singular solutions (see Figure 4.2):

$$v(x,t) = -\sqrt{\Delta}\left(\coth\frac{1}{2}\left(x - 2t\sqrt{\Delta} + \epsilon\right)\sqrt{\Delta} - 1\right)^2 \tanh\left(\frac{1}{2}\left(x - 2t\sqrt{\Delta} + \epsilon\right)\sqrt{\Delta}\right), \tag{4.15}$$

$$w\left(x,t\right)=-2\Delta\text{csch}^2\left(\frac{1}{2}\left(x-2t\sqrt{\Delta}+\epsilon\right)\sqrt{\Delta}\right), \tag{4.16}$$

providing that $\Delta=\lambda^2-4\mu>0,\ \lambda\neq 0, \mu\neq 0.$

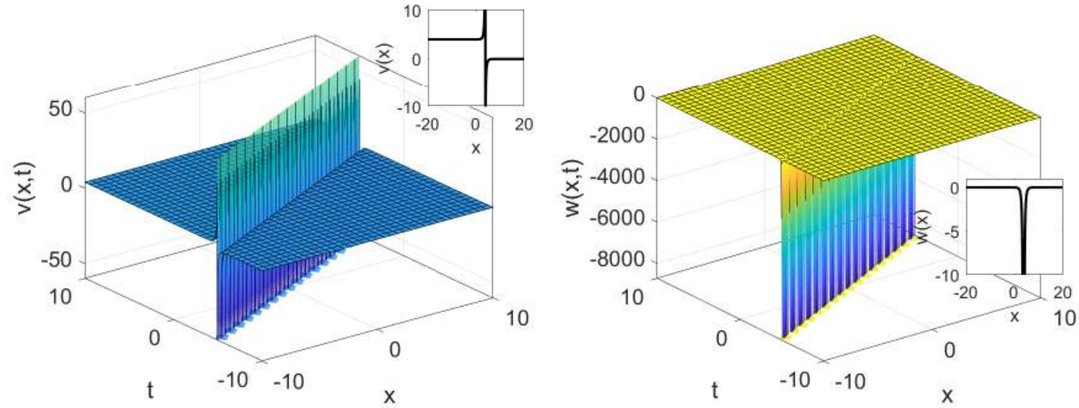

(a) Singular solution to equation (??)

(b) Singular solution to equation (??)

Figure 4.2. 3D and 2D graph of Eqs. (4.15) and (4.16) drawn when $\lambda=3,\mu=2,\epsilon=1$.

Case 3. When $a_0=b_0k+\frac{\sqrt{-{b_0}^2(k^2-8\mu)}}{\sqrt{2}}$, $a_1=\frac{1}{4}\left(b_0\left(8-\frac{4c_0}{d_1}\right)+\frac{\sqrt{2}k\sqrt{-{b_0}^2(k^2-8\mu)}}{\mu}\right)$, $a_2=-\frac{c_0\sqrt{-{b_0}^2(k^2-8\mu)}}{2\sqrt{2}d_1\mu}$, $c_2=2d_1\mu$, $d_0=0$, $c_1=0$, $b_1=\frac{\sqrt{-{b_0}^2(k^2-8\mu)}}{2\sqrt{2}\mu}$, $\lambda=\frac{\sqrt{-{b_0}^2(k^2-8\mu)}}{\sqrt{2}b_0}$, we have the following periodic singular solutions (see Figure 4.3):

$$v\left(x,t\right)=k+\sqrt{2}k\csc\left(\frac{k\left(-kt+x+\epsilon\right)}{\sqrt{2}}\right), \tag{4.17}$$

$$w\left(x,t\right)=-\frac{1}{4}k^2\left(1+\cot^4\left(\frac{k\left(-kt+x+\epsilon\right)}{2\sqrt{2}}\right)\right)\tan^2\left(\frac{k\left(-kt+x+\epsilon\right)}{2\sqrt{2}}\right). \tag{4.18}$$

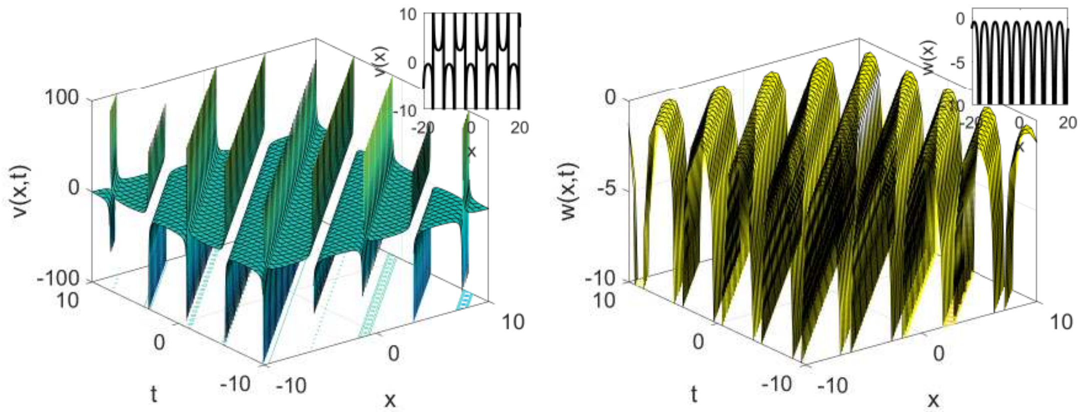

(a) Periodic singular solution to equation (4.17)

(b) Periodic singular solution to equation (4.18)

Figure 4.3. 3D and 2D graph of Eqs. (4.17) and (4.18) drawn when $\epsilon = 0.1, k = 1$.

Case 4. When $a_1 = b_1 k + \sqrt{{b_1}^2 (k^2 + 4\mu)}, a_2 = 2b_1, c_1 = -\frac{a_0 d_0}{b_1}, c_2 = -\frac{a_0 d_1}{b_1}, \lambda = \frac{\sqrt{{b_1}^2 (k^2+4\mu)}}{b1}, c_0 = 0, b_0 = 0$, we can construct and study the following solutions:

Solution 1. In case $\lambda^2 - 4\mu > 0, \mu \neq 0, \lambda \neq 0$, we get

$$v(x,t) = \frac{\mathrm{e}^{\frac{1}{2}k(-kt+x+\epsilon)} k \left(b_1 k + \sqrt{{b_1}^2 (k^2 + 4\mu)}\right)}{\sqrt{{b_1}^2 (k^2 + 4\mu)} \cosh\left(\frac{1}{2}k(-kt + x + \epsilon)\right) + b_1 k \sinh\left(\frac{1}{2}k(-kt + x + \epsilon)\right)}, \tag{4.19}$$

$$w(x,t) = \frac{2{b_1}^2 k^2 \mu}{\left(\sqrt{{b_1}^2 (k^2 + 4\mu)} \cosh\left(\frac{1}{2}k(-kt + x + \epsilon)\right) + b1k \sinh\left(\frac{1}{2}k(-kt + x + \epsilon)\right)\right)^2}. \tag{4.20}$$

Eqs. (4.19) and (4.20) are the kink type and soliton surfaces solutions of Eq. (4.1) as seen in Figure 4.4.

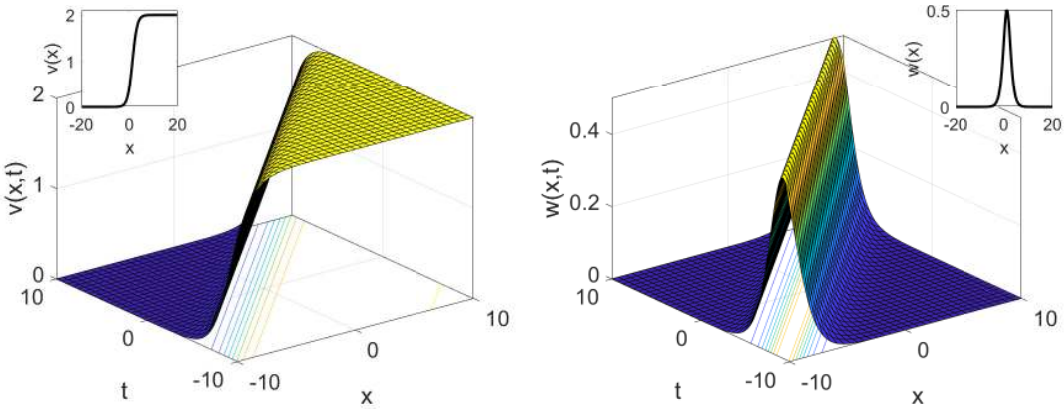

(a) The kink-type wave **(b)** The soliton surface

Figure 4.4. 3D and 2D graph of Eqs. (4.19) and (4.20) drawn when $\mu = 2, \epsilon = 0.1, k = 1, b_1 = 0.1$.

Solution 2. In case $\lambda^2 - 4\mu > 0, \mu = 0, \lambda \neq 0$, we gain

$$v(x,t) = k\left(1 + \coth\left(\frac{1}{2}k(-kt + x + \epsilon)\right)\right), \tag{4.21}$$

$$w(x,t) = -\frac{2k^2 e^{\frac{\sqrt{b_1{}^2k^2}(kt+x+\epsilon)}{b_1}}}{\left(e^{\frac{k\sqrt{b_1{}^2k^2}t}{b_1}} - e^{\frac{\sqrt{b_1{}^2k^2}(x+\epsilon)}{b_1}}\right)^2}. \tag{4.22}$$

Eqs. (4.21) and (4.22) are the singular solutions of Eq. (4.1) and represented graphically as shown in Figure 4.5.

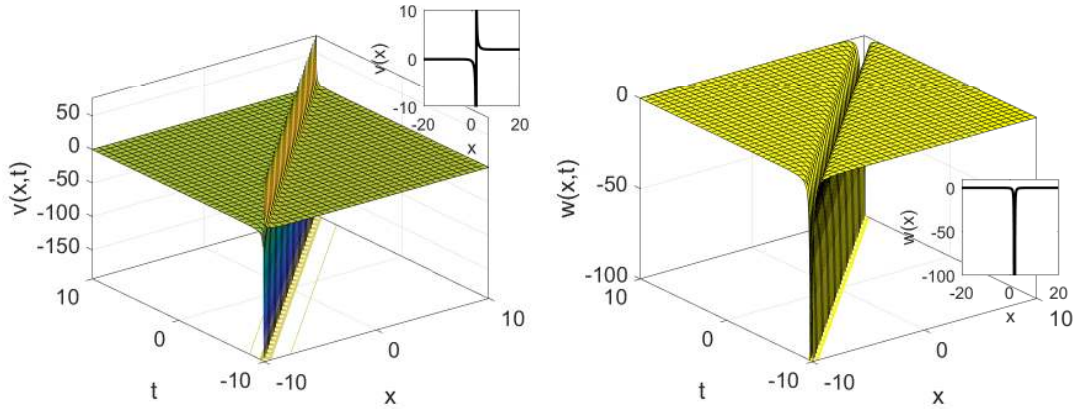

(a) Singular solution to Eq. (4.21) **(b)** Singular solution to Eq. (4.22)

Figure 4.5. 3D and 2D graph of Eqs. (4.21) and (4.22) drawn when $\mu = 0, \epsilon = 0.1, k = 1, b_1 = 0.1$.

Case 5. When $c_0 = -\frac{a_2 d_1}{b_1}, c_1 = -\frac{d_1\left(a_1 + \left(1 - i\sqrt{2}\right)b_1\lambda\right)}{b_1}, c_2 = -\frac{a_0 d_1}{b_1} - \frac{3d_1\lambda^2}{2}, k = i\sqrt{2}\lambda, \mu =$

$\frac{3\lambda^2}{4}, d_0 = 0, b_0 = 0$ and $\lambda^2 - 4\mu < 0$, we can construct the below solutions

$$v\left(x,t\right) = \sqrt{2}\lambda\left(\mathrm{i} - \tan\left(\frac{\left(x+\epsilon\right)\lambda}{\sqrt{2}} + \mathrm{i}t\lambda^2\right)\right), \tag{4.23}$$

$$w\left(x,t\right) = -\lambda^2 \mathrm{sec}^2\left(\frac{\left(x+\epsilon\right)\lambda}{\sqrt{2}} - \mathrm{i}t\lambda^2\right). \tag{4.24}$$

These are complex solutions to the studied equations as shown in Figure 4.6 and Figure 4.7.

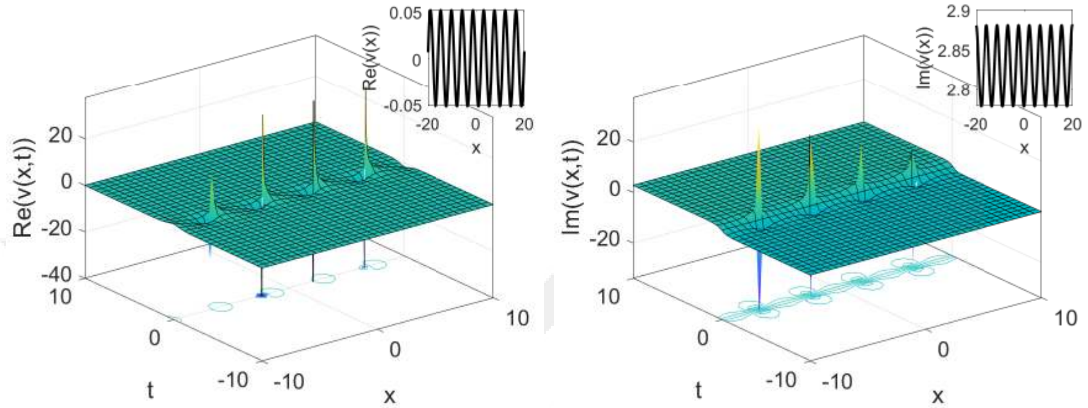

(a) Real wave solution

(b) Imaginary wave solution

Figure 4.6. 3D and 2D graph of Eq. (4.23) drawn when $\lambda = 1, \epsilon = 0.1, k = 1$.

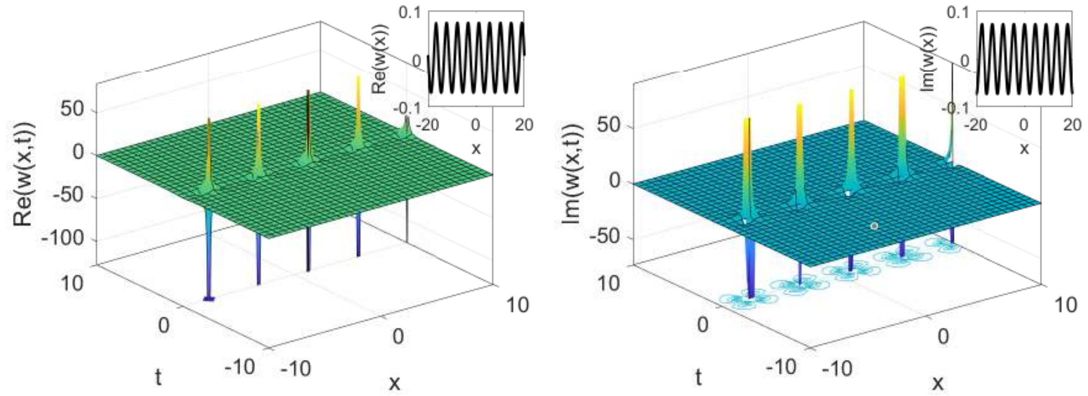

(a) Real wave solution

(b) Imaginary wave solution

Figure 4.7. 3D and 2D graph of Eq. (4.24) drawn when $\lambda = 1, \epsilon = 0.1, k = 1$.

4.3. Numerical Solutions

In this portion of work, we study the numerical solutions of Eq. (4.1) by using the Adomian decomposition scheme. Consider the (1+1)- dimensional Boussinesq equations in

Eq. (4.1), and rewrite it as below

$$Lv = -w_x - v\, v_x \tag{4.25}$$

$$Lw = -\left(wv_x + w_x v + v_{xxx}\right), \tag{4.26}$$

where $L = \frac{\partial}{\partial t}$. Now from Eqs. (4.13) and (4.14), one can find initial conditions that cover the Egs. (4.25) and (4.26) as shown below

$$v\left(x, 0\right) = \sqrt{\Delta}\left(1 + \tanh\left(\frac{1}{2}\left(x + \epsilon\right)\sqrt{\Delta}\right)\right), \tag{4.27}$$

$$w\left(x, 0\right) = \frac{\lambda^2 - 4\mu}{1 + \cosh\left(\left(x + \epsilon\right)\sqrt{\Delta}\right)}. \tag{4.28}$$

Defining the inverse operator $L^{-1}\left(*\right) = \int\limits_0^t \left(*\right)$ dt and applying it on Eqs. (4.25) and (4.26), we have

$$v = -\int\limits_0^t \left(w_x + v\, v_x\right)\mathrm{dt}, \tag{4.29}$$

$$w = -\int\limits_0^t \left(wv_x + w_x v + v_{xxx}\right)\mathrm{dt}. \tag{4.30}$$

Using Eqs. (4.27) and (4.28), and applying on Eqs. (4.29) and (4.30), we have

$$v = \sqrt{\Delta}\left(1 + \tanh\left(\frac{1}{2}\left(x + \epsilon\right)\sqrt{\Delta}\right)\right) - L^{-1}\left(w_x\right) - L^{-1}\left(v\, v_x\right), \tag{4.31}$$

$$w = \frac{\Delta}{1 + \cosh\left(\left(x + \epsilon\right)\sqrt{\Delta}\right)} - \left(L^{-1}wv_x + L^{-1}w_x v + L^{-1}v_{xxx}\right). \tag{4.32}$$

The solution of Eqs. (4.31) and (4.32) is defined as an infinite series, and the nonlinear terms are defined as below

$$A_i = \sum_{k=0}^{i} v_k v_{i-k}, \quad B_i = \sum_{k=0}^{i} w_k {v'}_{i-k}, \; C_i = \sum_{k=0}^{i} {w'}_k v_{i-k}, \;\; \forall i = 0, 1, 2, ..., n \tag{4.33}$$

where A_i, B_i, C_i are the Adomian polynomial of v_k, w_k. Plugging Eq. (4.33) into Eqs. (4.31) and (4.32), the first-two terms of solutions can be written as follows

$$v_0 = \sqrt{\Delta}\left(1 + \tanh\left(\frac{1}{2}\left(x + \epsilon\right)\sqrt{\Delta}\right)\right), \tag{4.34}$$

$$w_0 = \frac{\lambda^2 - 4\mu}{1 + \cosh\left(\left(x + \epsilon\right)\sqrt{\Delta}\right)}, \tag{4.35}$$

Table 4.1. Analytical and numerical solutions of $v(x,t)$ for the Eq. (4.1) and its absolute errors when $\lambda = 3, \mu = 2, \epsilon = 0$, and $t = 0.1$ under Eq. (4.13)

x_i	Exact Solution	Numerical solution	Absolute Error
0.01	0.9550303504	0.954955901	7.44484×10^{-5}
0.02	0.9600213196	0.959960033	6.12866×10^{-5}
0.03	0.9650142846	0.964966309	4.79749×10^{-5}
0.04	0.9700089967	0.969974480	3.45162×10^{-5}
0.05	0.9750052070	0.974984293	2.09135×10^{-5}
0.06	0.9800026662	0.979995496	7.1697×10^{-6}
0.07	0.9850011248	0.985007836	6.7119×10^{-6}
0.08	0.9900003333	0.990021061	2.07283×10^{-5}
0.09	0.9950000416	0.995034917	3.48762×10^{-5}

$$v_1 = -\frac{1}{2} t \Delta^{3/2} \text{sech}^2 \left(\frac{1}{2} \sqrt{\Delta} \left(x + \epsilon \right) \right), \tag{4.36}$$

$$w_0 = 4t\Delta^2 \text{csch}^3 \left(\sqrt{\Delta} \left(x + \epsilon \right) \right) \sinh^4 \left(\frac{1}{2} \sqrt{\Delta} \left(x + \epsilon \right) \right), \tag{4.37}$$

and in general forms, we have

$$v_{k+1} = - \left(L^{-1} \left(w'_k \right) + L^{-1} \left(v \, v'_k \right) \right), \qquad \forall k = 1, 2, 3, ... \tag{4.38}$$

$$w_{k+1} = - \left(L^{-1} w v'_k + L^{-1} w'_k v + L^{-1} v'''_k \right). \qquad \forall k = 1, 2, 3, .. \tag{4.39}$$

The findings are presented and discussed graphically and numerically as shown in Figure 4.8 and tables (4.1) and (4.2).

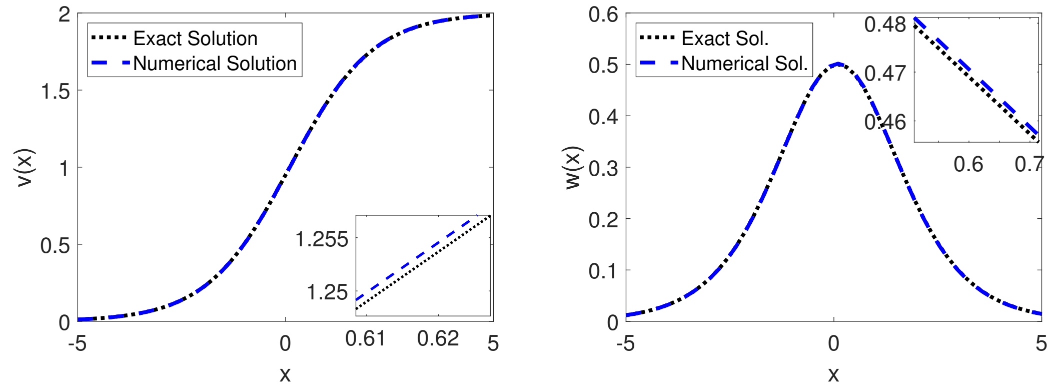

(a) Exact and numerical solution of $v(x,t)$

(b) Exact and numerical solution of $w(x,t)$

Figure 4.8. 2D graph of exact solutions under Eqs. (4.13), (4.14) and corresponding numerical solutions of Eq. (4.1) plotted when $\lambda = 3, \mu = 2, \epsilon = 0$.

Table 4.2. Analytical and numerical solutions of $w(x,t)$ for the Eq. (4.1) and its absolute errors when $\lambda = 3, \mu = 2, \epsilon = 0$, and $t = 0.1$ under Eq. (4.14)

x_i	Exact Solution	Numerical solution	Absolut Error
0.01	0.4989888653	0.5002974576	1.3085923×10^{-3}
0.02	0.4992008525	0.5005245744	1.3237219×10^{-3}
0.03	0.4993879998	0.5007265680	1.3385682×10^{-3}
0.04	0.4995502698	0.5009033929	1.3531231×10^{-3}
0.05	0.4996876301	0.5010550088	1.3673786×10^{-3}
0.06	0.4998000533	0.5011813804	1.3813270×10^{-3}
0.07	0.4998875168	0.5012824775	1.3949606×10^{-3}
0.08	0.4999500033	0.5013582752	1.4082719×10^{-3}
0.09	0.4999875002	0.5014087537	1.4212535×10^{-3}

4.4. Linear Stability Analysis to the coupled Boussinesq equation

In this section, the notion of linear stability analysis will be used to explore and study the stability analysis of the coupled Boussinesq equation. Assume that the perturbed solutions have the forms [**97**]:

$$v\left(x,t\right) = a_1 + a_2\, V\left(x,t\right), \tag{4.40}$$

$$w\left(x,t\right) = b_1 + b_2\, W\left(x,t\right), \tag{4.41}$$

where a_1, b_1 describe the steady-state solutions for Eq. (4.1) and a_2, b_2 are constants. Putting Eqs. (4.40) and (4.41) into Eq. (4.1) and making the linearization, the results yield:

$$a_2 V_t + a_1 a_2 V_x + b_2 W_x = 0, \tag{4.42}$$

$$b_2 W_t + a_2 b_1 V_x + a_1 b_2 W_x + a_2 V_{xxx} = 0. \tag{4.43}$$

Now, let the solutions of Eqs. (4.42) and (4.43) have the following functions:

$$V\left(x,t\right) = \epsilon_1 \mathrm{e}^{\mathrm{i}(kx+\Omega t)}, \tag{4.44}$$

$$W\left(x,t\right) = \epsilon_2 \mathrm{e}^{\mathrm{i}(kx+\Omega t)}, \tag{4.45}$$

here k symbolizes the normalized wave number. Inserting the above equations into Eqs. (4.42) and (4.43), we obtain

$$a_1 a_2 k \epsilon_1 + b_2 k \epsilon_2 + a_2 \epsilon_1 \Omega = 0, \tag{4.46}$$

$$a_2 k \left(k^2 - b_1\right) \epsilon_1 - b_2 \epsilon_2 \left(a_1 k + \Omega\right) = 0. \tag{4.47}$$

Collecting the terms of Eqs. (4.46) and (4.47) according to ϵ_1, ϵ_2, we set up

$$\begin{pmatrix} a_1a_2k + a_2\Omega & b_2k \\ a_2k\left(k^2 - b_1\right) & -b_2\left(a_1k + \Omega\right) \end{pmatrix} \begin{pmatrix} \epsilon_1 \\ \epsilon_2 \end{pmatrix} = \begin{pmatrix} 0 \\ 0 \end{pmatrix}. \tag{4.48}$$

Evaluating the determinant of Eq. (4.48), the result gives

$$-a_2b_2\left({a_1}^2k^2 - b_1k^2 + k^4 + 2a_1k\Omega + \Omega^2\right) = 0. \tag{4.49}$$

Finding the solution of Eq. (4.49) for Ω, the outcome yields:

$$\Omega\left(k\right) = -a_1k \mp \sqrt{b_1k^2 - k^4} = -a_1k \mp \mathrm{i}\sqrt{k^4 - b_1k^2}, \tag{4.50}$$

due to this result, we investigate the linear stability of coupled Boussinesq equations that is dependent on the values of steady-state parameters a_1, b_1. From equation (4.50), we observe that the real part will be negative in condition $k > 0$, therefore the dispersion is unstable while the situation will become stable when $k < 0$ as well as it occurs if $a_1 < 0$. In the case, $a_1 = 0$ the dispersion is called marginally stable, which is occur when the real part is equal to zero. In Figure 4.9, the effect of parameters a_1 and b_1 that describes the steady-state solutions is presented.

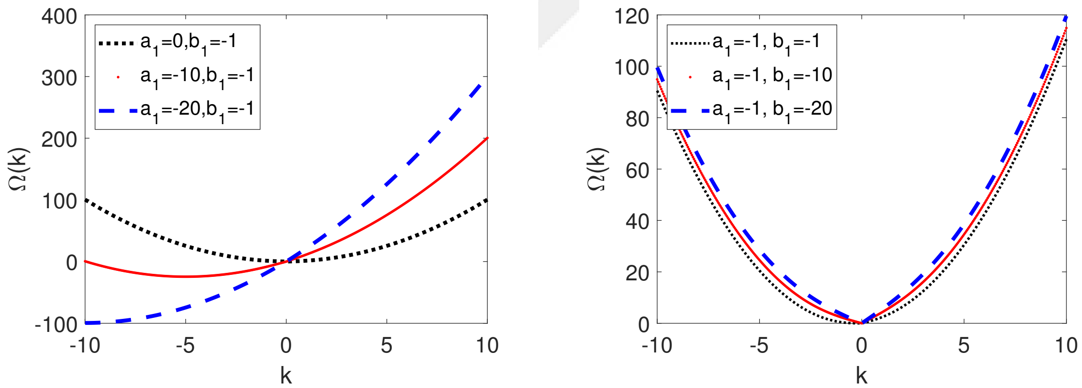

(a) Effect of the parameter a_1

(b) Effect of the parameter b_1

Figure 4.9. Frequency of the perturbation vs wave number.

4.5. Results and discussion

In this work, we are newly extended the MEFM to analyze and study some new solutions for partial differential equations. Applying this newly modified method on the studied equations leads to the new solutions, as well as gives us a more exact solutions, too. We have successfully applied this newly modified method to couple Boussinesq equation, and the results lead to new the solutions. The MEFM has been successfully implemented to the couple Boussinesq equation in Ref. [**48**], and two cases of the solutions are revealed. In this paper, the solutions observed in Eqs. (4.13), (4.14), (4.15), (4.16), and Eqs. (4.21), (4.22) are the same, but the solutions constructed in Eqs. (4.17), (4.18), and complex solutions (4.23), (4.24) are novel and successfully constructed via this method. This approach is straightforward, reliable, and easy-to-use as a mathematical tool that can be applied to other nonlinear models or nonlinear partial differential equations to study and depict real and complex solutions.

Conclusion

In this thesis, we have focused on the study several types of partial differential equations like the (2+1)-dimensional Bogoyavlenskii–Schieff equation, the extended (2+1)-dimensional shallow water wave model, the (2+1)-dimensional Bogoyavlenskii's generalized breaking soliton equation, the (2+1)-dimensional Date-Jimbo-Kashiwara-Miwa equation, the (2+1)-dimensional Bogoyavlensky-Konopelchenko equation, the (2+1)-dimensional Korteweg-De Vries equation with the extension of time-dependent coefficients, the (3+1)-dimensional generalized Kadomtsev-Petviashvili equation, and the (1+1)-dimensional Boussinesq equations. In this study, the simplified Hirota's method, a long wave method, computational method, newly modified expansion function method, and the Adomian decomposition technique are utilized.

Several partial differential equations including those with constant coefficients have been studied, for example, multiple soliton waves, lump waves, M-lump waves, and several interesting physical interactions for Bogoyavlenskii–Schieff equation have been constructed. For the extended shallow water wave model N-soliton waves, complex N-soliton waves, fusion soliton solutions, lump waves, interaction waves between one-lump and solitary waves, and periodic lump solutions have been revealed. To study Bogoyavlenskii's generalized breaking soliton equation, we focus on Hirota's and a long wave method to obtain multi-soliton waves, fusion solutions, M-lump waves, and several interesting physical collision solutions. The simplified Hirota's and a long wave method are applied on Bogoyavlenskii's generalized breaking soliton equation to report N-soliton waves, fusion waves, M-lump waves, and physical interactions phenomena. To investigate the Date-Jimbo-Kashiwara-Miwa equation, we have used two suggested methods to derive N-soliton waves, rational solutions, and interaction phenomena between one-M-lump wave and solitary waves. Complex multi-soliton waves, rational solutions, lump waves, and several interactions solutions such as mixed one-soliton-M-lump, mixed two-soliton-M-lump wave, and one-soliton-two-M-lump wave have been constructed for the Bogoyavlensky-Konopelchenko equation. Also, the (2+1)-dimensional KdV equation with time-variable and (3+1)-dimensional generalized KP equation are investigated. For the KdV equation, a class of lump waves, interaction physical phenomena solutions, and complex N-soliton solutions are explored. Dynamical features such as M-lump waves and mixed solutions through M-lump waves and N-soliton waves are revealed for the generalized KP equation.

Besides this, we newly extend the modified expansion function method in order to explore novel wave solutions for partial differential equations. This newly modified method provides us with novel and more exact solutions compared to the modified expansion function method. For this purpose, a newly modified method is applied to Boussinesq equations. Numerical solutions are presented successfully via tables and figures. Moreover, stability analysis of Boussinesq equations is also studied.

References

[1] Ismael, H. F.; Bulut, H. (2021). Nonlinear dynamics of (2+ 1)-dimensional Bogoyavlenskii–Schieff equation arising in plasma physics. *Mathematical Methods in the Applied Sciences*, 44(13), 10321-10330.

[2] Ismael, H. F.; Seadawy, A.; Bulut, H. (2021). Multiple soliton, fusion, breather, lump, mixed kink-lump and periodic solutions to the extended shallow water wave model in (2+ 1)-dimensions. *Modern Physics Letters B*, 35(08), 2150138.

[3] Ismael, H. F.; Bulut, H.; Osman, M. S. (2022). The N-soliton, fusion, rational and breather solutions of two extensions of the (2+ 1)-dimensional Bogoyavlenskii–Schieff equation. *Nonlinear Dynamics*, 107(4), 3791-3803.

[4] Ismael, H. F.; Ma, W. X.; Bulut, H. (2021). Dynamics of soliton and mixed lump-soliton waves to a generalized Bogoyavlensky-Konopelchenko equation. *Physica Scripta*, 96(3), 035225.

[5] Ismael, H. F.; Bulut, H.; Park, C.; Osman, M. S. (2020). M-lump, N-soliton solutions, and the collision phenomena for the (2+ 1)-dimensional Date-Jimbo-Kashiwara-Miwa equation. *Results in Physics*, 19, 103329.

[6] Ismael, H. F.; Murad, M. A. S.; Bulut, H. (2021). Various exact wave solutions for KdV equation with time-variable coefficients. *Journal of Ocean Engineering and Science*. https://doi.org/10.1016/j.joes.2021.09.014

[7] Ismael, H. F.; Murad, M. A. S.; Bulut, H. (2022). M-lump waves and their interaction with multi-soliton solutions for a generalized Kadomtsev–Petviashvili equation in (3+ 1)-dimensions. *Chinese Journal of Physics*. https://doi.org/10.1016/j.cjph.2022.03.039

[8] Bekir, A.; Taşcan, F.; Ünsal, Ö. (2015). Exact solutions of the Zoomeron and Klein–Gordon–Zakharov equations. *Journal of the Association of Arab Universities for Basic and Applied Sciences*, 17, 1-5.

[9] Matinfar, M.; Eslami, M.; Roshandel, S. (2015). The first integral method to study the (2+ 1)-dimensional Jaulent–Miodek equations. *Pramana*, 85(4), 593-603.

[10] Calogero, F.; Degasperis, A. (1977). Nonlinear evolution equations solvable by the inverse spectral transform.—II. *Il Nuovo Cimento B* (1971-1996), 39(1), 1-54.

[11] Vakhnenko, V. O.; Parkes, E. J.; Morrison, A. J. (2003). A Bäcklund transformation and the inverse scattering transform method for the generalised Vakhnenko equation. *Chaos, Solitons & Fractals*, 17(4), 683-692.

[12] Eltayeb, H.; Kılıçman, A. (2008). A note on solutions of wave, Laplace's and heat equations with convolution terms by using a double Laplace transform. *Applied Mathematics Letters*, 21(12), 1324-1329.

[13] Novikov, S., Manakov; S. V.; Pitaevskii, L. P.; Zakharov, V. E. (1984). *Theory of solitons: the inverse scattering method*. Springer Science & Business Media, New York.

[14] Qian, C.; Rao, J.; Mihalache, D.; He, J. (2018). Rational and semi-rational solutions of the y-nonlocal Davey–Stewartson I equation. *Computers & Mathematics with Applications*, 75(9), 3317-3330.

[15] Guner, O.; Bekir, A. (2016). Bright and dark soliton solutions for some nonlinear fractional differential equations. *Chinese Physics B*, 25(3), 030203.

[16] Guo, L.; Zhang Y.; Xu, S.; Wu, Z.; He, J. (2014). The higher order rogue wave solutions of the Gerdjikov–Ivanov equation. *Physica Scripta*, 89(3), 035501.

[17] Liu, C. S. (2008). Solving an inverse Sturm-Liouville problem by a Lie-group method. *Boundary Value Problems*, 2008, 1-18.

[18] Ismael, H. F.; Seadawy, A.; Bulut, H. (2021). Construction of breather solutions and N-soliton for the higher order dimensional Caudrey–Dodd–Gibbon–Sawada–Kotera equation arising from wave patterns. *International Journal of Nonlinear Sciences and Numerical Simulation*. https://doi.org/10.1515/ijnsns-2020-0169

[19] Ismael, H. F.; Bulut, H. (2021). Multi soliton solutions, M-lump waves and mixed soliton-lump solutions to the awada-Kotera equation in (2+ 1)-dimensions. *Chinese Journal of Physics*, 71, 54-61.

[20] Ismael, H. F.; Seadawy, A.; Bulut, H. (2021). Rational solutions, and the interaction solutions to the (2+ 1)-dimensional time-dependent Date–Jimbo–Kashiwara–Miwa equation. *International Journal of Computer Mathematics*, 98(12), 2369-2377.

[21] Manafian, J.; Ilhan, O. A.; Ismael, H. F.; Mohammed, S. A.; Mazanova, S. (2021). Periodic wave solutions and stability analysis for the (3+ 1)-D potential-YTSF equation arising in fluid mechanics. *International Journal of Computer Mathematics*, 98(8), 1594-1616.

[22] Ali, K. K.; Yilmazer, R.; Osman, M. S. (2022). Dynamic behavior of the (3+ 1)-dimensional KdV–Calogero–Bogoyavlenskii–Schiff equation. *Optical and Quantum Electronics*, 54(3), 1-15.

[23] Liu, D.; Ju, X., Ilhan; O. A., Manafian, J.; Ismael, H. F. (2021). Multi-waves, breathers, periodic and cross-kink solutions to the (2+ 1)-dimensional variable-coefficient Caudrey-Dodd-Gibbon-Kotera-Sawada equation. *Journal of Ocean University of China*, 20(1), 35-44.

[24] Ismael, H. F.; Bulut, H.; Baskonus, H. M. (2021). W-shaped surfaces to the nematic liquid crystals with three nonlinearity laws. *Soft Computing*, 25(6), 4513-4524.

[25] Ali, K. K.; Dutta, H., Yilmazer, R.; Noeiaghdam, S. (2020). On the new wave behaviors of the Gilson-Pickering equation. *Frontiers in Physics*, 8, 54.

[26] He, J.; Xu, S.; Porsezian, K. (2012). Rogue waves of the Fokas–Lenells equation. *Journal of the Physical Society of Japan*, 81(12), 124007.

[27] Zhang, Y.; Cheng, Y.; He, J. (2017). Riemann-Hilbert method and N-soliton for two-component Gerdjikov-Ivanov equation. *Journal of Nonlinear Mathematical Physics*, 24(2), 210-223.

[28] Peng, W. Q.; Tian, S. F.; Wang, X. B.; Zhang T. T.; Fang, Y. (2019). Riemann–Hilbert method and multi-soliton solutions for three-component coupled nonlinear Schrödinger equations. *Journal of Geometry and Physics*, 146, 103508.

[29] Zhang, S.; Tong, J. L.; Wang, W. (2008). A generalized $(G'G)$-expansion method for the mKdV equation with variable coefficients. *Physics Letters A*, 372(13), 2254-2257.

[30] Ali, K. K.; Yilmazer, R.; Yokus, A.; Bulut, H. (2020). Analytical solutions for the (3+ 1)-dimensional nonlinear extended quantum Zakharov–Kuznetsov equation in plasma physics. *Physica A: Statistical Mechanics and its Applications*, 548, 124327.

[31] Ali, K. K.; Seadawy, A. R.; Yokus, A.; Yilmazer, R.; Bulut, H. (2020). Propagation of dispersive wave solutions for (3+ 1)-dimensional nonlinear modified Zakharov–Kuznetsov equation in plasma physics. *International Journal of Modern Physics B*, 34(25), 2050227.

[32] Ali, K. K.; Yilmazer, R.; Bulut, H.; Yokus, A. (2022). New Wave Behaviours of the Generalized Kadomtsev-Petviashvili Modified Equal Width-Burgers Equation. *Appl. Math*, 16(2), 249-258.

[33] Mamun Miah, M.; Shahadat Ali H. M.; Ali Akbar, M.; Majid Wazwaz, A. (2017). Some applications of the $(G'/G, 1/G)$-expansion method to find new exact solutions of NLEEs. *The European Physical Journal Plus*, 132(6), 1-15.

[34] Ismael, H. F.; Bulut, H.; Baskonus, H. M. (2020). Optical soliton solutions to the Fokas–Lenells equation via sine-Gordon expansion method and $(m + (G'/G))$-expansion method. *Pramana*, 94(1), 1-9.

[35] Gao, W.; Ismael, H. F.; Husien, A. M.; Bulut, H.; Baskonus, H. M. (2019). Optical soliton solutions of the cubic-quartic nonlinear Schrödinger and resonant nonlinear Schrödinger equation with the parabolic law. *Applied Sciences*, 10(1), 219.

[36] Ismael, H. F.; Baskonus, H. M.; Bulut, H. (2021). Abundant novel solutions of the conformable Lakshmanan-Porsezian-Daniel model. *Discrete & Continuous Dynamical Systems-S*, 14(7), 2311.

[37] Ismael, H. F.; Atas, S. S.; Bulut, H.; Osman, M. S. (2021). Analytical solutions to the M-derivative resonant Davey–Stewartson equations. *Modern Physics Letters B*, 35(30), 2150455.

[38] Rehman, S. U.; Yusuf, A.; Bilal, M.; Younas, U.; Younis, M.; Sulaiman, T. A. (2020). Application of (G'/G^2)-expansion method to microstructured solids, magneto-electro-elastic circular rod and (2+ 1)-dimensional nonlinear electrical lines. *Mathematics in Engineering, Science & Aerospace*, 11(4).

[39] Gaber, A. A.; Aljohani, A. F.; Ebaid, A.; Machado, J. T. (2019). The generalized Kudryashov method for nonlinear space–time fractional partial differential equations of Burgers type. *Nonlinear Dynamics*, 95(1), 361-368.

[40] Arshad, M.; Seadawy, A. R.; Lu, D. (2017). Elliptic function and solitary wave solutions of the higher-order nonlinear Schrödinger dynamical equation with fourth-order dispersion and cubic-quintic nonlinearity and its stability. *The European Physical Journal Plus*, 132(8), 1-11.

[41] Wen, X. (2010). Construction of new exact rational form non-travelling wave solutions to the (2+ 1)-dimensional generalized Broer–Kaup system. *Applied Mathematics and Computation*, 217(4), 1367-1375.

[42] Tang, Y. (2013). Pfaffian solutions and extended Pfaffian solutions to (3+ 1)-dimensional Jimbo–Miwa equation. *Applied Mathematical Modelling*, 37(10-11), 6631-6638.

[43] He, X. J.; Lü, X.; Li, M. G. (2021). Bäcklund transformation, Pfaffian, Wronskian and Grammian solutions to the $(3+1)$-dimensional generalized Kadomtsev–Petviashvili equation. *Analysis and Mathematical Physics*, 11(1), 1-24.

[44] Konopelchenko, B. G. (1993). *Solitons in multidimensions: inverse spectral transform method.* World Scientific.

[45] Tarla, S.; Ali, K. K.; Yilmazer, R.; Osman, M. S. (2022). New optical solitons based on the perturbed Chen-Lee-Liu model through Jacobi elliptic function method. *Optical and Quantum Electronics*, 54(2), 1-12.

[46] Tarla, S.; Ali, K. K.; Sun, T. C.; Yilmazer, R.; Osman, M. S. (2022). Nonlinear pulse propagation for novel optical solitons modeled by Fokas system in monomode optical fibers. *Results in Physics*, 105381.

[47] Olver, P. J. (2014). *Introduction to partial differential equations*, Springer Nature Switzerland AG.

[48] Hirota, R. (2004). *The direct method in soliton theory.* Cambridge University Press, 155.

[49] Zhang, X.; Wang, L.; Liu, C.; Li, M.; Zhao, Y.C. (2020). High-dimensional nonlinear wave transitions and their mechanisms. *Chaos An Interdiscip. J. Nonlinear Sci.* 30, 113107 .

[50] Yu, S. J.; Toda, K.; Fukuyama, T. (1998). N-soliton solutions to a-dimensional integrable equation. *Journal of Physics A: Mathematical and General*, 31(50), 10181.

[51] Wazwaz, A. M. (2012). A study on two extensions of the Bogoyavlenskii–Schieff equation. *Communications in Nonlinear Science and Numerical Simulation*, 17(4), 1500-1505.

[52] Yong, C.; Biao, L.; Hong-Qing, Z. (2003). Generalized Riccati equation expansion method and its application to the Bogoyavlenskii's generalized breaking soliton equation. *Chinese Physics*, 12(9), 940.

[53] Saha Ray, S. (2020). Lie symmetry analysis, symmetry reductions with exact solutions, and conservation laws of (2+ 1)-dimensional Bogoyavlenskii-Schieff equation of higher order in plasma physics. *Mathematical Methods in the Applied Sciences*, 43(9), 5850-5859.

[54] Ma, W. X. (2022). N-soliton solutions and the Hirota conditions in (1+ 1)-dimensions. *International Journal of Nonlinear Sciences and Numerical Simulation*, 23(1), 123-133.

[55] Manakov, S. V.; Zakharov, V. E., Bordag; L. A., Its, A. R.; Matveev, V. B. (1977). Two-dimensional solitons of the Kadomtsev-Petviashvili equation and their interaction. *Physics Letters A*, 63(3), 205-206.

[56] Satsuma, J.; Ablowitz, M. J. (1979). Two-dimensional lumps in nonlinear dispersive systems. *Journal of Mathematical Physics*, 20(7), 1496-1503.

[57] Harun-Or-Roshid; Ma, W. X. (2018). Dynamics of mixed lump-solitary waves of an extended (2+ 1)-dimensional shallow water wave model. *Physics Letters A*, 382(45), 3262-3268.

[58] Solli, D. R.; Ropers, C., Koonath, P.; Jalali, B. (2007). Optical rogue waves. Nature, 450(7172), 1054-1057.

[59] Yan, Z. (2011). Vector financial rogue waves. *Physics letters A*, 375(48), 4274-4279.

[60] Grimshaw, R.; Pelinovsky, E.; Taipova, T.; Sergeeva, A. (2010). Rogue internal waves in the ocean: long wave model. *The European Physical Journal Special Topics*, 185(1), 195-208.

[61] He, J. S.; Charalampidis, E. G.; Kevrekidis, P. G.; Frantzeskakis, D. J. (2014). Rogue waves in nonlinear Schrödinger models with variable coefficients: application to Bose–Einstein condensates. *Physics Letters A*, 378(5-6), 577-583.

[62] Ma, W. X.; Zhou, Y. (2018). Lump solutions to nonlinear partial differential equations via Hirota bilinear forms. *Journal of Differential Equations*, 264(4), 2633-2659.

[63] Wang, H.; Tian, S.; Zhang, T.; Chen, Y. (2019). Lump wave and hybrid solutions of a generalized (3+ 1)-dimensional nonlinear wave equation in liquid with gas bubbles. *Frontiers of Mathematics in China*, 14(3), 631-643.

[64] Wang, M.; Tian, B.; Sun, Y.; Zhang, Z. (2020). Lump, mixed lump-stripe and rogue wave-stripe solutions of a (3+ 1)-dimensional nonlinear wave equation for a liquid with gas bubbles. *Computers & Mathematics with Applications*, 79(3), 576-587.

[65] Zhao, Z.; He, L. (2019). Multiple lump solutions of the (3+ 1)-dimensional potential Yu–Toda–Sasa–Fukuyama equation. *Applied Mathematics Letters*, 95, 114-121.

[66] Fokas, A. S.; Pelinovsky, D. E.; Sulem, C. (2001). Interaction of lumps with a line soliton for the DSII equation. *Physica D: Nonlinear Phenomena*, 152, 189-198.

[67] Toda, K.; Song-Ju, Y.; Fukuyama, T. (1999). The Bogoyavlenskii-Schiff hierarchy and integrable equations in (2+ 1) dimensions. *Reports on Mathematical Physics*, 44(1-2), 247-254.

[68] Bogoyavlenskii, O. I. (1990). Breaking solitons in 2+ 1-dimensional integrable equations. *Russian Mathematical Surveys*, 45(4), 1.

[69] Wazwaz, A. M. (2010). Multiple soliton solutions for the Bogoyavlenskii's generalized breaking soliton equations and its extension form. *Applied Mathematics and Computation*, 217(8), 4282-4288.

[70] Kadomtsev, B. B.; Petviashvili, V. I. (1970). On the stability of solitary waves in weakly dispersing media. *Dokl. Akad. Nauk SSSR*, 192(4), 753-756.

[71] Dorizzi, B.; Grammaticos, B.; Ramani, A.; Winternitz, P. (1986). Are all the equations of the Kadomtsev–Petviashvili hierarchy integrable?. *Journal of mathematical physics*, 27(12), 2848-2852.

[72] Date, E.; Jimbo, M.; Kashiwara, M.; Miwa, T. (1982). Transformation groups for soliton equations: IV. A new hierarchy of soliton equations of KP-type. *Physica D: Nonlinear Phenomena*, 4(3), 343-365.

[73] Wang, S. N.; Hu, J. (2019). Grammian solutions for a (2+ 1)-dimensional integrable coupled modified Date–Jimbo–Kashiwara–Miwa equation. *Modern Physics Letters B*, 33(10), 1950119.

[74] Guo, F.; Lin, J. (2019). Interaction solutions between lump and stripe soliton to the (2+ 1)-dimensional Date–Jimbo–Kashiwara–Miwa equation. *Nonlinear Dynamics*, 96(2), 1233-1241.

[75] Adem, A. R.; Yildirim, Y.; Yaşar, E. (2019). Complexiton solutions and soliton solutions: $(2+1)$-dimensional Date–Jimbo–Kashiwara–Miwa equation. *Pramana*, 92(3), 1-12.

[76] Yuan, Y. Q.; Tian, B.; Sun, W. R.; Chai, J.; Liu, L. (2017). Wronskian and Grammian solutions for a $(2+1)$-dimensional Date–Jimbo–Kashiwara–Miwa equation. *Computers & Mathematics with Applications*, 74(4), 873-879.

[77] Singh, M.; Gupta, R. K. (2018). On Painlevé analysis, symmetry group and conservation laws of Date–Jimbo–Kashiwara–Miwa equation. *International Journal of Applied and Computational Mathematics*, 4(3), 1-15.

[78] Sajid, N.; Akram, G. (2018). The application of the $\exp(-\Phi(\xi))$-expansion method for finding the exact solutions of two integrable equations. *Mathematical Problems in Engineering*, 2018, 5191736.

[79] Bogoyavlenskiĭ, O. I. (1990). Overturning solitons in new two-dimensional integrable equations. *Mathematics of the USSR-Izvestiya*, 34(2), 245.

[80] Chen, S. T.; Ma, W. X. (2018). Lump solutions to a generalized Bogoyavlensky-Konopelchenko equation. *Frontiers of Mathematics in China*, 13(3), 525-534.

[81] Chen, S. T.; Ma, W. X. (2019). Exact solutions to a generalized Bogoyavlensky-Konopelchenko equation via maple symbolic computations. *Complexity*, 2019.

[82] Wazwaz, A. M. (2016). The simplified Hirota's method for studying three extended higher-order KdV-type equations. *Journal of Ocean Engineering and Science*, 1(3), 181-185.

[83] Wazwaz, A. M. (2017). A new integrable nonlocal modified KdV equation: Abundant solutions with distinct physical structures. *Journal of Ocean Engineering and Science*, 2(1), 1-4.

[84] Shamseldeen, S.; Latif, M. A.; Hamed, A. A.; Nour, H. M. (2017). New doubly-periodic solutions for the new integrable non local modified KdV equation. *Journal of Ocean Engineering and Science*, 2(4), 245-247.

[85] Karunakar, P.; Chakraverty, S. (2019). Effect of Coriolis constant on Geophysical Korteweg-de Vries equation. *Journal of Ocean Engineering and Science*, 4(2), 113-121.

[86] Nuruddeen, R. I. (2018). Multiple soliton solutions for the (3+ 1) conformable space–time fractional modified korteweg–de-vries equations. *Journal of Ocean Engineering and Science*, 3(1), 11-18.

[87] Huda, M. A.; Akbar, M. A.; Shanta, S. S. (2017). Abundant general solitary wave solutions to the family of KdV type equations. *Journal of Ocean Engineering and Science*, 2(1), 47-54.

[88] Meng, Q.; Zhang, C. (2016). A third-order KdV solution for internal solitary waves and its application in the numerical wave tank. *Journal of Ocean Engineering and Science*, 1(2), 93-108.

[89] Boiti, M.; Leon, J. P.; Manna, M.; Pempinelli, F. (1986). On the spectral transform of a Korteweg-de Vries equation in two spatial dimensions. *Inverse problems*, 2(3), 271.

[90] Wazwaz, A. M. (2020). Two new Painlevé-integrable (2+ 1) and (3+ 1)-dimensional KdV equations with constant and time-dependent coefficients. *Nuclear Physics B*, 954, 115009.

[91] Liu, J. G.; Zhu, W. H. (2020). Various exact analytical solutions of a variable-coefficient Kadomtsev–Petviashvili equation. *Nonlinear Dynamics*, 100(3), 2739-2751.

[92] Liu, J. G.; Tian, Y.; Zeng, Z. F. (2017). New exact periodic solitary-wave solutions for the new (3+ 1)-dimensional generalized Kadomtsev-Petviashvili equation in multi-temperature electron plasmas. *AIP Advances*, 7(10), 105013.

[93] Liu, J. G.; Zhu, W. H.; Zhou, L. (2020). Interaction solutions and abundant exact solutions for the new (3+ 1)-dimensional generalized Kadomtsev-Petviashvili equation in fluid mechanics. *Journal of Applied Analysis & Computation*, 10(3), 960-971.

[94] Wazwaz, A. M.; El-Tantawy, S. A. (2016). A new (3+ 1)-dimensional generalized Kadomtsev–Petviashvili equation. *Nonlinear Dynamics*, 84(2), 1107-1112.

[95] Peregrine, D. H. (1967). Long waves on a beach. *Journal of fluid mechanics*, 27(4), 815-827.

[96] Jawad, A. M.; Petković, M. D.; Laketa, P.; Biswas, A. (2013). Dynamics of shallow water waves with Boussinesq equation. *Scientia Iranica*, 20(1), 179-184.

[97] Zeeshan, A.; Ismael, H. F.; Yousif, M. A.; Mahmood, T.; Rahman, S. U. (2018). Simultaneous effects of slip and wall stretching/shrinking on radiative flow of magneto nanofluid through porous medium. *Journal of Magnetics*, 23(4), 491-498.

CURRICULUM VITAE

Hajar Farhan Ismael

[redacted]

[redacted] [redacted]

[redacted]

[redacted]

[redacted]

[redacted]

[redacted] [redacted]

[redacted] [redacted]

[redacted] [redacted]

[redacted] [redacted]

[redacted] [redacted]

[redacted]

[redacted] [redacted]

ACADEMIC ACTIVITIES

Paper

1. Gao, W., Ismael, H. F., Mohammed, S. A., Baskonus, H. M., & Bulut, H. (2019). Complex and real optical soliton properties of the paraxial non-linear Schrödinger equation in Kerr media with M-fractional. Frontiers in Physics, 7, 197.

2. Gao, W., Ismael, H. F., Husien, A. M., Bulut, H., & Baskonus, H. M. (2019). Optical soliton solutions of the cubic-quartic nonlinear Schrödinger and resonant nonlinear Schrödinger equation with the parabolic law. Applied Sciences, 10(1), 219.

3. Ismael, H., & Bulut, H. (2020). On the wave solutions of (2+ 1)-dimensional time-fractional Zoomeron equation. Konuralp Journal of Mathematics (KJM), 8(2), 410-418.

4. Gao, W., Ismael, H. F., Bulut, H., & Baskonus, H. M. (2020). Instability modulation for the (2+ 1)-dimension paraxial wave equation and its new optical soliton solutions in Kerr media. Physica Scripta, 95(3), 035207.

5. Ismael, H. F., Bulut, H., Baskonus, H. M., & Gao, W. (2020). Newly modified method and its application to the coupled Boussinesq equation in ocean engineering with its linear stability analysis. Communications in Theoretical Physics, 72(11), 115002.

6. Ismael, H. F., Bulut, H., & Baskonus, H. M. (2020). Optical soliton solutions to the Fokas–Lenells equation via sine-Gordon expansion method and $(m + (G'/G))$-expansion method. Pramana, 94(1), 1-9.

7. Ismael, H. F., Bulut, H., Park, C., & Osman, M. S. (2020). M-lump, N-soliton solutions, and the collision phenomena for the (2+ 1)-dimensional Date-Jimbo-Kashiwara-Miwa equation. Results in Physics, 19, 103329.

8. Ismael, H. F., Ma, W. X., & Bulut, H. (2021). Dynamics of soliton and mixed lump-soliton waves to a generalized Bogoyavlensky-Konopelchenko equation. Physica Scripta, 96(3), 035225.

9. Ismael, H. F., Bulut, H., & Baskonus, H. M. (2021). W-shaped surfaces to the nematic liquid crystals with three nonlinearity laws. Soft Computing, 25(6), 4513-4524.

10. Ismael, H. F., Seadawy, A., & Bulut, H. (2021). Construction of breather solutions and N-soliton for the higher order dimensional Caudrey–Dodd–Gibbon–Sawada–Kotera equation arising from wave patterns. International Journal of Nonlinear Sciences and Numerical Simulation.

11. Ismael, H. F., Seadawy, A., & Bulut, H. (2021). Multiple soliton, fusion, breather, lump, mixed kink-lump and periodic solutions to the extended shallow water wave model in (2+ 1)-dimensions. Modern Physics Letters B, 35(08), 2150138.

12. Ismael, H. F., & Bulut, H. (2021). Nonlinear dynamics of (2+ 1)-dimensional Bogoyavlenskii–Schieff equation arising in plasma physics. Mathematical Methods in the Applied Sciences, 44(13), 10321-10330.

13. Ismael, H. F., Bulut, H., Baskonus, H. M., & Gao, W. (2021). Dynamical behaviors to the coupled Schrödinger-Boussinesq system with the beta derivative. AIMS Mathematics, 6(7), 7909-7928.

14. Ismael, H. F., & Bulut, H. (2021). Multi soliton solutions, M-lump waves and mixed soliton-lump solutions to the awada-Kotera equation in (2+ 1)-dimensions. Chinese Journal of Physics, 71, 54-61.

15. Ismael, H. F., Baskonus, H. M., & Bulut, H. (2021). Abundant novel solutions of the conformable Lakshmanan-Porsezian-Daniel model. Discrete & Continuous Dynamical Systems-S, 14(7), 2311.

16. Manafian, J., Ilhan, O. A., Ismael, H. F., Mohammed, S. A., & Mazanova, S. (2021). Periodic wave solutions and stability analysis for the (3+ 1)-D potential-YTSF equation arising in fluid mechanics. International Journal of Computer Mathematics, 98(8), 1594-1616.

17. Ismael, H. F., Atas, S. S., Bulut, H., & Osman, M. S. (2021). Analytical solutions to the M-derivative resonant Davey–Stewartson equations. Modern Physics Letters B, 35(30), 2150455.

18. Ismael, H. F., Murad, M. A. S., & Bulut, H. (2021). Various exact wave solutions for KdV equation with time-variable coefficients. Journal of Ocean Engineering and Science.

19. Ismael, H. F., Seadawy, A., & Bulut, H. (2021). Rational solutions, and the interaction solutions to the (2+ 1)-dimensional time-dependent Date–Jimbo–Kashiwara–Miwa equation. International Journal of Computer Mathematics, 98(12), 2369-2377.

20. Ismael, H. F., Bulut, H., & Osman, M. S. (2022). The N-soliton, fusion, rational and breather solutions of two extensions of the (2+ 1)-dimensional Bogoyavlenskii–Schieff equation. Nonlinear Dynamics, 107(4), 3791-3803.

21. Ismael, H. F., Okumuş, İ., Aktürk, T., Bulut, H., & Osman, M. S. (2022). Analyzing study for the 3D potential Yu-Toda-Sasa-Fukuyama equation in the two-layer liquid medium. Journal of Ocean Engineering and Science.

22. Ismael, H. F., Murad, M. A. S., & Bulut, H. (2022). M-lump waves and their interaction with multi-soliton solutions for a generalized Kadomtsev–Petviashvili equation in (3+ 1)-dimensions. Chinese Journal of Physics.

Proceedings: :

1. Ismael, H. F., & Bulut, H. (2019, April). On the solitary wave solutions to the (2+ 1)-dimensional Davey-Stewartson equations. In International Conference on Computational Mathematics and Engineering Sciences (pp. 156-165). Springer, Cham.

2. Abdulkareem, H. H., Ismael, H. F., Panakhov, E. S., & Bulut, H. (2019, April). Some novel solutions of the coupled Whitham-Broer-Kaup equations. In International Conference on Computational Mathematics and Engineering Sciences (pp. 200-208). Springer, Cham.